Charles University in Prague
Faculty of Sciences
Department of Plant Physiology

Following the Arp2/3-based processes in plant cells

Ph.D. Thesis

Mgr. Jindřiška Fišerová roz. Pokorná

Specialization: Plant Physiology
Supervizor: Prof. RNDr. Zdeněk Opatrný, CSc.
Consultants: RNDr. Kateřina Schwarzerová, Ph.D.
Mgr. Lukáš Fischer, Ph.D.

Department of Plant Physiology, Faculty of Science
Charles University in Prague, Czech Republic

Prague 2006

This work was supported by grants from the Ministry of Education, Youth and Sports of the Czech Republic, no. VZ113100003 and from the Grant Agency of the Charles University in Prague, no. 165/B-BIO/PrF.

I declare that this thesis is my own work and has not previously been submitted for a degree at any education institution. All sources have been acknowledged and my contribution is clearly identified in the thesis. For any work in the thesis that has been co-published with other authors, I have the permission of the co-authors to include this work in my thesis.

.....

ACKNOWLEDGEMENT/PODĚKOVÁNÍ

I would like to thank my supervisor Prof. RNDr. Zdeněk Opatrný, Csc. for giving me the chance to work on an exciting project in his laboratory. I would also like to thank all people who participated on this project. The work presented in this thesis was done in the Department of Plant Physiology, Charles University in Prague, Czech Republic, and at School of Biological and Biomedical Sciences, University of Durham, UK.

I thank Dr. Kathleen L. Gould, Vanderbilt University, Nashville, USA, for the kind gift of rabbit polyclonal sera against fission yeast ARP2 and ARP3. The psmGFP vector was kindly provided by Prof. Seth J. Davis, University of Wisconsin-Madison, USA, via *Arabidopsis* Biological Resource Center, while the pCP binary vector was a kind gift of Dr. Ratet (Institut des Sciences Végétales CNRS, Gif sur Yvette, France).

My further thanks are in Czech...

Především děkuji za možnost pracovat tvořivě, svobodně a v míru uprostřed kolektivu lidí vnitřně krásných a opravdových. Bez této možnosti a bez mých nejbližších spolupracovníků a přátel by moje práce postrádala mnoho ze své radosti a smyslu. Můj dík je adresován všem minulým i současným rukám, jejichž dílem je naše dnešní společnost a díky nimž se rodí příležitost nejen k vypracování jedné disertační práce. Každému zvlášť a všem dohromady děkuji za každý okamžik poctivého života, jímž vtisknou světu nesmazatelnou a nesmírně krásnou pečeť. Pán Bůh jistě chápe a odpustí, že zůstává skryt na pozadí těchto řádků – samozřejmě, jako tomu bylo, je a bude.

Svému školiteli, Prof. Zdeňkovi Opatrnému, děkuji za mnohé. Děkuji za poskytnutí vynikajícího materiálního zázemí, pomoci při zařizování zahraničních stáží, neméně pak za přátelský přístup, smělé diskuse nad výsledky i vlastním textem práce.

Katce Schwarzerové děkuji za podnětné impulsy, cenné diskuse a rady při směrování vlastních experimentů, psaní publikací i této práce, a zejména za ochotu a obětavost, s jakou se mi vždy věnovala.

Lukášovi Fischerovi děkuji za oporu při prvních krocích na poli molekulárně biologických metod, za cenné rady, ochotu je vždy poskytnout na jakoukoliv vzdálenost a za pomoc při psaní této práce.

Dr. Andrei Smertenkovi děkuji za veškerou pomoc a inspiraci, a za vstřícnost vůbec při mém pobytu v laboratoři prof. Husseyho, jenž zasluží dík za poskytnutí věcného zázemí laboratoře.

RNDr. Janu Patráškovi děkuji za inspirativní diskuse.

Kolektivu Laboratoře buněčné biologie a biotechnologie, zejména pak Lence Havelkové, děkuji za ochotu, pomoc a příjemnou atmosféru v laboratoři.

Výše uvedeným patří můj dík za podporu v těžších chvílích a za vytvoření týmu, v němž bylo radostí pracovat. Jim a mnoha dalším vděčím za radost z každodenního údivu nad krásou světa a člověka.

Naposled děkuji svým rodičům. Při pomyšlení na jejich nekonečnou lásku a samozřejmou obětavost se mi téměř zastavuje srdce.

TABLE of CONTENT

ABREVIATIONS

AFs	Actin filaments
ARP	Actin related protein
ARPC	Actin related protein complex component
ASB	Actin stabilizing buffer
BY-2	Tobacco cell line Bright Yellow 2
DIC	Nomarski differential interference contrast
DMSO	Dimethyl sulfoxide
DTT	Dithiothreitol
ECL	Enhanced chemiluminiscence
EDTA	Ethylenediamine tetraacetic acid
EGTA	Ethylenebis(oxyethylenenitrilo)tetraacetic acid
ER	Endoplasmic reticulum
F-actin	Filamentous actin
FDA	Fluorescein diacetate
FITC	Fluorescein isothiocyanate
G-actin	Globular actin
GFP	Green fluorescent protein
HEPES	N-[2-Hydroxyethyl]piperazine-N'-[2-ethansulfonic acid]
IPTG	Isopropylthio-β-galactoside
Lat B	Latrunculin B
MES	2-morpholinoethanesulfonic acid
MS salts	Murashige and Skoog
MTs	Microtubules
PBS	Phosphate buffered saline
PCR	Polymerase chain reaction
PFA	Paraformaldehyde
PIPES	Piperazine-1,4-bis (2-ethanesulfonic acid)
PMSF	Phenylmethylsulfonyldifluoride
PVDF	Polyvinyldene difluoride
SAN	Site of AF nucleation
SDS	Sodium dodecyl sulfate
SDS-PAGE	Sodium dodecylsulfate-polyacrylamid gel electrophoresis
Scar	Supressor of cAMP
VCA	Verprolin cofilin acidic domain
TCA	Trichloracetic acid
TRITC	Tetramethylrhodamine isothiocyanate
WASP	Wiscott-Aldrich syndrome protein
WAVE	WASP family verprolin homologous

1. ABSTRACT

An actin cytoskeleton comprises an essential cytoskeletal structure that organizes a cytoplasm during number of processes occurring in animal and plant cells, such as cell division and growth, formation of membrane protrusions and cellular movement or cytoplasmic streaming. A dynamic actin net and an exact spatial and temporal actin filament organization is, therefore, necessary for correct growth processes and development of multicellular organism.

Depolymerization and re-establishment of actin arrays is mediated by actin associated proteins. Among them, an Arp2/3 complex (actin related protein 2 and 3) plays an important role as a catalyst of the actin filament nucleation and, thus, enables the formation of dynamic actin network. In non-plant cells, Arp2/3 complex-dependent polymerization of actin filaments is required for movement of whole cells (fibroblasts or keratocytes), it drives organels and pathogens throughout the cell or mediates endocytic processes. The role of the Arp2/3 complex in non-motile plant cells is despite the considerable effort over last three years far from being understood. Unlike animals, where loss-of-function mutations in the Arp2/3 complex are lethal, only limited number of cell types show significant phenotype in *Arabidopsis* mutants. The evidence exists that the complex is essential for some tip-growing cells, but a mosaic showing a mechanism of actin filament nucleation and the action of the Arp2/3 complex in plant is quite fragmentary.

My Ph.D. thesis is focused on the processes of the actin filament initiation and polymerization in tobacco BY-2 cells. To observe the processes of the polymerization of actin filaments, I took an advantage of the depolymerization effect of low temperature on actin filaments and during subsequent recovery, I observed the first steps of actin filament initiation. Consequently, I investigated a localization of Arp2/3 complex subunits in untreated BY-2 cells and in cells recovering their actin network either by immunolabelling using various antibodies against Arp2/3 complex subunits or in living cells by fusion of green fluorescent protein with ARP3 subunit of the complex. Further, I aimed to uncover the potential role of the Arp2/3 complex during tip-growth of tobacco pollen tubes. The results will be discussed taking into consideration the most recent knowledge and theories on the disputed role of the Arp2/3 complex in plants will be challenged.

2. INTRODUCTION

Actin filaments (AFs) represent dynamic directional polymers of an eukaryotic cell carrying out multiple cellular functions, such as cell division, growth and differentiation, intracellular transport, signal transduction, cell polarity determination, etc. The proper function of AFs is dependent on the exact spatial and temporal interplay of wide range of associated proteins, some of which can nucleate globular actin (G-actin), others stabilize, cap, cross-link, sever or degrade polymers of filamentous actin (F-actin), and so regulate formation and destruction of the complex actin net.

De novo nucleation and side-directed branching of AFs are essential for numerous motility processes in animal cells, including the extension of membrane protrusions, phagocytosis or chemotaxis. Plants do not posses motile cells, however, various cell shapes essential for the constitution of the complex plant body rise by means of complex processes including the spatial organization of AFs. The following text shortly summarises the recent knowledge on AFs assembly and formation of branched AFs network, with the emphasis on special character of plant cells.

2.1. Basic facts about actin

The major component of the actin cytoskeleton, actin, is an ATP-binding protein that exists in two forms in cell: as the monomer (G-actin or globular actin) and as the polymer (F-actin or filamentous actin). When new actin filament polymerizes, the formation of actin dimer and trimer is required before elongation step itself. Actin dimers and trimers can form spontaneously in solution if the concentration of G-actin increases above the critical concentration of polymerization, but seeds containing these forms of actin are extremely unstable. Since all incorporated actin subunits face the same direction, AFs are polar structures, and the two ends have distinct biochemical properties. The polymerization occurs primarily at the fast growing end (barbed; B-end or + end), while the depolymerization takes place at the slow growing end (pointed; P-end or – end). Rate constants for these reactions are known (Pollard 1986, Kuhn and Pollard 2005). Both processes are tightly controlled by monomer- and filament-binding proteins that regulate the monomer pool, supervise the nucleation and polymerization step, organize bundling of filaments and finally depolymerize filaments and ensure recycling of monomers (reviewed in Pollard et al. 2000).

In animals, different nucleators of AFs are known; among them an Arp2/3 complex, formins and spire are the best-known candidates. Since the text summarizing all available information on

AFs nucleation and polymerization would extensively expand, in accordance to my research focus I concentrate on processes mediated by the Arp2/3 complex.

2.2. The Arp2/3 complex in animals

2.2.1. Structure of the Arp2/3 complex

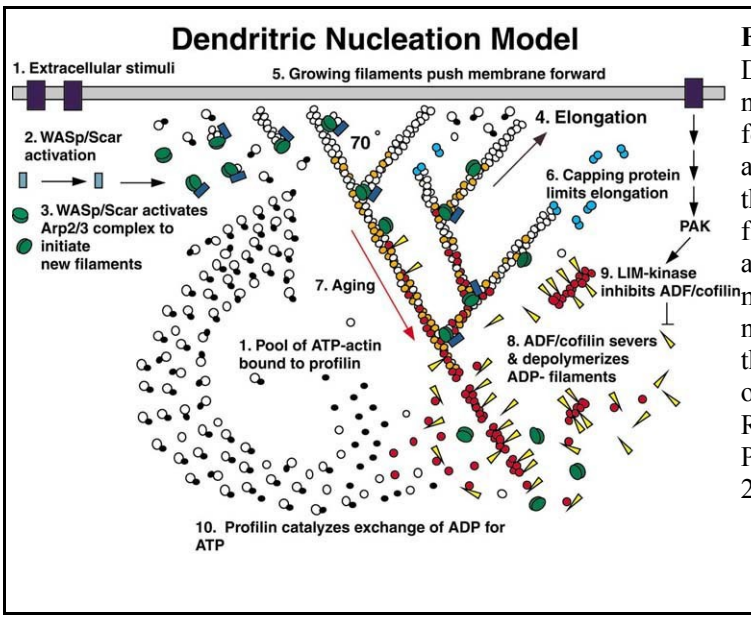

Figure 1. Dendritic nucleation model for the assembly and recycling of the branched actin filament network at leading edge of motile cells. The numbers refer to the postulated order of events. Reproduced from Pollard et al. 2000.

Eight years ago, a dendritic model of AF nucleation was published (Mullins et al 1998, Fig. 1) to explain the formation of branched AFs with the assistance of the Arp2/3 complex in motile cells. The complex was first isolated from *Acanthamoeba castellanii* (*A. castellanii*) based on its affinity for the actin monomer-binding protein profilin (Machesky et al. 1994) and was subsequently purified from several other organisms including humans (Welch et al. 1997a), other vertebrates (Ma et al. 1998, Rohatgi et al. 1999), and the yeast *Saccharomyces cerevisiae* (*S. cerevisiae*) (Winter et al. 1997). Its subunit composition is conserved in all of these organisms and comprises seven tightly associated subunits (Machesky et al. 1994) that include the actin-related proteins ARP2 and

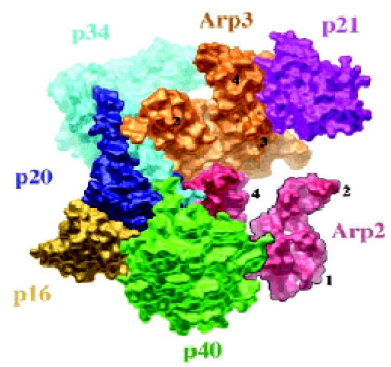

Figure 2. Space-filling model of the 2 Ä crystal stucture of bovine Arp2/3 complex. Robinson et al. 2001.

ARP3 and five additional proteins called ARPC1-ARPC5 (Fig. 2). The complex is poorly active on its own, but when activated by nucleation promoting factors, it nucleates new AFs from the surface of an existing filament at an angle of 70° relative to the "parental" filament (Fig. 3). Based on the sequences of *ARP2* and *ARP3* (Kelleher et al. 1995) and the X-ray crystallography of the structure of the Arp2/3 complex (Robinson et al. 2001), ARP2 and ARP3 within the activated complex were predicted to mimic an actin dimer to which a G-actin needs to bind to create an actin nucleus competent for rapid elongation.

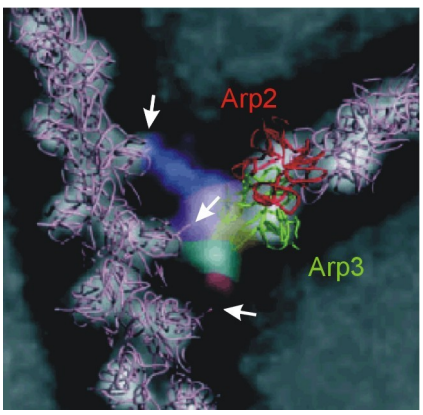

Figure 3. Model of Arp2/3 complex in Y-branch. Arrows indicate the three bridges of density observed to connect the Arp2/3 complex to the mother filament. Borth and Welch 2002.

2.2.2. Signalling to the Arp2/3 complex

Activation of the Arp2/3 complex is catalysed by a number of proteins and protein complexes. These include *Listeria monocytogenes* (*L. monocytogenes*) ActA protein (Welch et al. 1997b), the Wiscott-Aldrich syndrome protein (WASP) (Yarar et al. 1999), N-WASP (Rohatgi et al. 1999), supressor of cAMP (Scar)/WASP family verprolin homologous (WAVE) proteins (Machesky and Gould 1999), yeast myosin I (Evangelista et al. 2000), metazoan cortactin (Uruno et al. 2001, Weaver et al. 2001) yeast Abp1p (Goode et al. 1999) or yeast Pan1p (Duncan et al. 2001). Readers interested in regulation of the Arp2/3 complex can find more details reviewed by Welch and Mullins (2002), Stradal et al. (2004) or Stradal and Scita (2006). The following text summarises recent knowledge on the only known regulator of the Arp2/3 complex in plant cells - Scar/WAVE.

Three isoforms of WAVE are expressed in mammals (WAVE1-3), just one in *Dictyostelium discoideum* (*D. discoideum*), *Caenorhabditis elegans* (*C. elegans*) and *Drosophila melanogaster* (*D. melanogaster*), but no homolog of WAVE was found in yeasts (for review see Ibarra et al. 2005). WAVE proteins share their conserved C-terminal "catalytic" domain (VCA domain) with

WASP and N-WASP. This module enables them to form a tripartite unit with G-actin and the Arp2/3 complex (Marchand et al. 2001, Zallen et al. 2002). Conversely, there is a remarkable divergence in their N-terminal regions that underlines significant differences in their activity and regulation. For example, full-length WASP and N-WASP are regulated directly by small GTPases, while the regulation of Scar/WAVE downstream of GTPases occurs through formation of protein complexes.

In cell, Scar/WAVE is present in a complex with four other proteins: Pir121, Nap1, Abi1 and HSP300 (Eden et al. 2002, Gautreau et al. 2004, Innocenti 2004). WAVE complexes have been postulated to exert both positive and negative modes of regulation. In the negative model of regulation, the complex represses the activity of Scar/WAVE until released by binding of small GTPases (Blagg et al. 2003, Bogdan and Klambt 2003). In the positive model of regulation, binding of small GTPase induces conformational change within the complex leading to its active state (Innocenti et al. 2004 , Steffen et al. 2004). Nowadays, the biochemical evidence seems to support positive model, however, taking into account that various experimental organisms and species were used, it is feasible that both modes of regulation take place at different cellular contexts, or even in different cell types and species.

2.2.3. The role of the Arp2/3-driven AFs polymerization in animals

As mentioned previously, the Arp2/3 driven AFs polymerization generally takes part in processes based on dynamical actin network, which was mostly confirmed *in vivo* studies by localisation of the complex subunits with GFP fusion or using antibodies. Many information about the function of the Arp2/3 complex comes from studies on various mutants in genes coding for proteins of the Arp2/3 complex and its regulatory agents.

Subunits of the Arp2/3 complex were detected in cells of many species. Both ARP2 and ARP3 are strongly enriched in the cortex of *A. castelanii* (Kelleher et al. 1995), a single-celled motile organism, strains of which can colonize human tissue. During infection, *A. castelanii* migrates through the extracellular matrix of the host; *in vitro*, the migration of *A. castelanii* is actin-dependent and is achieved through the formation of actin-rich membrane extensions.

D. discoideum resembles neutrophils in its capability to rapidly adjust its cortical actin system in response to environmental cues. Within seconds, both types of cells respond to adhering particles by forming of phagocytic cup, and to chemoatractants by establishing a new leading edge (Devreotes and Zigmond 1988). *D. discoideum* cells can project leading edges from any part of their surface, and their cortical actin cytoskeleton is higly dynamic (Bretschneider at al. 2004). In *D. discoideum* cells, ARP3 and p41 (ARPC1) were shown to localize to the substrate-attached actin-

rich spots, macropinosomes and phagosomes (Bretschneider at al. 2004, Cvrckova et al. 2004). ARP3 was also reported to be associated with mitochondria of *D. discoideum* (Murgia et al. 1995).

In human or chicken fibroblast, subunits of the Arp2/3 complex localized to lamellipodia in stationary cells, but also to leading lamellipodia of motile cells (Welch et al. 1997a, Svitkina et al. 2003; Fig. 4), supporting its role in formation of membrane ruffles and in generating forces, which results in movement of the whole cell body. Apart from it, the Arp2/3-driven AFs polymerization also propels parasites or organels. The pathogenic bacterium *L. monocytogenes* is capable of direct movement within the cytoplasm of infected host cells. The propulsion is driven by actin polymerization at the bacterial cell surface, and moving bacteria leave in their wave a tail of AFs (comet tail). ARP3, p34 (ARPC2) and p21 (ARPC4) localized throughout actin comet tails of *L. monocytogenes* (Welch et al. 1997b).

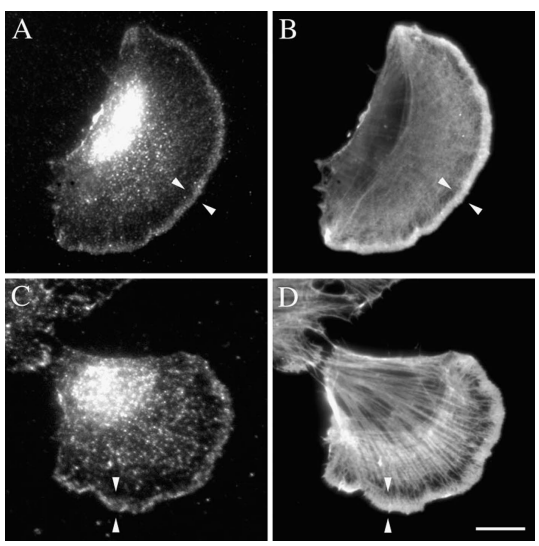

Figure 4. Localization of Arp2/3 complex subunits in primary culture fibroblasts from embryonic chicken hearts by indirect fluorescence. (A) Distribution of Arp3 and (B) of actin in the same cell. (C) Distribution of ARPC2 and (D) of actin in the same cell. The arrowheads indicate the possition of the lamellipodia. Bar 10 μM. Welch et al. 1997a.

In yeasts, the Arp2/3 complex was shown to participate in several cellular processes. The disruption of any subunit of the Arp2/3 complex generally led to several growth defections or even to deaths, depending on the strain of yeast and growth conditions (Moreau et al. 1996, Winter et al. 1997, Morrell et al. 1999). Mutants showed affected organization of highly dynamic cortical actin patches (actin patches and actin cables are the two AFs structures found in yeasts; the actin patches concentrate at cellular surface and participate in membrane-based processes, such as exocytosis and endocytis) and disrupted endocytic processes, which are believed to be the reason for reduced

cellular viability.

Consistently with a possible function of the Arp2/3 complex in regulating of the dynamic actin, ARP2 and ARP3 localized to highly dynamic cortical actin patches at all stages of cell cycle (Moreau et al. 1996; Winter et al. 1997; Morrell at al. 1999). In yeasts, the role of the Arp2/3 complex in membrane-based processes, such as vesicle formation in a trans-Golgi network (Carreno et al. 2004), regulation of both retrograde (Golgi-to-endoplasmic reticulum; ER) (Luna et al. 2002) and anterograde (ER-to-Golgi) (Matas et al. 2004) protein transport, vacuole fusion (Eitzen et al. 2002) or endocytic internalization (Kaksonen et al. 2003; reviewed in Merrifield 2004 and Ayscough 2005) was frequently reported. Finally, ARP2 was found to co-localize with mitochondria and yeast cells bearing the mutation in ARP2 or ARPC1 genes showed decreased velocities of mitochondrial movement and defects in mitochondrial morphology (Boldogh et al. 2001). Therefore, it was hypothesized that the movement of mitochondria in yeasts is actin polymerization driven and that this movement requires the Arp2/3 complex .

Finally, the role of the Arp2/3 complex during embryonal development of several species has been proposed. In *C. elegans*, RNAi of various subunits of the Arp2/3 complex resulted in the inhibited hypodermal cell migration accompanied by the reduction of F-actin formation. Consistently, the subunits of the Arp2/3 complex localized at the leading edges of migrating hypodermal cells (Sawa et al. 2003). Mutations in all of the genes of the Arp2/3 complex resulted in the lethality before the adult stage in *D. melanogaster* (Hudson and Cooley 2002). Therefore, the phenotypes and the function of the Arp2/3 complex were examined in clones of mutant cells in specific tissue types, such as germline cells. Weaker mutants in ARPC1 and Scar exhibited defects in the uniform spacing of interfaze nuclei, abnormal nuclear morphogenesis and several defects in the AFs arrangement during oogenesis (Zallen et al. 2002). The requirement of the Arp2/3 complex during oogenesis was further supported by Hudson and Cooley (2002). Loss of ARP3 or ARPC1 led to defects in the expansion of ring canals, where both proteins were immunolocalized (ring canals are large intracellular bridges allowing a flow of the cytoplasm from the nurse cell to the oocyte during oogenesis), however, many cellular processes such as cell division, remained unaffected (reviewed in Miller 2002). The Arp2/3 complex was therefore proposed to be required for ring canal expansion during oogenesis. Moreover, in *D. melanogaster* cultured motile cells, the knockdown of the Scar/WAVE resulted in a strong inhibition of lamellipodia and filopodia formation and the cell spreading. AFs in mutants were markedly reduced (Biyasheva et al. 2004). Within this context the fact falls that the disruption of the Scar gene in *D. discoideum* predictably reduced the levels of cellular F-actin together with macropinocytosis, phagocytosis and endosomal membrane flow (Seastone et al. 2001). Interestingly, when Pir121, other subunit of the Scar/WAVE complex, was disrupted, mutant cells maintained an excessive portion of their actin in a polymerized state,

displaying severe defects in movement and chemotaxis (Blagg et al. 2003).

2.3. Back to plants

Following the Arp2/3 story, readers could not miss the fact that, in animals, the Arp2/3 complex exhibits an essential role mainly during various motility processes. However, plant cells do not move at all, moreover, they are tightly packed inside cell walls. When searching for plant "leading edges", one would pay attention to at least forward the tip-growing cells, such as pollen tubes or root hairs. What importance have the Arp2/3-driven processes in plant organisms? What processes involving the Arp2/3 complexes in motile cells could be equally important for non-motile cells? Studies aimed to uncover the role of the Arp2/3-driven processes in plant cells (unfortunately quite single-tracked concerning methods used) revealed surprising results and pointed to new aspects of the growth processes and shape differentiation of plant cells. But before meeting the Arp2/3 story in plant context, let us shortly summarize the recent knowledge on actin nucleation in plants generally.

2.3.1. Actin filament nucleation in plants

In plants, actin associated proteins known to accelerate turnover of AFs, such as profilin or ADF, were under intensive investigation for years. Nevertheless, not a single study revealed the mechanisms of F-actin nucleation and initiation until picking up animal models of AFs nucleation driven by the Arp2/3 complex or formins. These proteins and corresponding nucleation processes stayed behind the boundary of view of plant scientists until 2003 and 2004, respectively. Since then, however, they – and especially the Arp2/3 complex – attract extensive attention. As a consequence of their popularity, our knowledge expanded as well as number of arising questions. In agreement with goals of my thesis, I focus on recent discoveries of the Arp2/3 complex-mediated actin assembly, leaving the reader interested in formins with relevant reviews (Deeks et al. 2002, Cvrčková et al. 2004).

2.3.2. The Arp2/3 complex in a plant genome

All seven subunits of the Arp2/3 complex are encoded in the *Arabidopsis thaliana* (*A. thaliana*) genome (Klahre and Chua 1999, Vantard and Blanchoin 2002, Li et al. 2003). In contrast to eight actin genes expressed in *A. thaliana* tissues, only one copy of ARP2, ARP3, ARPC3, ARPC4 and ARPC5, and two copies of ARPC1 and ARPC2 are present (McKinney et al. 2002, Mathur 2005). Moreover, all members of the Scar/WAVE complex have been identified in *A. thaliana* genome (Table 1). These are Scar/WAVE (Brembu et al. 2004, Deeks et al. 2004, Frank et al. 2004**,** Basu et al. 2005), NAPP/NAP1/GNARLED (homolog of Nap1; Brembu et al. 2004, Deeks at al. 2004, El Assal et al. 2004), PIROGI/PIRP (homolog of Pir121; Basu et al. 2004, Brembu et al. 2004), ABI (homolog of Abi1; Deeks et al. 2004) and BRICK1 (homolog of HSP300; Zhang et al. 2005, Djakovic et al. 2006, Le et al. 2006). In *A. thaliana* genome, Scar/WAVE and ABI are present in four copies, but PIPP, NAPP and BRICK1 are single copy genes. Expression of BRICK was firstly reported in maize (Frank and Smith 2002; Frank et al. 2003) which along with one maize Scar (Frank et al. 2003) broadens requirements for the Arp2/3-based processes overall plant kingdom. None of the other known activators of the Arp2/3 complex in animals, such as

Subunit	**Mutation**	**Published in**
ARP2	WURM	Le et al. 2003 Li et al. 2003 Mathur et al. 2003a
ARP3	DISTORTED1	Le et al. 2003 Li et al. 2003 Mathur et al. 2003a
ARPC1	Not characterized	Not characterized
ARPC2	DISTORTED2	Saedler et al. 2004 El Assall et al. 2004
ARPC3	Not characterized	Not characterized
ARPC4	----------	Li et al. 2003
ARPC5	CROOKED	Li et al. 2003 Mathur et al. 2003b
SCAR2	DISTORTED3 ITB1	Basu et al. 2005 Zhang et al. 2005
NAP1	GNARLED	Brembu et al. 2004 El Assal et al. 2004 CB Deeks et al. 2004
PIR121	PIROGI	Basu et al. 2004 Brembu et al. 2004
HSP300	BRICK1	Brembu et al. 2004 Djakovic et al. 2006 Le et al. 2003

Table 1. Characterized mutations in the Arp2/3 complex and Scar/WAVE complex in *A. thaliana*

cortactin, coronin, Abp1p or WASP, was found in *A. thaliana* genome except for two paralogs of the budding yeast Arp2/3 activator Pan1p (Szymanski 2005).

Because the plant Arp2/3 complex has not been isolated and biochemically characterized, it is still unclear whether its composition and function correspond to its animal counterparts. Sequence homologies, the complementation of *A. thaliana* mutants by respective animal homologs (Mathur et al. 2003a), and the rescue of yeast mutants by plant homologs (Le et al. 2003, El Assall et al. 2004) suggest a high degree of functional conservation of the complex in plants.

2.3.3. Lessons from mutants

Most information about the role of the Arp2/3 complex and possible modes of its regulation come from studies of "distorted" group of *A. thaliana* mutants. At least eight genes (ALIEN, CROOKED, DISTORTED1, DISTORTED2, GNARLED, KLUNKER, SPIRRIG and WURM) falls within the "distorted" group of mutations that are characterized by randomly distorted phenotype of trichomes. During the last three years, it became evident that mutant genes are allelic to genes for proteins of the Arp2/3 complex or for subunits of the Scar/WAVE complex. The more information, the more surprise.

As shown above, in non-plant organisms, a loss of the Arp2/3 complex is lethal or results in severe developmental defects. Surprisingly, *A. thaliana* plants harbouring null mutations for the Arp2/3 complex genes (to date characterized mutants in all genes except for ARPC1 and ARPC3; see Table 1) or Scar/WAVE complex genes (except for ABI) have mild phenotype: the plants are vigorous but have a modest reduction in shoot fresh weight, they have a normal seed set and overall plant architecture (reviewed in Szymanski 2005). The distorted phenotype is characterized mainly

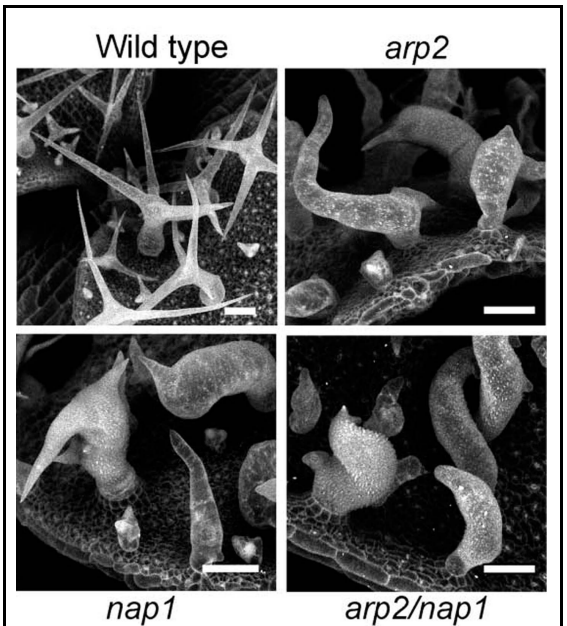

Figure 5. Trichome phenotype of *nap1* and *arp2* mutants. Deeks et al. 2004.

by a deformation of trichomes (Fig. 5) and defects in an expansion of leaf pavement and hypocotyle epidermal cells. Some of these defects can be induced by treatment of wild-type plants with actin-depolymerizing drugs (Mathur et al. 1999, Szymanski et al. 1999, Saedler et al. 2004). However, expectable abnormalities in tip-growing cells, such as pollen tubes and root hairs, that have strict growing requirements for the actin cytoskeleton, were not confirmed and the tip growing cells of these mutants do not have clear phenotypes. Changes in the root hair growth and morphology have been described only by Mathur and colleagues (2003a) in conditions inducing rapid root hair elongation, but no further evidence has been reported. The obvious hypothesis is that Arp2/3 complex is not required for the cell viability and expansion, since alternative signalling pathways may exist to regulate the Arp2/3-driven AFs polymerization in pollen tubes and root hairs. Another possibility is that in pollen tubes or root hairs, knockdown of one of the Arp2/3 complex subunits does not result in knockdown of the whole complex function.

ARPC1 and ARPC3 subunits mutants have not been characterized yet and none of the remaining four distorted mutants map to the same chromosomal location as these genes. The mutations in these genes might result in embryo lethality in plants as well as in animals, as suggested by Deeks and Hussey (2005). Alternatively, specific growth conditions might be required for eliciting a mutant phenotype for these genes (Mathur 2005).

2.3.4. Expression profiles of the Arp2/3 and WAVE complex subunits

Interestingly, the first evidence concerning an involvement of the Arp2/3 complex in a plant development came from the investigation of transcript levels of the ARP2 in various *A. thaliana* tissues (Klahre and Chua 1999). Nothern hybridization revealed that the ARP2 transcript was present in all plant tissues at very low levels and that it was down-regulated by light. GUS-expression studies, however, showed that the ARP2 promoter directs activity predominantly to a very small number of cells: cells immediately adjacent to xylem organs and pollen grains. Consequently, some of the following mutant studies took notice on expression profile of various subunits of both Arp2/3 and Scar/WAVE complexes. Transkript analysis showed that the genes were expressed ubiquitously at low levels in a plant, concentrated into extending parts of the plant such as the inflorescence stem, expanding siliques or rozette leaves and young seedlings (Li et al. 2003, Frank et al. 2004, Basu et al. 2005). Just Li and colleagues (2003) explored the transcript levels of genes in pollen. They discovered very low levels of expression of all Arp2/3 complex subunits except for well-expressed ARPC3. Nevertheless, taking into account that results of different authors slightly varied, it becomes evident that growth conditions and the method used significantly influences obtained results.

2.3.5. Distorted cytoskeleton in mutant cells

All the Arp2/3 complex mutants and the Scar/WAVE complex mutants show defects in actin cytoskeleton organization during later stage of trichome development, as it may be expected that the intact actin cytoskeleton is necessary to maintain polarized growth after branch initiation (Szymanski et al. 1999).

In wild type *A. thaliana* trichomes in later stage of a development, actin filaments are organized into a dense network of fine and bundled, longitudinally extended cables (Kost et al. 1998, Sheahan et al. 2004). Changes in the organization of AFs detected in Scar/WAVE or Arp2/3 mutants differed depending, in part, on the method used for detection of actin cytoskeleton. When observed in living cells using GFP fused to actin binding protein talin, actin filaments were typically organized into thick, cross-linked, short bundles accompanied by an increased number of dense actin patches at the cell cortex (Mathur et al. 2003a, b, Saedler et al. 2004). On the other hand, when the actin cytoskeleton was visualized in living cells with GFP fused to actin binding domain of fimbrin (FABD2), or using antibodies or phalloidin, a disorganization of actin bundles followed by reduction in the levels of AFs was revealed (Le et al. 2003, Basu et al. 2004, Deeks et al. 2004, El Assal et al. 2004, El Assall et al. 2004, Zhang et al. 2005; Fig. 6).

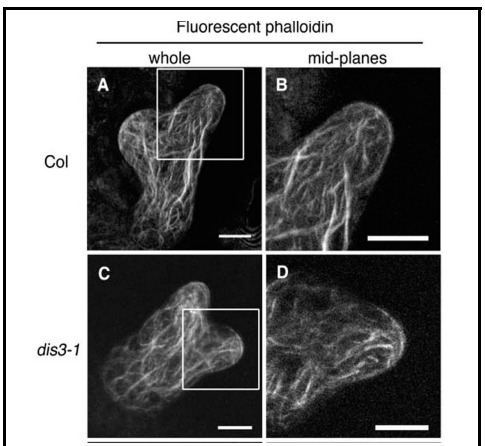

Figure 6. The actin cytoskeleton of wild-type and *dis3-1* trichomes. Basu et al. 2005

Comparing to numerous information about AFs in trichomes, the organization of AFs in mutant epidermal leaf cells was described only by Li and colleagues (2003) using GFP fused to talin. Mutant cells exhibited - similarly to the wild type - extensive F-actin cables, nevertheless they oriented perpendicularly to the cell axis comparing to more randomly oriented AFs in wild type.

Apart from the disarrangement of AFs, defects in microtubule cytoskeleton in mutant trichomes have been severally reported (Saedler et al. 2004, Basu et al. 2005, Zhang et al. 2005). Two populations of MTs in *A. thaliana* trichomes have been described: cortical and endoplasmic

MTs. Endoplasmic MTs were shown to play the main role in reorienting the growth in *A. thaliana* trichomes (Mathur and Chua 2000). Consistently, cortical MTs followed general contours of the distorted cell in mutant trichomes, but endoplasmic MTs showed specific alterations, which referred to close relation of AFs and MTs during trichome development.

In conclusion, the mutants exhibit strong phenotypic similarities suggesting that, in higher plants, the complex functions as a whole, that each subunits plays a role in maintaining its integrity, and that Scar/WAVE complex positively regulates the Arp2/3 complex. The lack of the Arp2/3 complex-derived actin network results in distorted trichomes and several defects in various cell types. However, the phenotype of cells (trichomes still capable of anisotropical growth; lobes of epidermal cells initiated) demonstrates that there is significant remaining control on the direction of inhibited or even misdirected cellular expansion. Inhibited trichome growth and epidermal lobe expansion were hypothesized to be a result of changes in AFs and MTs organization and relating disruption of controlled vesicle targeting (Mathur et al. 1999, Li et al. 2003). A considerably mild phenotype of mutants may suggest that only selected cell types depend fully of the dendritic mode of assembly proposed by the Arp2/3 complex in plants.

2.3.6. Leading edge in plants?

In plant and fungi, tip-growing cells may serve as an interesting parallel to the protrusive membranes of animal motile cells. The tip-growing cells have a particular lifestyle, that is characterized by the following features: (1) their growth is based on the occurrence of elongation exclusively at the apex; (2) tip-growing cells are able to penetrate their growth environment, thus they have to withstand considerable external forces; (3) the growth velocity of tip-growing cells is among the fastest in biological systems (Geitmann and Emons 2000). This rapid growth is underlied by polarized ions gradients and fluxes, turnover of cytoskeletal elements (AFs mainly), and endocytosis and exocytosis of membrane vesicles. This occurs, in addition to root hairs and pollen tubes, in hyphae of fungi and oomycetes, moss chloronemata and caulonemata, fern protonemata or algal and moss rhizoids.

The tip-growing cells typically exhibit a high degree of polarized zonation along the radial and longitudinal axes. Growing pollen tubes are well characterised by a clear zone filled with secretory vesicles at the extreme apex (Hepler et al. 2001). The apex represents growth zone of the tube. The adjacent cytoplasmic zone (subapex) is characterized by a cytoplasm densely packed with organels. The remaining part represents the “basal” part of the tube. AFs have been shown to play a crucial role in tip-growth of pollen tubes and their arrangement was subjected to extensive studies. In the basal region of pollen tubes, AFs form long longitudinally oriented cables present in both

cortical and endoplasmic regions. However, their arrangement in apical and subapical domains is still controversial, reflecting problems with fixing and labeling of extremely fragile AFs in rapidly growing cells (reviewed in Geitmann and Emons 2000, Vidali and Hepler 2001). Some authors observed a clear zone in the apex and short actin bundles and cortical actin ring in the subapical region of tobacco and lily pollen tubes (Kost et al. 1998, Fu et al. 2001, Lovy-Wheeler et al. 2005). Using different method of AF detection, the others found longitudinal F-actin extending to the very tip of the pollen tube (Lovy-Wheeler et al. 2005, Wilsen et al. 2006).

Different mechanisms of an action of AFs in pollen tubes growth have been proposed. One model postulates that AFs complement cell wall as a structure that can oppose turgor pressure (Picton and Steer 1982). Another model proposes that the force of actin polymerization generates a force that causes cell growth similarly to filopodial and lamellipodial extension (Pollard et al. 2000). The second model was further supported by Vidali et al. (2001), who used AFs inhibitors Latrunculin B and Cytochalasin D to observe the effect of AFs depolymerization on a pollen tube growth. They found out that the pollen tube growth was more sensitive to drug treatment than cytoplasmic streaming and that there were no correlations between streaming and growth rates. This result suggests that tip growth requires actin polymerization participating in elongation processes either as a force generator or as an organiser of the apical cytoplasm (Vidali et al. 2001).

Taking into account the above mentioned information, the results obtained by studies of mutant plants of "distorted" group (Chapter 2.3.3.) were rather surprising: sinous root hairs described only by Mathur et al. (2003a) in plants deprived of ARP2 and ARP3 seemed to be the only effect of a loss of function of the Arp2/3 complex. Fertile seeds represented an indirect evidence that the pollen tube growth occurred normally. Therefore, the researches suggested a presence of another actin filament nucleator that would play a central role in the elongation of pollen tubes and in root hairs.

On the other hand, one recent study took advantage of an approach commonly used in animal mutational analyses – knockdown of ARPC1 subunit by RNAi in the moss *Physcomitrella patens* (*P. patens*) (Harries et al. 2005). Their results are of highest importance. The loss-of-function mutants showed dramatic defects in cell morphology manifested as short, irregularly shaped cells with abnormal division patterns. The moss also lacked rapidly tip-elongating caulonemal cell types found in wild type protonemal tissue, which resulted in lacking of gametophores (protonemal tissue is composed of two distinct cell types: chloronema and caulonema; caulonemal cells can produce a meristematic bud that will grow into a leafy gametophore). ARPC1 mutants showed increased sensitivity to osmotic shock and their ability to establish the polarized outgrowth was inhibited. Latrunculin B treatment mimicked phenotype of the mutants, which implicates an importance of the

AFs polymerization in a development of moss. In conclusion, results showed the importance of Arp2/3 complex for controlling of polarized growth and cell division in the moss.

Accompanied by the immunolocalization experiments of Van Gestel et al (2003), who detected ARP3 subunit of the complex in the tips of extending root hairs, the study of Harries and colleagues (2005) shed different light on the role of Arp2/3-mediated processes in plant cells and highlighted the necessity of generating diverse approaches to study biological events such as AFs assembly.

2.3.7. Conclusions

A current evidence available, mostly based on the analysis of mutants, force us to conclude that (1) the Arp2/3 complex seems to be dispensable for most processes of plant cell growth and differentiation, (2) its role somehow relates to the AFs organization. However, the story of hunting the role of the plant Arp2/3 complex emphasizes the importance of a wide spectra of methods, models and investigative approaches used to achieve better understanding of such a complex event. The exact function of the Arp2/3 complex in plants and, simultaneously, the function of the dynamic actin network or even the force generated by the Arp2/3-based actin polymerization in various types of plant cells still remains to be uncovered. With the exception of a study of Van Gestel et al. (2003), where various heterologous antibodies against animal and fungal ARPs were used to study the potential co-localization with AFs, the localization of the Arp2/3 complex proteins have not been studied in plants. Moreover, no direct links between ARPs and the mechanism of the AF nucleation have been reported.

2.4. Low temperature as a tool to study the cytoskeleton

To study the processes of cytoskeleton dynamics in plant cells, various stress factors can be used to induce its destruction and subsequent recovery. Among others, low temperature is known to depolymerize cytoskeletal polymers. The reversibility of this process can be taken as advantage for studying a mode of the organization of the cytoskeletal structures. The described approach was effectively used in the study of Hasezawa et al. (1997) to follow the early phases of the initiation of MTs in tobacco BY-2 cells during cell cycle progression. Experiments revealed that the sites of MTs organization are localized in perinuclear and cortical region and that combination of drug and cold treatment does not affect their distribution and function. Except from report of Hasezawa and colleagues (1997), several older studies followed the re-organization of MTs in algae after the

destruction by various treatments (Hogetsu 1986, Wasteneys and Williamson 1989). Besides, the structure of MT arrays in cells subjected to cold treatment has been studied thoroughly (Akashi et al. 1990, Mizuno 1992) and cold-induced depolymerization of MTs has been documented to vary in a wide range of plant species (for review see Nick 2000).

On the contrary, much less information is available concerning low temperature-induced changes in the actin cytoskeleton. The role of AFs was studied in relation to cold-induced cessation of cytoplasmic streaming (Quader et al. 1989) and changes in membrane fluidity (Örvar et al. 2000), but information about the effects of cold on the organization of AFs and the sites of their initiation is sparse. In my thesis, I was inspired by the described approach of reversible destruction of cytoskeletal polymers, and during subsequent recovery, I followed the processes of re-polymerization of actin filaments in tobacco BY-2 cells.

3. AIMS

The aim of my study was to investigate nucleation mechanisms of actin cytoskeleton in tobacco BY-2 cells with the respect to the role of the Arp2/3 complex, and to find out the discussed role of the complex in tip-growing pollen tubes. Partial goals reflect consecutive steps necessary to gain the desired result.

1) To describe the dynamic processes of cold-induced AFs depolymerization and their subsequent recovery in tobacco BY-2 cells

2) To characterize the localization of proteins of the Arp2/3 complex in tobacco BY-2 cells using immunostaining

- To produce tobacco specific antibodies against selected proteins of the Arp2/3 complex
- To detect these proteins in tobacco BY-2 cells
- To describe the localization of these proteins in cells recovering from cold-induced AFs depolymerization

3) To characterize the localization of proteins of the Arp2/3 complex in living tobacco BY-2 cells

- To isolate the genes encoding for selected proteins of the tobacco Arp2/3 complex and to fuse them with GFP
- To produce and characterize stably transformed tobacco BY-2 cells
- To produce and observe transiently transformed tobacco leaf epidermal cells

4) To characterize the role of the Arp2/3 complex in growing tobacco pollen tubes

4. MATERIALS & METHODS

4.1. Plant material

4.1.1. Tobacco cell line BY-2

The tobacco cell line BY-2 (*Nicotiana tabacum* L. cv. Bright Yellow; Nagata et al. 1992) was cultured in a liquid medium containing MS salts, 1 mg/l thiamine, 200 mg/l KH_2PO_4, 100 mg/l inositol, 30 g/l sucrose and 0.2 mg/l 2,4-dichlorophenoxyacetic acid (2,4-D), pH 5.8 (all chemicals obtained from Sigma-Aldrich, St. Louis, USA). Every seven days, 1.5 ml of cells were transferred to 30 ml of fresh medium and cultured in darkness at 25 ° C on a horizontal shaker (IKA KS501, IKA Labortechnik, Germany; 120 rpm, orbital diameter 30 mm).

4.1.2. Tobacco cultivation in soil

Tobacco plants (*Nicotiana benthamiana*) were cultivated in common garden soil at 16 h day, 8 h night, 22 ° C. After 3-4 weeks, the seedlings were placed into their own pots and grown for 2-3 weeks until infiltration.

4.1.3. Tobacco pollen tubes cultivation

Tobacco pollen (*Nicotiana tabacum* cv. Samsun) was kind gift of Doc. Fatima Cvrčková, Dr. rer. Nat. Frozen (-20 ° C) pollen was kept for 15 min at 25 ° C to recover, then re-suspended in simple germination medium (10% [w/v] sucrose [P-Lab], 1.6 mM H_3BO_3 [P-Lab]) and incubated on a rotary shaker (100 rpm) at 25 ° C. After 60-90 min, pollen tubes were collected for staining procedures.

4.2. Cellular biology

4.2.1. Assessment of cellular viability

Cellular viability was assessed with fluorescein diacetate (FDA) according to the method of Widholm (1972). 40 ml of 0.2% (w/v) FDA stock solution in acetone were diluted in 7 ml of culture medium, and an aliquot mixed 1:1 (w/v) with cell suspension on a microscopic slide. After 1 minute incubation with FDA, the viability was determined from at least ten optical fields on each of five separate slides as a percentage of fluorescing cells (a total of around 400 cells were counted in each sample). I control cells, the viability reached almost 100 % during the whole 7-day growth cycle. Prior to the measurement of viability of cold-treated cells, aliquots of cell culture were taken, filtered, re-suspended in the same volume of cultivation medium at 25 ° C, and cultivated on a

horizontal shaker (IKA KS501, IKA Labortechnik, Germany) at 120 rpm and 25 ° C for 2 hours.

4.2.2. Cold and drug treatment and recovery experiments

Tobacco BY-2 cells from cultures in the exponential (3-day-old) and stationary (7-day-old) phase of growth were used. Cultivation conditions and cold treatment were carefully optimized to exclude any additional stresses. Cell suspensions in Erlenmayer flasks were placed into an ice water bath (0 ° C) and shaken on a horizontal shaker at 100 rpm (IKA KS501) in darkness. After required period (5 minutes - 12 hours), flasks were taken out from the ice water bath and the cells were immediately collected by filtering on a nylon mesh (pore diameter 20 μm). They were then re-suspended in medium at the control temperature (25 ° C) and further cultivated at this temperature.

For treatments with latrunculin B (LatB, Sigma-Aldrich), appropriate volumes of a 2.5 mM stock solution of LatB in dimethyl sulfoxide (DMSO, Sigma-Aldrich) were added to the cell suspension to give final concentrations of 100 or 500 nM LatB (final concentration of DMSO less than 0.015 %). To depolymerize AFs for subsequent recovery experiments, 500 nM LatB was applied for 12 hours. Subsequently, the cells were collected by filtering on a nylon mesh (pore diameter 20 μM), washed at least three times in fresh MS medium to remove LatB and re-suspended in fresh medium. They were then further cultivated for the desired period (5–60 minutes). Samples of cell culture were collected for cytological observations during cold and LatB treatment, and subsequent recovery.

4.2.3. Staining of BY-2 cells

Immunostaining of AFs and actin-related proteins

AFs and ARPs were visualized by the modified method of Collings et al. (1998). Briefly, 3-day-old cell culture was pre-fixed in actin-stabilizing buffer (ASB, 100 mM PIPES [Piperazine-1,4-bis (2-ethanesulfonic acid, Sigma-Aldrich], 5 mM EGTA (ethylenebis(oxyethylenenitrilo) tetraacetic acid [Sigma-Aldrich], 10 mM $MgSO_4$, [P-Lab, Prague, Czech Republic], pH 6.4, 25 ° C) supplemented with 200 μM MBS (N-succinimidyl 3-maleimidobenzoate, Fluka, Buchs, Switzerland) for 20 min. Cold-treated cells were pre-fixed in the solution chilled to 0 ° C. The cells were subsequently fixed in 2% (w/v) paraformaldehyde (PFA, Serva Electrophoresis GmbH, Heidelberg, Germany) and 1% (w/v) glutaraldehyde (Fluka) in ASB supplemented with 0.05% Triton X-100 (Sigma-Aldrich) and 200 mM phenylmethylsulfonyldisluoride (PMSF; Sigma-Aldrich) for 20 min. The cells were then washed in ASB twice for 10 min, digested with 0.05% (w/v) pectolyase Y-23 (Kyowa Chemical Products Co. LTD, Tokyo, Japan) in ASB for 20 min and rinsed again with ASB (twice for 10 min). After a wash in 1% (w/v) bovine serum albumin (Fluka) in phosphate buffered saline (PBS, 0.15 M NaCl, 2.7 mM KCl, 1.2 mM KH_2PO_4, 6.5 mM Na_2HPO_4,

all components obtained from P-Lab) for 30 min, the cells were transfered into 1.5 ml microcentrifuge tubes and incubated with primary antibodies (for antibodies and concentrations used see Table 2) for 2 hours. After washes with PBS (3 x 10 min), secondary antibodies were applied for 2 hours at 25 ° C. If AFs were stained with conjugated phalloidin, stock solution of rhodamine-phalloidin (Sigma) was diluted with PBS to get final concentration of 0.66 μM. 200 μL of diluted phalloidin solution were added to 200 μL of specimens for 35 min. Specimens were washed in PBS supplemented with Hoechst 33258 (bisbenzimide, 2-(4-ethoxyphenyl)-5-(4-methyl-1-piperazinyl)-2,5′-bi-1H-benzimidazole, 0.1 mg/ml, Sigma-Aldrich) to stain nuclei, embedded in Vectashield® Mounting Medium (Vector Laboratories, Inc., Burlingame, CA) and observed immediately.

Primary Antibodies	Final Dilution
Mouse monoclonal anti-actin 69100 clone C4 antibody (ICN Biomedicals Inc.)	1:400 Immunostaining 1:4000 Western Blotting
Rabbit polyclonal serum against fission yeast ARP2 (anti-SpARP2; Morrell et al. 1999) or ARP3 (anti-SpARP3; McCollum et al. 1996)	1:1000 Immmunostaining 1:2000 Western Blotting
Mouse polyclonal serum against tobacco ARP3 (anti-NtARP3)	1:1000 Immunostaining 1:5000 Western Blotting
Rabbit polyclonal serum anti-Green Fluorescent Protein (anti-GFP; Molecular Probes)	1:5000 Immunostaining 1:1000 Western Blotting
Secondary Antibodies for Immunostaining	
Fluorescein isothiocyanate (FITC)-conjugated anti-mouse antibody (Sigma-Aldrich)	1:50
Tetramethylrhodamine isothiocyanate (TRITC)-conjugated anti-rabbit antibody (Sigma-Aldrich)	1:100
Fluorescein isothiocyanate (FITC)-conjugated anti-rabbit antibody (Sigma-Aldrich)	1:100
Tetramethylrhodamine isothiocyanate (TRITC)-conjugated anti-mouse antibody (Sigma-Aldrich)	1:200
Secondary Antibodies for Western Blotting	
Peroxidase-conjugated antibody to mouse (ICN Biomedicals Inc.)	1:1000
Peroxidase-conjugated antibody to rabbit (Sevapharma, Prague, Czech Rep.)	1:1000

Table 2. List of primary and secondary antibodies used for immunostaining and western blotting

Rhodamine-phalloidin staining of AFs

AFs were visualized by the method of Kakimoto and Shibaoka (1987) modified according to Olyslaegers & Verbelen (1998). A 1 ml of 3-day-old cell culture was fixed for 10 minutes in 1.8% (w/v) paraformaldehyde (PFA) in ASB buffer (100 mM PIPES [Sigma-Aldrich]), pH 6.4, 10 mM

$MgCl_2$ [P-Lab], 5 mM EGTA [Sigma-Aldrich]). Cold-treated cells were pre-fixed for 5 minutes in fixation solution chilled to 0 ° C. After a subsequent 10 minutes of fixation in ASB buffer containing 1% (w/v) glycerol, cells were rinsed twice for 10 minutes with ASB buffer. Then, cells were incubated for 35 minutes with TRITC – phalloidin (final concentration of TRITC-phalloidin 0.33 μM). Cells were then washed three times for 10 minutes in PBS and observed immediately in the microscope.

4.2.4. Staining of pollen tubes

To stain actin and ARPs in tobacco pollen tubes, the method described above (Chapter 4.2.3.) was slightly modified: enzyme mixture was composed of 0.1% (w/v) pectolyase Y-23 (Kyowa Chemical Products Co. LTD), 0.5% (w/v) macerozyme (Serva), 0.5% (w/v) cellulase (Serva) and 0.1% (w/v) Triton X-100 (Sigma-Aldrich).

4.2.5. Production and staining of plasma membrane "ghosts"

To prepare plasma membrane ghosts (separated membranes of BY-2 cells attached to poly-L-lysin coated coverslips), the modified method according to Collings et al. (1998) was used as follows. Whole cells were used 2-3 days after subculturing. The cell walls were digested in a MS medium containing 1% (w/v) cellulase (Serva), 1% (w/v) pectolyase Y-23 (Kyowa Chemical Products Co. LTD) and 0.45 M mannitol (Sigma-Aldrich). Cells were shaken on horiozntal shaker (IKA KS501, IKA Labortechnik; 100 rpm, orbital diameter 30 mm) for 3-5 hours. The resulting protoplasts were pelleted, washed twice in wash buffer (10 mM PIPES [Sigma-Aldrich], pH 6.8, 100 mM KCl [P-Lab], 285 mM mannitol [Sigma-Aldrich]) and re-suspended in wash buffer. Protoplasts were attached to poly-L-lysine coated coverslips (poly-L-lysine obtained from Sigma-Aldrich). Wash buffer was removed and the buffer for protoplast lysis was applied (7 mM PIPES [Sigma-Aldrich], 2 mM EGTA [Sigma-Aldrich], 10 mM $MgCl_2$ [P-Lab], buffered to pH 6.9 with KOH [P-Lab], 1% (w/v) DMSO [Serva], 6 mM dithiothreitol [DTT, ICN Biomedicals Inc.], 300 μM PMSF [Sigma-Aldrich]). Protoplasts were lysed by a "quick flick" of the glass slide. The resulting membrane ghosts were then fixed for 25 minutes in 1.8% (w/v) PFA in ASB buffer (Chapter 4.2.3.). When fixed, AFs and ARPs were stained as described in Chapter 4.2.3.

4.2.6. Quantification of cold-induced changes in the arrangement of AFs

The percentages of cells with distinct cytoskeleton arrangements were determined from at least ten optical fields on each from at least three separate slides (a total of around 300 cells were

counted in each sample) in one representative experiment. For a quantification of structural changes in AFs during control temperature, the following categories were defined: 1) cells with transversely oriented AFs (in further text referred to as transversal AFs); 2) cells without unified orientation of AFs (no uniform orientation); 3) damaged cells. For a quantification of structural changes in AFs during cold treatment, the following categories were defined: 1) cells retaining intact cytoskeletal filaments or their fragments (polymers or fragments); 2) cells with totally depolymerized cytoskeleton (no polymers); 3) cells with cold-induced actin structures (transient actin structures; this category comprised actin dots, rods and dotted filaments); 4) damaged cells. The category of "damaged cells" included cells with disrupted cytoplasm, broken cell walls, or cells with plasma membrane detached from the cell wall. The phase of cells within the cell cycle was determined microscopically after staining the nuclei with Hoechst 33258. Only interphase cells were used for quantification experiments.

4.2.7. Microscopy and image analysis

Samples were observed with an epifluorescence microscope (Olympus Provis AX 70, Olympus Optical Co., Ltd., Japan) equipped with standard filter sets for FITC, TRITC and Hoechst 33258 fluorescence detection, and Nomarski differential interference contrast (DIC). Fluorescence images were grabbed with a monochromatic integrating CCD camera (COHU 4910, Cohu, Inc., USA) and digitally stored with LUCIA image analysis software (Laboratory Imaging, Prague, Czech Republic).

Confocal microscopy was performed using either Leica TCS SP2 AOBS confocal laser scanning microscope (Leica TCS NT, Heidelberg, Germany) or Zeiss Axiovert 200M microscope (Carl Zeis MicroImaging GmBH, Gottingen, Germany) fitted with a Zeiss LSM 510 laser scanning system. Both microscopes were equipped with an ArKr laser using filter sets for FITC and GFP (excitation at 488 nm, emission at 500–530 nm) and HeNe laser using filter sets for TRITC (excitation at 543 nm, emission at 545–590 nm). An objective lens Plan Apo (magnification 63´, numerical aperture 1.2) was used for all observations.

4.3. Molecular biology

4.3.1. *E. coli* and A. *tumefaciens* strains

Escherichia coli strains

XL-1 blue and DH5α recombination deficient *Escherichia coli* (*E. coli*) strains for common

plasmid cloning were used (Sambrook and Russell 2001). BL21(DE3), BL21(DE3)pLysS and BL21(DE3)Rosetta™ (Novagen, Madison, WI) strains were adopted for expression of recombinant proteins.

Agrobacterium tumefaciens strains

For stable transformation of BY-2 cells, C58C1 strain of *Agrobacterium tumefaciens* (*A. tumefaciens*) carrying pGV2206 plasmid was used (Deblaere et al. 1985). For transient transformation of tobacco epidermal leaf cells, GV3101 strain of *A. tumefaciens* was used, carrying pMP90 (pTiC58DR-DNA) plasmid (Koncz and Schell 1986).

4.3.2. Production of competent cells

Electrocompetent *E. coli* and *A. tumefaciens*

To obtain electrocompetent *E. coli* and *A. tumefaciens* cells (strain C85C1), methods according to Dower at al. (1988) and McCormac et al. (1998) were used, respectively.

Single bacterial colony from fresh agar plate was inoculated into a flask containing 20 ml of LB media (for *E. coli*) or 20 ml of YEB media (for *A. tumefaciens*), for media composition see Table 3, and incubated overnight at 37 ° C (*E. coli*) or 28 ° C (*A. tumefaciens*) with vigorous shaking (180 rpm in rotary shaker).

LB	1% (w/v) peptone (tryptone) (Serva), 0.5% (w/v) yeast extract (Serva), 1% (w/v) NaCl (P-Lab)
YEB	1% (w/v) pepton (tryptone), 0.1% (w/v) yeast extract, 0.5% (w/v) sucrose (P-Lab), 0.05% $MgSO_4$ (P-Lab)
YEB recovery	1% (w/v) pepton (trypton), 0.1% (w/v) yeast extract, 200 mM sucrose, 100 mM NaCl (P-Lab), 25 mM KCl (P-Lab), 100 mM $MgCl_2$ (P-Lab), 100 mM $MgSO_4$ (P-Lab)
SOB	2% (w/v) peptone (tryptone), 0.5% (w/v) yeast extract, 10 mM NaCl, 2.5 mM KCl, 10 mM $MgCl_2$, 10 mM $MgSO_4$, pH 6.7-7.0
TB	10 mM PIPES (Sigma-Aldrich), 55 mM $MnCl_2$ (Sigma-Aldrich), 15 mM $CaCl_2$ (Merk, Darmstadt, Germany), 250 mM KCl (P-Lab), pH 6.7
SOC	2% (w/v) pepton (trypton), 0.5 % (w/v) yeast extract, 20 mM glucose (P-Lab), 10 mM NaCl, 2.5 mM KCl, 10 mM $MgCl_2$, 10 mM $MgSO_4$

Table 3. Composition of media used for transformation of bacterial cells

Two 250 ml aliquots of LB/YEB medium were inoculated with 6 ml of overnight bacterial culture and incubated at 37 ° C with agitation 190 rpm in rotaty shaker till OD_{600} reached 0.5-0.6. Culture was chilled in ice-water bath for 15-30 min, centrifuged (15 min, 4000 g, 4 ° C) and re-

suspended subsequently in 500 ml of ice-cold pure dH_2O, 250 and 10 ml of ice-cold 10% (w/v) glycerol. Finally, pellet was re-suspended in 0.5 - 1 ml of ice-cold GYT medium (10% [w/v] glycerol [Serva], 0.125% [w/v] yeast extract [Serva], 0.25% [w/v] tryptone [Serva]), frozen in liquid nitrogen (40 µL and 100 µL aliquots for *E. coli* and *A. tumefaciens*, respectively) and stored at -70 ° C.

Chemically-competent *A. tumefaciens*

1 ml of overnight culture of *A. tumefaciens* strain GV3101 in YEB medium was used to inoculate 50 ml of YEB. Suspension was shaken vigorously at 30 ° C till OD_{600} reached 0.5-0.6. Cells were pelleted (5 min, 3000 g, 4 ° C), re-suspended in 50 ml ice-cold 0.15 M NaCl (P-Lab), kept on ice for 15 min, pelleted and re-suspended in 250 µL of ice-cold 20 mM $CaCl_2$ (Merk), 50 µL aliquots were frozen in liquid nitrogen and stored at -70 ° C.

4.3.3. Transformation of *E. coli* and *A. tumefaciens*

Electroporation

Electrocompetent cells together with DNA to be electroporated were thawed on ice. 1-3 µL of the DNA (10 pg – 50 ng) was added and incubated on ice for 1 min. Mixture was pipetted into ice-cold electroporation cuvette (d=2 mm) and puls of electricity was delivered (Bio-Rad Gene Pulser Apparatus) to the cells at following settings of 25 µF capacitance, 200 ohm resistance and 2.5 kV or 2.0 kV for *E. coli* or *A. tumefacien*s, respectively. Time constant ranged between 4-5 milliseconds. 1 ml of SOC medium (*E.coli*, Table 3) or YEB recovery medium (*A. tumefaciens*m, Table 3) was added quickly at 25 ° C. Cells were transferred into tubes and incubated with gentle rotation (150 rpm) for 1 hour at 37 ° C (*E. coli*) or 3 hours at 30 ° C (*A. tumefaciens*). Suspension was plated onto LB medium with appropriate antibiotics and grown at 37 ° C overnight or 28 ° C for 3 days for *E. coli* or *A. tumefaciens*, respectively.

Transformation of chemically-competent *A. tumefaciens*

A. tumefaciens (GV3101) competent cells and DNA to be electroporated were thawed on ice. 1-3 µL of the DNA (10 pg – 50 ng) were added, quickly frozen in liquid nitrogen and heated at 37 ° C for 5 min. 1 ml of YEB recovery medium was added quickly at 25 ° C. Cells were transferred into tubes and incubated with gentle rotation (150 rpm) for 3 hours at 30 ° C. Suspension was plated onto LB medium with appropriate antibiotics and grown at 28 ° C for 3 days.

4.3.4. Cloning of *NtARP2* and *NtARP3*

BLAST toolkit at the National Centre for Biotechnology Information (http://www.ncbi.nlm.nih.gov/BLAST) was used to search for sequences of various plant *ARP2* and *ARP3* to design specific primers for amplification of tobacco genes encoding for ARP2 (NtARP2) and ARP3 (NtARP3) subunits of Arp2/3 complex (for sequences used to design primers and sequences of both *NtARP2* and *NtARP3* see Supplemental data, for primer sequences see Table 4). Tobacco cDNA (prepared from exponential BY-2 cells by Zdeněk Pilát, Diploma thesis 2005) was

Primer	**Sequence**	**Reaction**
ARP2Forward	5` ATG GAC AGT AGA AAT GTC ATC GTT 3`	PCR1
ARP2Reverse	5` TCA TGC CTG ACC ACA CTT GCT 3`	PCR1
ARP3Forward	5` ATG GAC CCT TCT ACC TCT CG 3`	PCR1, PCR2
ARP3Reverse	5` TCA ATA CAT TCC CTT GAA TAC AGG 3`	PCR1
ARP3GFPReverse	5`GC TGA ATA CAT TCC CTT GAA TAC AGG 3`	PCR2

Table 4. Primer sequences used for cloning of *NtARP2* and *NtARP3*

used as a template for amplification of entire genes *NtARP2* and *NtARP3* by PCR (PCR conditions see Table 5, reaction PCR1; all reaction components obtained from Fermentas International Inc., Burlington, Canada). PCR reactions were mixed as shows Table 6. After blunting with T4 Dna Polymerase (Fermentas International Inc.), the genes were cloned into EcoRV restriction site of pBluescript II KS (+) (Fermentas International Inc.) (allowing blue/white selection) and transformed into *E. coli* cells. Plasmid DNA was isolated from positive colonies using

PCR1 – temperature program			**PCR2** – temperature program		
Initial denaturation	94°C	5 min	Initial denaturation	94°C	5 min
Denaturation	94°C	30 sec	Denaturation	94°C	30 sec
Annealing	58°C	45 sec	Annealing	64°C	45 sec
Elongation	72°C	1 min 30 sec	Elongation	72°C	1 min 30 sec
Number of cycles	35		Number of cycles	25	

Table 5. Conditions of PCR used to amplify genes for *NtARP2* and *NtARP3*

PCR buffer	10x concentrated
MgCl2	25 mM
dNTP	10 mM
Taq polymerase	1 U/1 μL
Primers	10 μM
template	2 μL of cDNA 10-20 ng (plasmid DNA)
dH_2O	up to final volume

Table 6. Composition of PCR reaction

Wizard®Plus SV Minipreps DNA purification kit (Promega, Madison, USA) according to manufacturer protocol. Sequences were verified by sequencing.

4.3.5. Fusion of genes coding for *NtARP3* and *GFP*

Entire sequence of *NtARP3* was re-amplified using pBluescript containing *NtARP3* as a template (PCR conditions see Table 5, reaction PCR2). Gene was subsequently cloned into blunted BamHI site of psmGFP vector (kindly provided by Prof. SJ Davies; Davis and Vierstra 1998). Reverse primer (Table 4) was designed so that stop codon was removed and a reading frame was preserved between *NtARP3* and *GFP* genes. C-terminal fusion of *NtARP3* and *GFP* was verified by sequencing.

Fusion gene *NtARP3::GFP* was re-cloned into HindIII/SstI restriction sites of the binary vector pCP60 (kindly provided by Prof. Ratet). Transformation of *E. coli* and selection of positive clones took place as described above (Chapter 4.3.3). Cloning vectors are summarized in Table 7.

Vector	**Resistence**	**Genes cloned**	**Restriction sites used**	**Used for**
pBluescript	ampicillin	ARP2, ARP3	EcoRV	Primary cloning vector
psmGFP	ampicillin	ARP3	blunted BamHI	C-terminal GFP fusion
pCP60	kanamycin	ARP3::GFP	HindIII/SstI	Transformation of plant cells
pET28a	kanamycin	ARP2, ARP3	HindIII/BamHI	Protein expression
pET32b	ampicillin	ARPC5	NotI/SalI	Protein expression
pET42a	kanamycin	ARP2, ARP3	HindIII/BamHI	Protein expression

Table 7. Vectors used for cloning and expression of *NtARP2* and *NtARP3*

4.3.6. Expression of recombinant NtARP2 and NtARP3

Full-lengths genes were re-cloned from pBlueescript into HindIII/BamHI – digested pET28a and pET42a vectors (Novagen). The sequence of each clone was verified by sequencing. The expression vectors were transformed into *E. coli* [BL21(DE3), BL21(DE3)Rosetta, or BL21(DE3)pLysS, see Table 8] and expressed as follows: 5 large colonies were inoculated into 15 ml of LB with appropriate selection [kanamycin for BL21(DE3), kanamycin and chloramphenicol for BL21(DE3) Rosetta and BL21(DE3)pLysS] and grown overnight at 37 ° C with agitation.

Gene in Vector	**Expressed in**
ARP2 in pET28a	BL21(DE3), BL21(DE3) Rosetta, BL21(DE3)pLysS
ARP3 in pET28a	BL21(DE3), BL21(DE3) Rosetta, BL21(DE3)pLysS
ARP2 in pET42a	BL21(DE3), BL21(DE3) Rosetta
ARP3 in pET42a	BL21(DE3), BL21(DE3) Rosetta
ARPC5 in pET32b	BL21(DE3) Rosetta

Table 8. Bacterial strains used for expression of recombinant proteins

Overnight culture was used to inoculate 2 L of LB with selection and incubated at 30 ° C (temperature conditions of 4 ° C and 14 ° C also tested) with shaking. When OD_{600} reached 0.45, expression of heterologous genes was induced by the addition of isopropylthio-β-galactoside (IPTG) to a final concentration of 1 mM. At the same time, 50 µg/mL of kanamycin and 15 µg/ml of chloramphenicol were added. The culture was then incubated at the optimal temperature with shaking at 200 rpm for 3 hours. The bacteria were pelleted (4000 g, 10 min, 25 ° C), re-suspended in 10 ml of protein extraction buffer (50 mM HEPES {N-[2-Hydroxyethyl]piperazine-N'-[2-ethansulfonic acid, Sigma-Aldrich}, pH 7.5, 300 mM NaCl [P-Lab], 5 mM β-mercaptoethanol [Serva], 8M Urea [Serva]) and sonicated (Soniprep 150; Sanyo, Herts, UK; 10 pulses at amplitude of 26 µm, the length of each pulse was 1s/mL of extraction buffer). The bacterial lysates were centrifuged at 30 000 g for 30 min, filtred through 20-µm nitrocellulose membranes, and applied to the columns containing 1-2 mL of Ni-NTA agarose resin (Quiagen, Crawley, UK). The columns were washed three times with protein extraction buffer containing (1) 20 mM imidazole (Sigma-Aldrich), 6 mM Urea (Serva), (2) 40 mM imidazole, 4M Urea and (3) 60 mM imidazole, 3 M Urea. The specifically bound proteins were eluted with 250 mM imidazole in elution buffer (50 mM HEPES [Sigma-Aldrich], pH 7.0, 300 mM NaCl [P-Lab], 2M Urea [Serva]). Proteins were concentrated in Vivaspin concentration tubes (Sartorius AG, Goettingen, Germany). For antibody production, proteins were dialysed overnight in dialysis buffers of various composition (dialysis buffer composition see Table 9). However, the effort to re-nature proteins did not meet success and so denatured protein must have been used to immunize mice. Because ARP2 was not expressed well at any conditions tested, recombinant ARP3 (expressed in pET28a in BL21(DE3)Rosetta) was used in following experiments.

Basic dialyzis buffer	Other additives tested
100 mM PIPES (Sigma Aldrich), pH 6.8 20%(w/v) glycerol (Serva) 5 mM β-merkaptoethanol (Serva) 2mM $MgSO_4$ (P-Lab) 5 mM EDTA (Sigma-Aldrich)	0.1 M or 0.5 M NaCl (P-Lab) 0.2% (w/v) Triton X-100 (Serva) 5% (w/v) NDSB* 195, 201, 211, 256 (ICN Biomedicals Inc.)

*NDSB 's are a group of zwitterionic compounds that can reduce aggregation and aid in refolding proteins found in inclusion bodies and bacterial expression systems [Vuillard et al. (1995)]

Table 9. Components of dialysis buffers tested to re-nature proteins

4.3.7. Production of anti-NtARP3 polyclonal antibody

For raising NtARP3 antiserum in mice, denatured ARP3 was used for every mouse and boost in concentration of 100 µg in total volume of 30 µL of dialysis buffer (100 mM PIPES [Sigma-Aldrich], pH 6.8, 20% (w/v) glycerol [Serva], 5 mM β-mercaptoethanol [Serva], 2 mM $MgCl_2$ [P-

Lab], 5 mM EDTA [Sigma-Aldrich], 2 M Urea [Serva]). Three mice were immunized with 4 boosts (immunization 1st, 3rd, 5th and 10th week) and bleeded 10 days after the last boost. The serums were spinned (20 min, 13 000 g, 4 ° C) and supernatants were taken for further tests.

4.3.8. Production of anti-NtARPC5 polyclonal antibody

Entire sequence of NtARPC5 subunits of the Arp2/3 complex was cloned into NotI/SalI – digested pET32b (prepared by Zdeněk Pilát, Diploma thesis 2005) and expressed in *E. coli* [BL21(DE3)Rosetta] as described in Chapter 4.3.6. For rabbit immunization, re-natured recombinant ARPC5 was used in concentration of 35 µg per mouse in a total volume of 150 µL of dialysis buffer (100 mM PIPES [Sigma-Aldrich], pH 6.8, 20% [w/v]) glycerol [Serva], 5 mM β-mercaptoethanol [Serva], 2 mM $MgCl_2$ [P-Lab], 5 mM EDTA [Sigma-Aldrich]). One rabbit was immunized with 4 boosts (immunization 1st, 3rd, 5th and 7th week). The rabbit was bleeded 10 days after last immunization.

4.3.9. Transient transformation *of Nicotiana benthamiana* by leaf infiltration

To infiltrate *Nicotiana bentamina* epidermal leaf cells for transient expression of ARP3::GFP, the methods according to Voinnet et al. (2003) and Romeis et al. (2001) were adapted. Single colonies of *A. tumefaciens* (GV3101 strain) containing a (1) vector, and (2) silencing suppressor p19, were used to inoculate 5 ml of YEB media with appropriate antibiotics and grown at 30 ° C with aeration until OD_{600} reached 0.5-1. Cells were pelleted (2000 g, 5 min, 4 ° C), washed twice with 1 ml of infiltration medium (10 mM 2-morpholinoethanesulfonic acid [MES, Sigma-Aldrich], pH 6.5, 10 mM $MgCl_2$ [P-Lab], 200 µM acetosyringone [Sigma-Aldrich]) and incubated at 25 ° C for 2-5 hours. Both bacterial suspensions were mixed together (final volume 2 ml) and infiltrated into abaxial epidermis using plastic syringe. Plants were cultivated for 2 - 4 days at 20-22 ° C to optimize infection. Square of leave was cut, mounted in dH_2O and observed with laser scanning confocal microscope.

4.3.10. Stable transformation of tobacco cell line BY-2

The basic transformation protocol of An (1985) was used. For stable transformation of the tobacco cell line BY-2, 4 ml of cell suspension in exponential phase of growth were co-cultivated with 150 µL of freshly grown *A. tumefaciens* suspension (clone C58C1 transformed with a binary vector to be introduced) in darkness on solid MS without selection. 1 µL of 20 mM stock of acetosyringone (Sigma-Aldrich) was added per 1 ml of cell suspension. *A. tumefaciens* was washed out after 3 days of cultivation. Cells were re-suspended in 5 ml of fresh MS medium, poured on solid MS containing appropriate selection and incubated at 25 ° C in darkness. After 3-5 weeks,

positive cali selection was performed according to fluorescence intensity of individual cali.

4.4. Biochemistry

4.4.1. Protein extractions from plant cells

Extraction procedure I – Total protein fraction

Tobacco BY-2 cells were harvested by filtration on nylon mesh. 1 g of cells or whole leaves of *Nicotiana benthamiana* were homogenized immediately in liquid nitrogen with a pestle and mortar. The frozen powder was mixed 1:1 with twice-concentrated denaturing buffer (50 mM Tris-HCl [Serva], pH 6.9, 2% [w/v] sodium dodecyl sulfate [SDS, ICN Biomedicals Inc.], 30% [w/v] glycerol [Serva], 5% [w/v] β-mercaptoethanol [Serva], 0.5% [w/v] bromophenol blue [Sigma-Aldrich]). Maximal amount of proteins was loaded on SDS-PAGE.

Extraction procedure II – Soluble and membrane protein fractions

Cells were harvested by filtration on a nylon mesh and 1 g of biomass was homogenized immediately in liquid nitrogen with a pestle and mortar. The frozen powder was mixed 1:1 with twice-concentrated extraction buffer (25 mM MES [Sigma-Aldrich], 5 mM EGTA [Sigma-Aldrich], 5 mM $MgCl_2$ [P-Lab], 1 M glycerol [Serva], 1 mM GTP [Sigma-Aldrich], 1 mM DTT [ICN Biomedicals Inc.], 1 mM PMSF [Sigma-Aldrich], 1 mM aprotinin [ICN Biomedicals Inc.], 1 mM leupeptin [Sigma-Aldrich], 1 mM pepstatin [Sigma-Aldrich], pH 6.9). The mixture was allowed to thaw on ice, and was then centrifuged at 3000 g for 15 minutes at 4 ° C. The supernatant was centrifuged again at 100 000 g for 1 hour at 4 ° C. The resulting supernatant represented the soluble fraction and the pellet the membrane fraction. All fractions were precipitated with 10% (w/v) trichloracetic acid (TCA, Sigma-Aldrich) and diluted in denaturing buffer (50 mM Tris-HCl [Serva], pH 6.9, 2% [w/v] SDS [ICN Biomedicals Inc.], 36% [w/v] urea [Serva], 30% [w/v] glycerol [Serva], 5% [w/v] β-mercaptoethanol [Serva], 0.5% [w/v] bromophenol blue [Sigma-Aldrich]). Protein concentration was determined after staining with amido black (Popov et al. 1975).

4.4.2. Protein electrophoresis and immunoblotting

Protein samples were vortexed, boiled for 5 minutes and separated by SDS-PAGE on 10% (w/v) polyacrylamide gels. Specificity of anti-NtARPC5 (molecular mass of NtARPC5 is of approximately 16 kDa) was tested on 15% (w/v) polyacrylamide gel. Separated proteins were either visualized by staining with Coomassie Brilliant Blue (Sigma-Aldrich) or transferred onto

polyvinyldene difluoride (PVDF) membranes (ICN Biomedicals Inc.) by semi-dry electroblotting for probing with antibodies (for antibodies and concentrations used see Chapter 4.2.3., Table 2). After incubation with primary and secondary antibodies (both for 1.5 hours) the reactions were visualized with a chemiluminescence ECL detection kit (Amersham Biosciences, Uppsala, Sweden) on X-ray films (Foma, Hradec Králové, Czech republic).

To test for cross-reactivity between the anti-actin and anti-ARP2 antibodies, proteins from the soluble and total fractions were separated by SDS-PAGE and transferred onto a PVDF membrane. One line of separated proteins was cut longitudinally into 3 strips and each strip was incubated separately with anti-actin, anti-SpARP2 and anti-SpARP3 antibodies. Strips were then placed back together before visualization with the ECL detection kit.

5. RESULTS

5.1. Sites of actin filament polymerization in cold treated tobacco BY-2 cells

5.1.1. Tobacco cell line BY-2 during growth cycle

During the 7-day growth cycle, characteristic changes in the phenotype are detectable in tobacco BY-2 cells (Fig. 7). Cells in exponential phase of growth (1.-4.-day-old) divide intensively. In interphase cells, the nucleus is located in the centre of the cell and many radial cytoplasmic strands connect perinuclear and cortical regions (Fig. 7A). For the stationary cells (5.-7.-day-old), the elongation processes are typical. Their nuclei are relocated from the centre close to the plasma membrane. Fusion of smaller vacuoles into a big central vacuole is accompanied by disappearing of cytoplasmic strands (Fig. 7B). Obviously, not only the size, shape and the structure of the cell, but also the organization of AFs depend on the actual position of the cell within the growth cycle (see Chapter 5.1.2.).

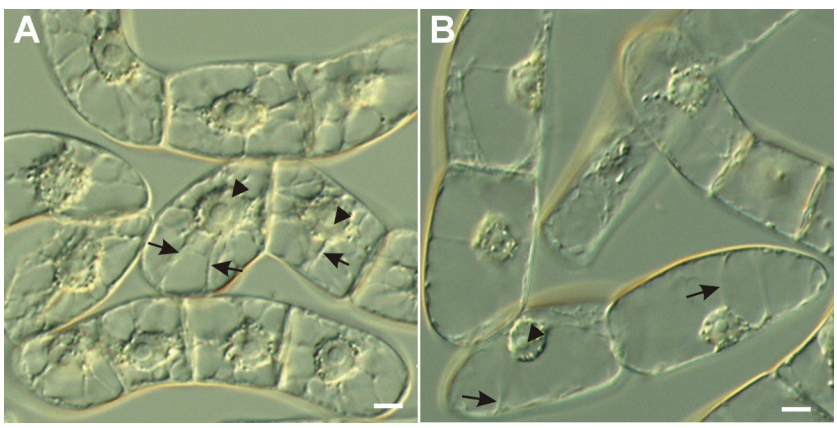

Figure 7. Tobacco BY-2 cells during growth cycle. Nomarski DIC. **A** 3-day-old cells. **B** 7-day-old cells. Arrows indicate position of cytoplasmic strands, arrowheads depict the position of the nuclei. Bars: 10 µM.

5.1.2. Organization of AFs in untreated BY-2 cells

In tobacco BY-2 cells maintained at 25 ° C, AFs were detectable in three cytoplasmic regions (Fig. 8): in a perinuclear region, in the transvacuolar cytoplasmic strands and in the cortical layer of the cytoplasm. AFs in the perinuclear region formed a basket-like structure around the nucleus (Fig. 8A, C). Cytoplasmic strands (prominent in 3-day old cells but rare in stationary cells) connecting the perinuclear and cortical regions were filled with thick AFs, forming a radial AF array (Fig. 8A). The character of AFs in the cortical layer of cytoplasm was dependent on the position of the cell within 7-day growth cycle (Graph 1). AFs of cells in exponential phase of growth formed a dense network of more or less fine filaments traversing the cortical cytoplasm apparently in all directions. A subpopulation of cells with fine AFs oriented transversely to the long cell axis was often detectable (data not shown). AFs of vacuolated stationary cells formed thicker cables uniformly arranged perpendicularly to the cell axis (Fig. 8D). As shown in Graph 1, 7-day-old cells were generally more difficult to be stained successfully than 3-day-old cells.

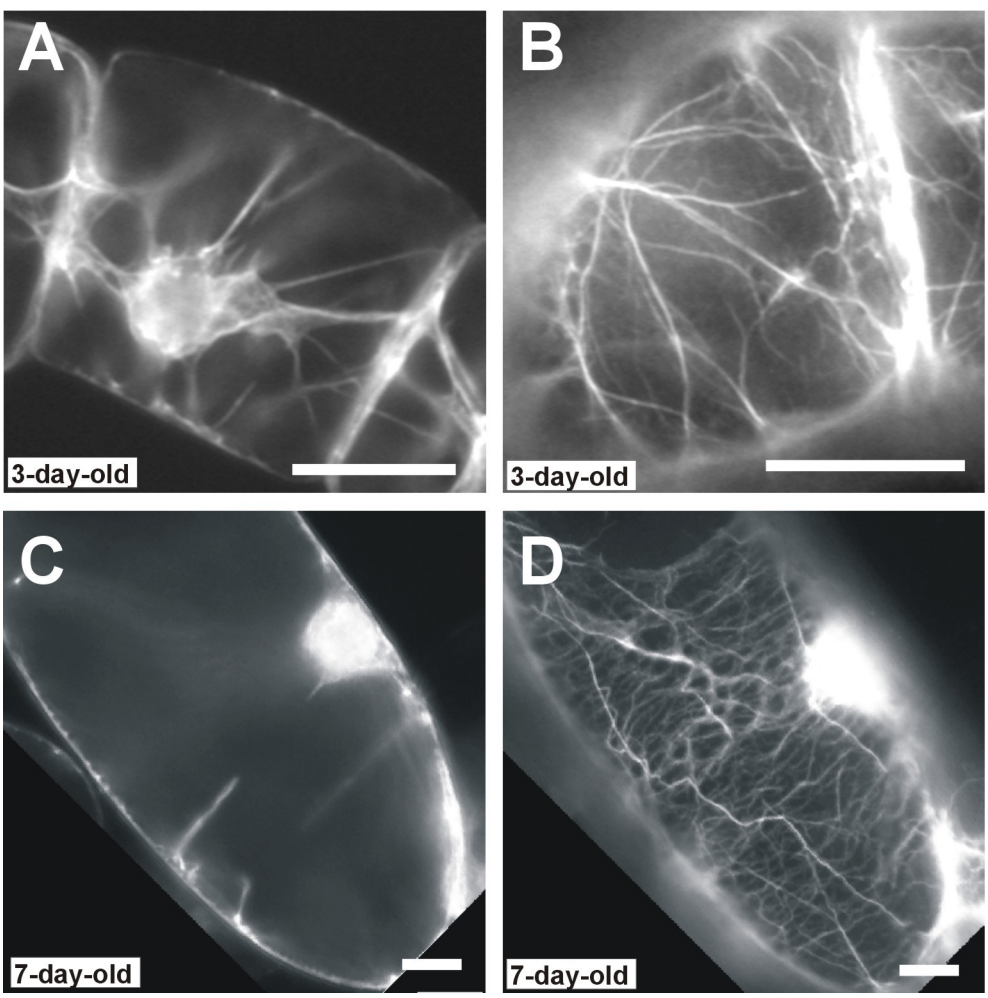

Figure 8. Changes in AFs organization during subculturing interval in tobacco BY-2 cells. Fluorescence microscopy. Rhodamin-phalloidin staining. **A** and **C** AFs in transvacuolar strands and around nucleus in 3-day-old cell (A) and 7-day-old cell (C). **B** and **D** A complex actin network in the cortical cytoplasm of 3-day-old cell (B) and 7-day-old cell (D). Bars: 10 μM.

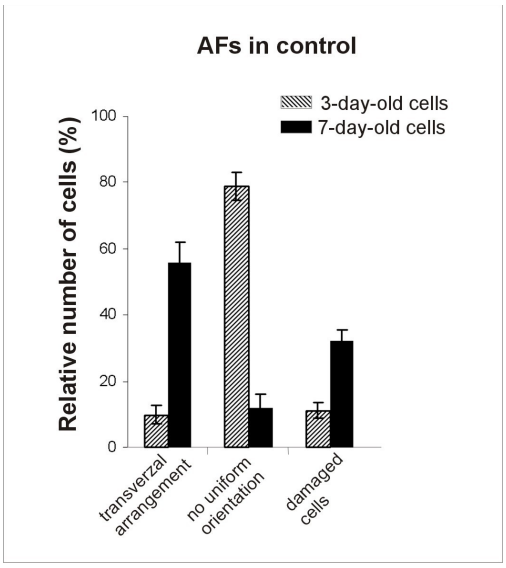

Graph 1. Changes in spatial distribution of cortical AFs in control tobacco BY-2 cells. Frequencies of individual categories in 3-day-old (shaded columns) and 7-day-old cells (black columns). Error bars represent SE (n=5 slides, 300 cells assessed on each).

5.1.3. Architecture and viability of cold-treated cells

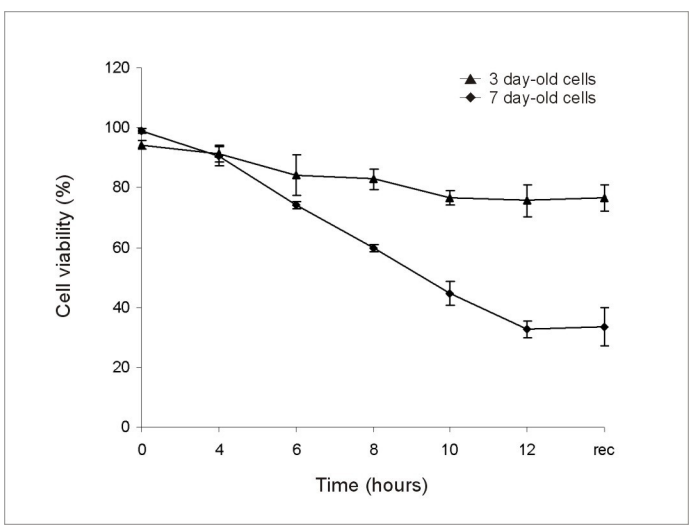

Graph 2. Viability of 3-day-old and 7-day old tobacco BY-2 cells maintained at 0 ° C. The graph shows a representative trend in the decrease in viability during the cold treatment. Error bars represent SE (n=5 slides, 400 cells were assessed on each slide).

When cultivated at the control temperature, interphase cells formed many radially oriented cytoplasmic strands connecting the cortical and perinuclear regions (Chapter 5.1.1.). Cold treatment in ice water (0 ° C) led to gradual disruption of the cytoplasmic strands, starting in all cells after only 5 minutes of cold treatment (data not shown). The cytoplasmic strands then gradually disappeared, the vacuolar complex fused into one big central vacuole, and the nucleus shifted into the layer of cortical cytoplasm. After 12 hours at 0 ° C, virtually no cytoplasmic strands were observed (data not shown). Restoration of cytoplasmic strands in the surviving cells started within 5 minutes after transfer to 25 ° C, and numerous cytoplasmic strands re-appeared after 20 minutes (data not shown).

The viability of cells gradually declined during 12 hours at 0 ° C (Graph 2). At the end of 12 hours at 0 ° C, the viability of 3-day-old cells varied between 30 % and 50 % in 4 independent experiments. In contrast, the decline in viability of 7-day-old cells was not so prominent and the

viability maintained between 75 % and 85 % in 3 independent experiments.

5.1.4. AFs completely depolymerize in cells exposed to 0 ° C

Cells in exponential and stationary phase of growth were cultivated at 0 ° C for 5 min - 12 hours and collected for AFs visualisation every 2 hours. In exponential cells (Fig. 9A-F), the first observable effects of the cold treatment, which became apparent after 5 minutes at 0 ° C, were a degradation of cytoplasmic strands and a disappearance of the radial AF array (Fig. 9A). After 20 minutes, the fine AFs in the cortex disappeared and actin formed a network of disordered, thick and branched AFs in the cortical layer of the cytoplasm (Fig. 9B). This network gradually thinned out during the first 6 hours of cold treatment, leaving only a sparse actin network in the cortical region (Fig. 9C). Very rarely (in about 1 % of cells), brightly shining actin rods (or less frequently actin dots) appeared in the cortex and around the nucleus (Fig. 9F). In Graph 3, they are altogether referred to as transient actin structures. Such actin rods (or dots) were never detected in the controls. After 12 hours of the cold treatment (follow the Graph 3A), only 19 % of cells retained few, short, sometimes branched AFs (Fig. 9D), while the number of cells with actin rods (or dots) in the cortex and around the nucleus increased to 18 %. 24 % of cells did not contain any detectable actin filaments (Fig. 9E), and 39 % of cells were damaged (see Materials and Methods, Chapter 4.2.6.).

As expected, the degradation of AFs in the cortical layer of stationary cells (Fig. 9G-I) started similarly to the exponential cells during 1 hour of cold treatment, and the progressive degradation of AFs was observed. During 2-12 hours, cortical AFs depolymerized gradually (Fig. 9G, H), but there were still 1-3 thick cables in polymerized state left even after 12 hours of the cold period (in about 57 % of cells, Graph 3B). Only 7 % of cells contained no polymerized filaments (Fig. 9I) and, interestingly, low amount of cells containing transient actin rods (or dots) appeared (about 5 %) comparing to cells in exponential phase of growth.

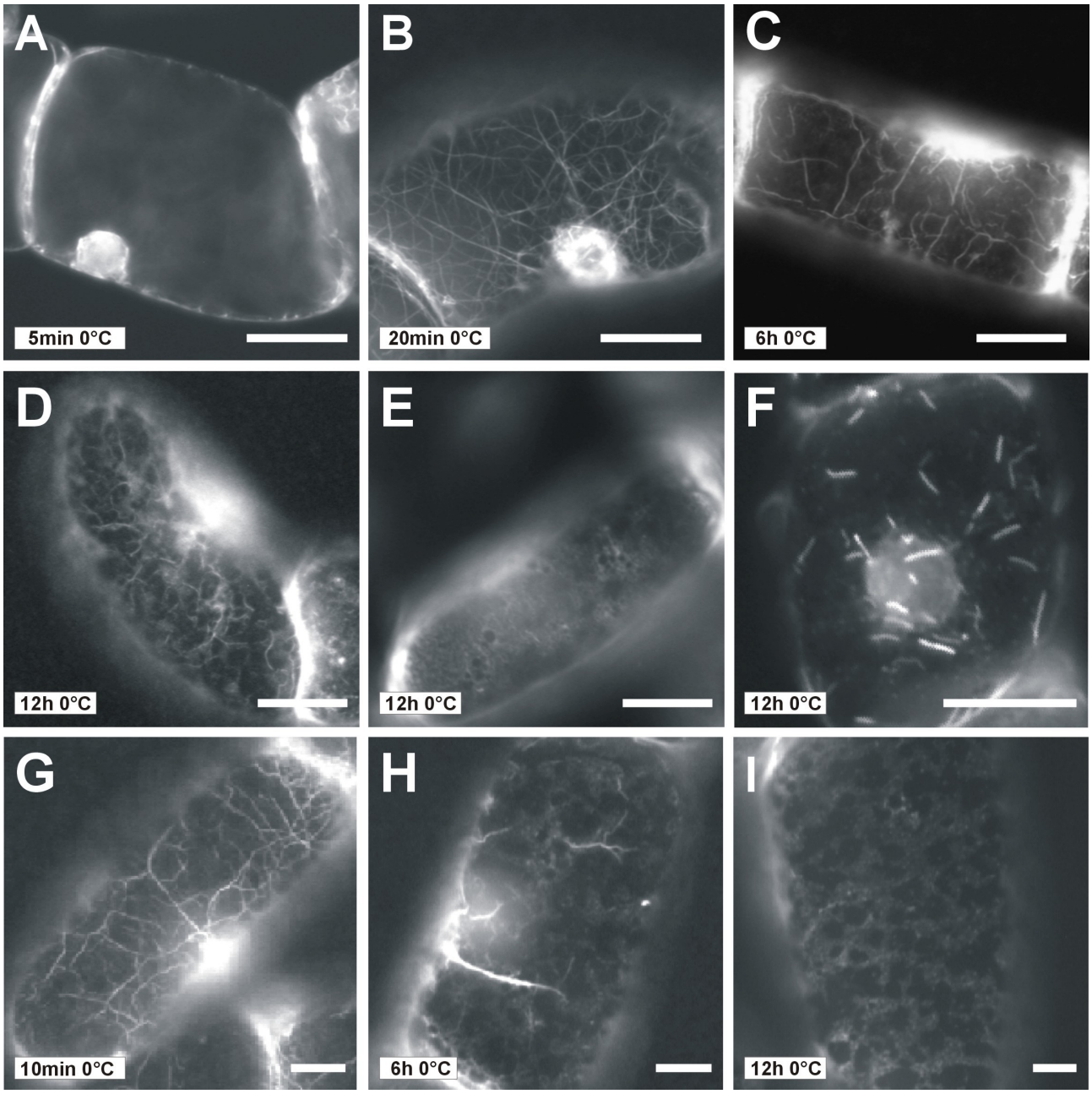

Figure 9. AFs in tobacco BY-2 cells maintained at 0 ° C for 5 min – 12 h. Fluorescence microscopy. Rhodamin-phalloidin staining. **A-F** Depolymerization of AFs in 3-day-old cells. **A** Loss of radial AFs in transvacuolar strands and around nucleus in control cells. Median optical section. **B** Absence of fine AFs and formation of a cortical network of thick, disoriented AFs in cells incubated at 0°C for 20 min. **C** Advanced disassembly of AFs in cortical cytoplasm of cells exposed to 0 ° C for 6 h. **D-F** A few thick AFs remaining in the cortical cytoplasm (D), completely disassembled AFs (E), and actin rods (F) in cells exposed to 0 ° C for 12 h. **G-I** Gradual depolymerization of AFs in 7-day-old cells. **G** Cortical AFs in cell exposed to 0 ° C for 10 min. **H** Few actin cables remained in cells treated with 0°C for 6 h. **I** Completely disassembled network in cell after 12 hours at 0 ° C. Bars: 10 μM.

5.1.5. Re-polymerization of AFs during recovery from cold treatment

After 12 hours at 0 ° C, cells were transferred to standard temperature (25 ° C) to observe whether re-polymerization of filaments occurs. During the period of 1 to 5 minutes at 25 ° C, various forms of polymerized actin were detectable in the cortical cytoplasm as well as around the nucleus in exponential cells (Graph 3). The actin forms were: a) actin dots (Fig. 10A); b) actin rods often connected with thin AFs (Fig. 10B); c) actin dots connected with thin branched AFs resembling "beads-on-string". Brightly shining dots often localized to the junction of Y-shaped filament (Fig. 10C, D). Actin dots, rods or “beads on string” appeared only transiently during the early phases of the recovery period (30 s - 30 min) and therefore, in following text, they are called “transient actin structures”. In addition, the cells with a very dense network of thin filaments were observable (Fig. 10F). After 2 minutes at 25 ° C, the number of cells containing detectable polymerized filaments reached 38 %, while after 20 minutes at 25 ° C, around 56 % of cells re-formed the network of AFs (see Graph 3). The transient actin structures were still detectable in about 25 % and 17 % of the cells

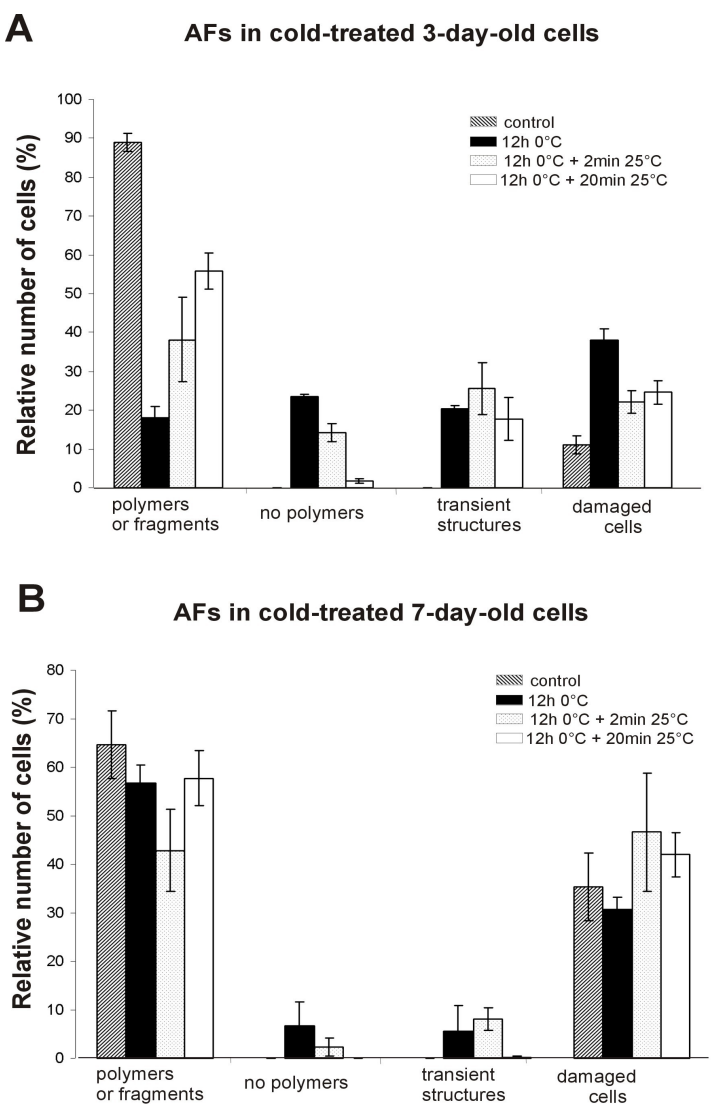

Graph 3. Distribution of cortical AF in control cells, cold treated cells and cells recovering from cold. **A** 3-day-old cells. **B** 7-day old cells. Frequencies of individual categories of AFs in control cells (shaded columns); cells maintained at 0 ° C for 12 h (black columns); in cells recovering from cold (12 h at 0 ° C) for 2 min (dotted columns) and 20 min (white columns). Error bars represent SE (n=3 slides, 300 cells assessed on each).

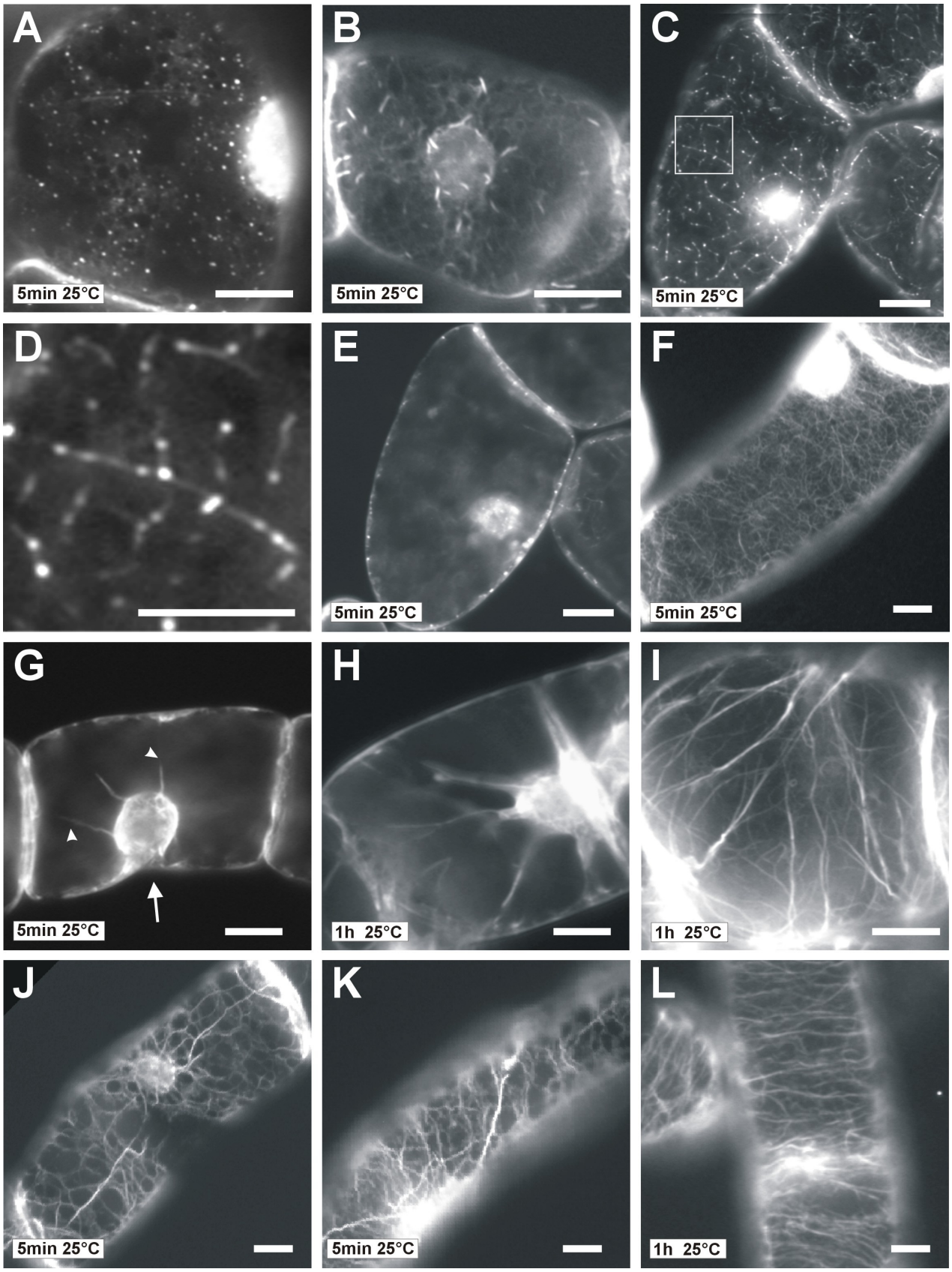

Figure 10. Recovery of AFs after 12 h at 0 ° C and subsequent incubation at 25 ° C in 3-day-old cells (A-I) and 7-day-old cells (J-L). Fluorescence microscopy. Rhodamin-phalloidin staining. **A-E** Transient actin structures formed in cortical region and around nucleus during 5 min recovery at 25°C. **A** Actin dots; **B** short actin rods with thin filaments; **C** disoriented branched thin actin filaments with a dotted signal in the cortical cytoplasm; **D** magnification of Y-shaped actin filaments with dotted signal; **E** actin dots around the nucleus; **F** dense cortical network that consisted of very thin AFs. **G** Basket-like actin structures formed around the nucleus (arrow) after 5 min at 25 ° C. AFs emerging from the basket towards the cortical region are indicated with arrowheads. **H** Formation of AFs in transvacuolar strands after 1 hour at 25 ° C. **I** Cortical actin network after 1 h at 25 ° C. **J-K** Formation of cortical AFs network after 5 min at 25 ° C in 7-day-old cells. **L** Cortical actin network after 1 h at 25 ° C in 7-day-old cells. Bars: 10 µM.

recovering for 2 and 20 minutes, respectively. After 1 hour at 25 ° C, no transient actin structures were detectable and stained cells contained control-like AFs network in the cortical cytoplasm (Fig. 10I). Simultaneously with the re-assembly of the cortical actin network, re-organization of the actin cytoskeleton also occurred around the nucleus. Initially, the diffuse signal from depolymerized AFs that was detectable during the cold treatment re-formed into filaments, sometimes decorated with dots (Fig. 10E). After 5-15 minutes at 25 ° C, AFs formed a dense basket surrounding the nucleus (Fig.10G, arrow). At the same time, other AFs emerged from the basket, pointing towards the cortical region (Fig. 10G, arrowheads). After 15 minutes of the recovery, AFs of cytoplasmic strands also re-formed (Fig. 10H).

In stationary cells (Fig. 10J-L), the structures typical for actin recovery in exponential cells (dots, rods, etc.) were observed with much lower intensity (in about 8 % of cells after 2 minutes at 25 ° C; Graph 3) and AF network re-appeared gradually (Fig. 10J, K). After 20 minutes at 25 ° C, almost no cells containing transient actin structures were detectable and number of cells with polymerized net increased to 57 %. Control actin configuration was recovered in 95 % of cells after 1 hour at 25 ° C (Fig. 10L).

To determine whether incidence of transient actin structures during recovery of AFs is connected with the degree of previous depolymerization of AFs, the 6-hour period of cold treatment (0 ° C) was used to treat exponential cells before recovery experiments (25 ° C) to induce partial depolymerization of AFs. Graph 4 shows that such a treatment resulted in decreased number of cells with transient actin structures. This may suggest that AFs have to be completely depolymerized for the formation of transient actin structures during subsequent recovery processes.

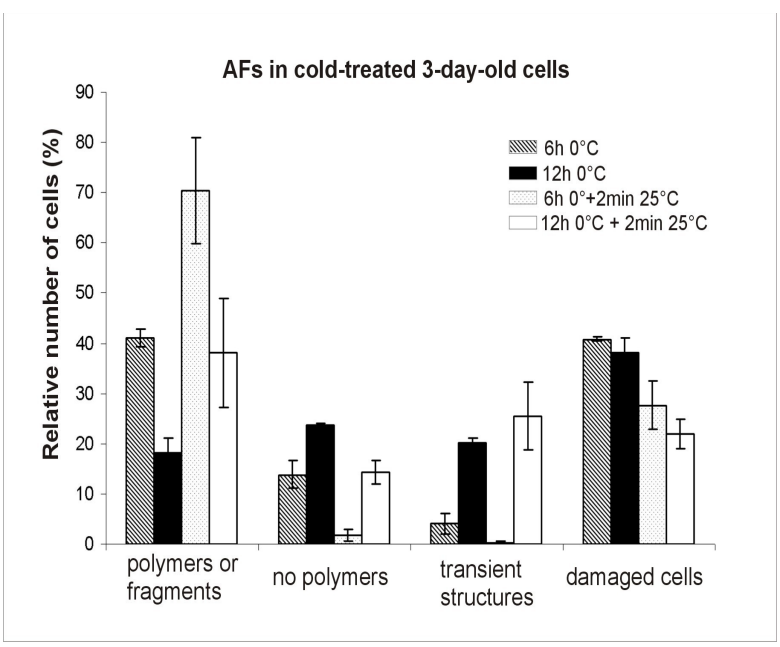

Graph 4. Distribution of cortical AFs in 3 day-old cells treated with 0 ° C for 6 and 12 h and subsequently recovered at 25 ° C. Frequencies of individual categories of AFs in cells maintained at 0 ° C for 6 h and 12 h (shaded and black columns, respectively); and in cells recovering for 2 min from 6 h and 12 h at 0 ° C (dotted and white columns, respectively). Error bars represent SE (n=5 slides, 300 cells assessed on each).

5.1.6. Western bolt analysis of actin during cold treatment

To test for possible changes in amount of actin during the cold treatment of exponential cells, total, soluble and sedimentable protein fractions were analyzed by SDS-PAGE and immunoblotting. Equal amounts of proteins from all fractions taken at two-hour intervals during 12 hours at 0 ^{o} C were loaded onto gels for the analysis. The immunoblots showed no changes in the relative amounts of actin in any of tested protein fractions during the cold treatment (Fig. 11).

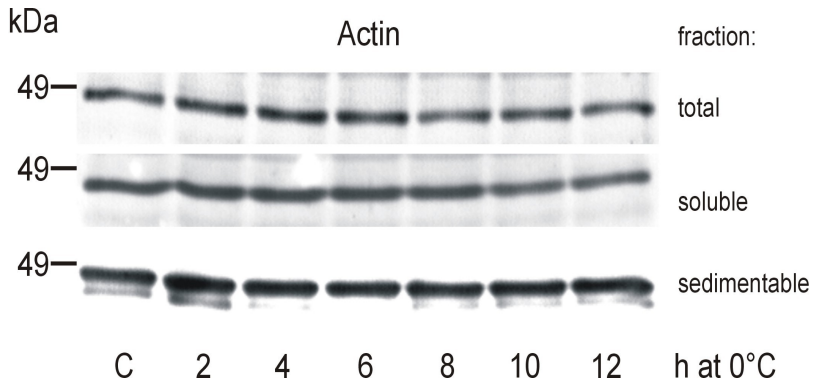

Figure 11. Western blot analysis of actin in total, soluble, and sedimentable protein extracts from BY-2 cells incubated for 0-12 hours at 0 ° C. Immunoblots were probed with anti-actin antibody. C – control.

5.2. ARP2 and ARP3 are localized to sites of actin filament nucleation in tobacco BY-2 cells

5.2.1. Immunobloting of ARPs and ARPC5

To visualize the distribution of ARPs in cells, antibodies against SpARP2 and SpARP3 were used. Besides this heterologous system, a plant specific antibody against tobacco ARP3 (NtARP3) was prepared. Prior the use of ARPs antibodies for *in situ* immunodetection, I performed immunoblot analysis with soluble and membrane protein fractions from BY-2 cells in the exponential phase of growth (Fig. 12). The antibody against SpARP2 recognized a protein of apparent molecular mass of about 44 kDa in the soluble fraction but not in the membrane fraction (Fig. 12A). The antibodies against ARP3 (anti-SpARP3 and anti-NtARP3) recognized a proteins of apparent molecular mass slightly larger than 45 kDa in the membrane fraction, but not in the soluble fraction (Fig. 12A, B). The anti-actin antibody detected a band of apparent molecular mass that was distinct from those of ARP2 and ARP3 (approximately 45 kDa, Fig. 12C).

The antibody raised against NtARPC5 detected many proteins of various sizes on western blot (Fig. 12D), therefore the antibody was found to be non-specific and was not used for further experiments.

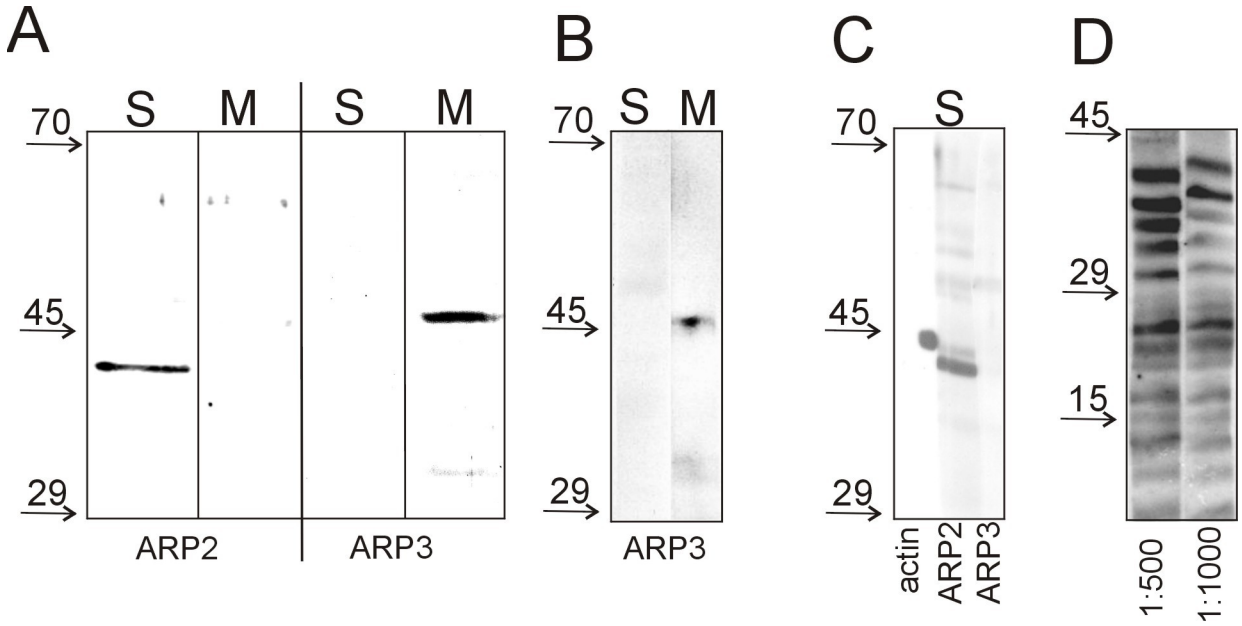

Figure 12. Immunoblot detection of ARP2, ARP3 and ARPC5 in 3-day-old BY-2 cells. **A**, **B** Soluble (S) and membrane (M) protein fractions were blotted and stained with antibodies against SpARP2 and SpARP3 (A) and with antibody against NtARP3 (B). **C** A cross-reactivity test between anti-actin, anti-SpARP2 and anti-SpARP3 antibodies (details in Material and Methods). **D** Total protein fraction was immunoblotted with antibody against NtARPC5.

The tobacco BY-2 cells and tobacco leaf epidermal cells were transformed with fusion gene *ARP3::GFP* to localize ARP3 subunit of the Arp2/3 complex in living cells. Results are described and discussed further (see Chapters 5.2.6. and 6.8.). Moreover, the transformed cells served for further testing of the specificity of anti-NtARP3 (Fig. 13). Total protein extracts from tobacco BY-2 cells and tobacco leaf epidermal cells transformed with fusion gene *ARP3::GFP* were used. As a control, proteins extracted from untransformed tobacco BY-2 cells and tobacco leaves were used. In control, anti-NtARP3 detected bands of about 30 kDa and 50 kDa. In transformed cells probed with anti-NtARP3, an extra band of approximately 80 kDa appeared, exactly maching a band recognized by anti-GFP. The bands of 50 kDa and 80 kDa correspond to the predicted molecular masses of NtARP3 (50 kDa) and NtARP3 fused to GFP (80 kDa), respectively.

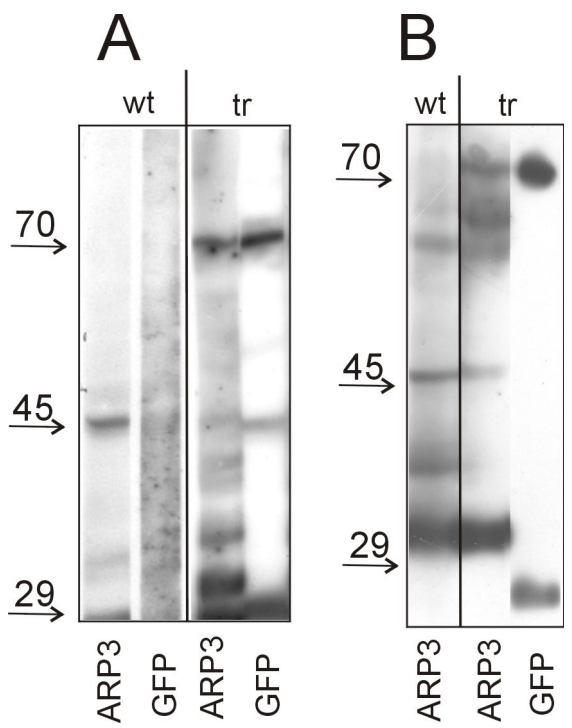

Figure 13. Immunoblot detection of ARP3 in BY-2 cells and tobacco leaf epidermal cells transformed with *ARP3::GFP*. **A** Total protein fractions of control and transformed 3-day-old BY-2 cells were immunoblotted with anti-NtARP3 and rabbit polyclonal anti-GFP. **B** Total protein fractions of control and transformed tobacco leafs were immunoblotted with anti-NtARP3 and rabbit polyclonal anti-GFP. Molecular mass standards are indicated by arrows. (wt) – not transformed, (tr) – transformed with fusion gene *ARP3::GFP*. One line of separated proteins was cut longitudinally into 2 strips and each strip was incubated separately with anti-GFP and anti-NtARP3. Strips were then placed back together before visualization with the ECL detection kit.

5.2.2. ARP2 and ARP3 localize as dots along AFs and at filament branching points in control BY-2 cells

Since immunoblot confirmed the specificity of antibodies, the distribution of ARPs in control BY-2 cells was assessed by immunodetection. All antibodies (anti-SpARP2, anti-SpARP3 and anti-NtARP3) produced similar staining pattern within the cells. ARP2 and ARP3 were detected as dots in all regions of AF occurrence, namely in the cortical layer of the cytoplasm (Fig. 14A–D), around the nucleus and in cytoplasmic strands (Fig. 14E–H). The ARP dots in the cortical layer of the cytoplasm often co-localized with AFs (Fig. 14B–D, arrowheads) and were also found at points of

AFs branching (Fig. 14B–D, arrows). Isolated ARP dots without any contact with AFs were observed very rarely, approximately in 5% of all dots. The co-localization of ARP dots and AFs was confirmed using standard fluorescence microscopy as well as laser scanning confocal microscopy (Fig. 14I-L).

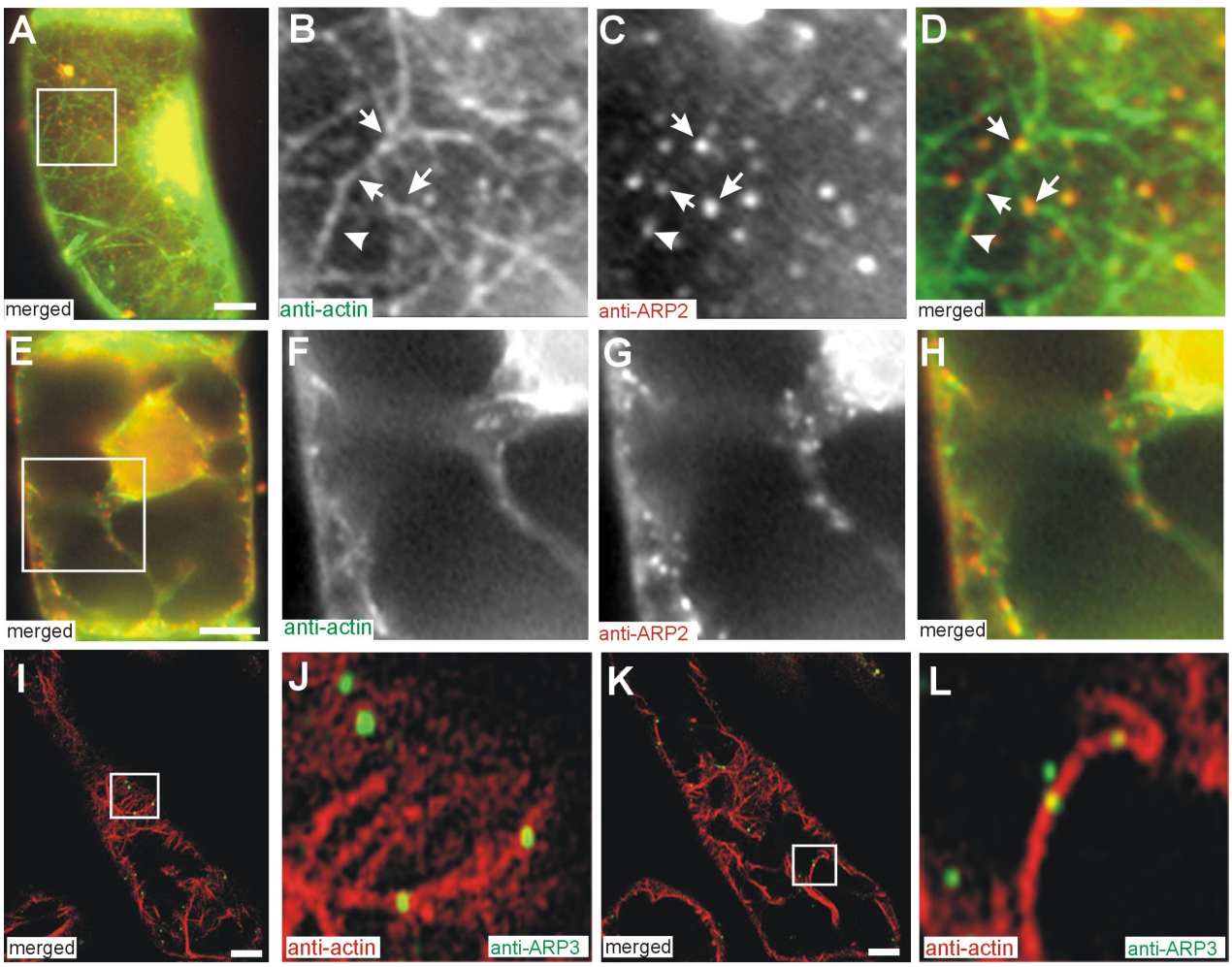

Figure 14. Localization of ARP2 and ARP3 in 3-day-old BY-2 cells. Immunofluorescence staining with anti-actin (A-H green channel; I-L red channel), anti-SpARP2 (A-H, red channel) and anti-NtARP3 (I-L, green channel) antibodies. Fluorescence microscopy (A–H) and confocal microscopy (I–L). Details boxed in panels A, E, I and K are shown in panels B–D, F–H, J and L, respectively. **A–D** Co-localization of ARP2 and AFs at the sites of AF branching (arrows) and along AFs (arrowhead) in the cortical cytoplasm. **E–H** Co-localization of ARP2 and AFs in cytoplasmic strands and in the perinuclear region. **I-L** A single optical sections showing co-localization of ARP3 and AFs at the site of AF branching and along AF. Bars = 10 μm.

5.2.3. ARP3 localizes to plasma membrane in BY-2 cells

To confirm the putative membrane localization of ARP3, “membrane ghosts” were prepared. Isolated membranes attached to a glass slide retain proteins interacting with a plasma membrane in living cells. Among other, actin was shown to be associated with plasma membrane in tobacco BY-2 cells. ARP3 was immunodetected on “membrane ghosts” prepared from tobacco BY-2 cells. Figure 15 shows that ARP3 dots indeed localized along actin filaments and close to AFs branching on isolated membranes from BY-2 cells.

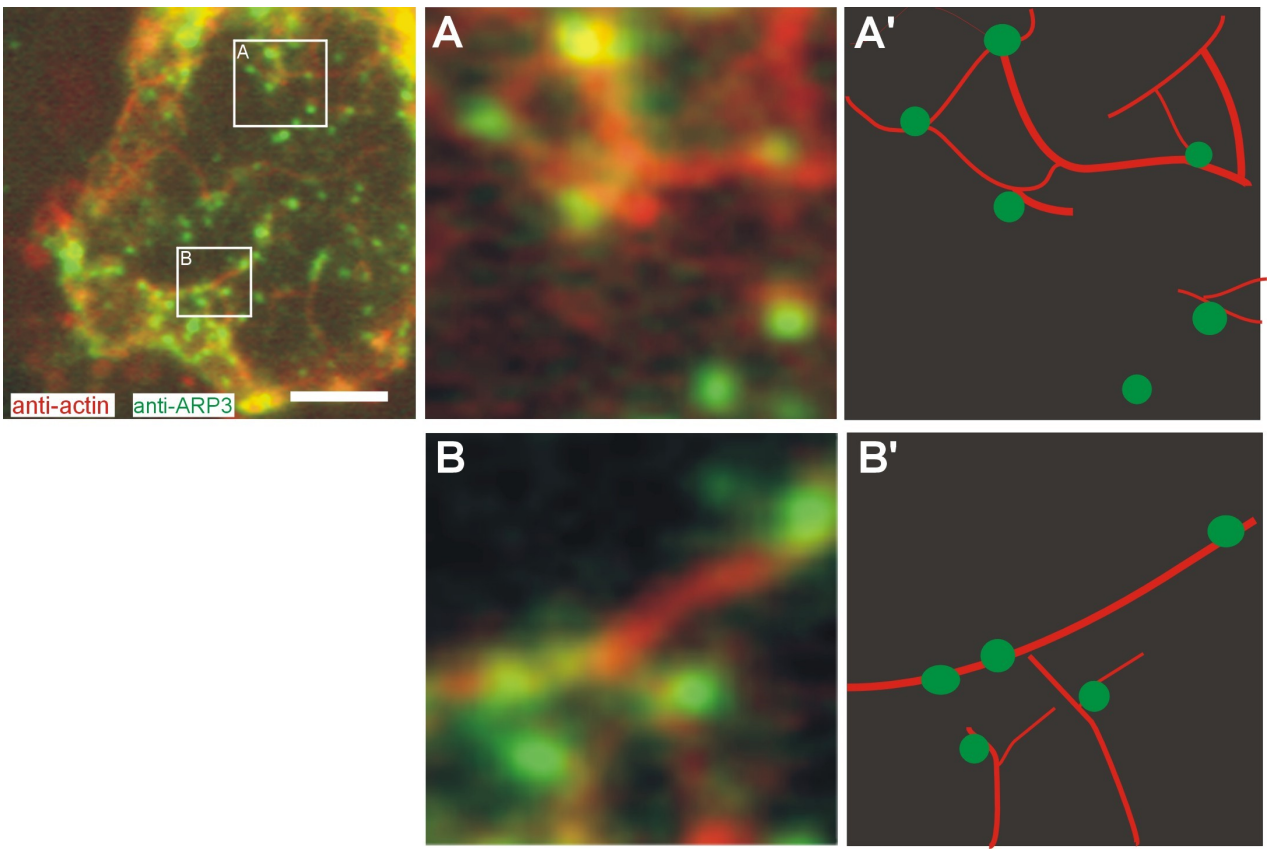

Figure 15. Co-localization of AFs and ARP3 on isolated membrane of 3-day-old tobacco BY-2 cell. Immunofluorescence staining with anti-NtARP3 (green channel) antibody and rhodamine-phalloidine (red channel). Details boxed are shown in panels A and B. Schematic pattern of details is depicted in panels A` and B`. Bar = 10 μm.

5.2.4. ARP2 and ARP3 co-localize with transient actin dots

To test whether transient actin structures represent early phases of AF nucleation and correspond to sites of AFs nucleation (SANs), I performed double immunostaining of ARPs and actin during the early phase of AFs recovery after their complete cold-induced depolymerization. As in the control cells, both ARP2 and ARP3 antibodies stained dots in the cortical layer of cytoplasm (Fig. 16 for anti-SpARP2 antibody). These ARP dots co-localized with transient actin dots (Fig. 16A–D) and junctions of Y-shaped actin structures (Fig. 16F–H, arrows), and were localized along newly formed cortical AFs (Fig. 16E, white arrowheads). Isolated ARP dots without any co-localization with AFs were rarely observed (Fig. 16E, black arrowheads).

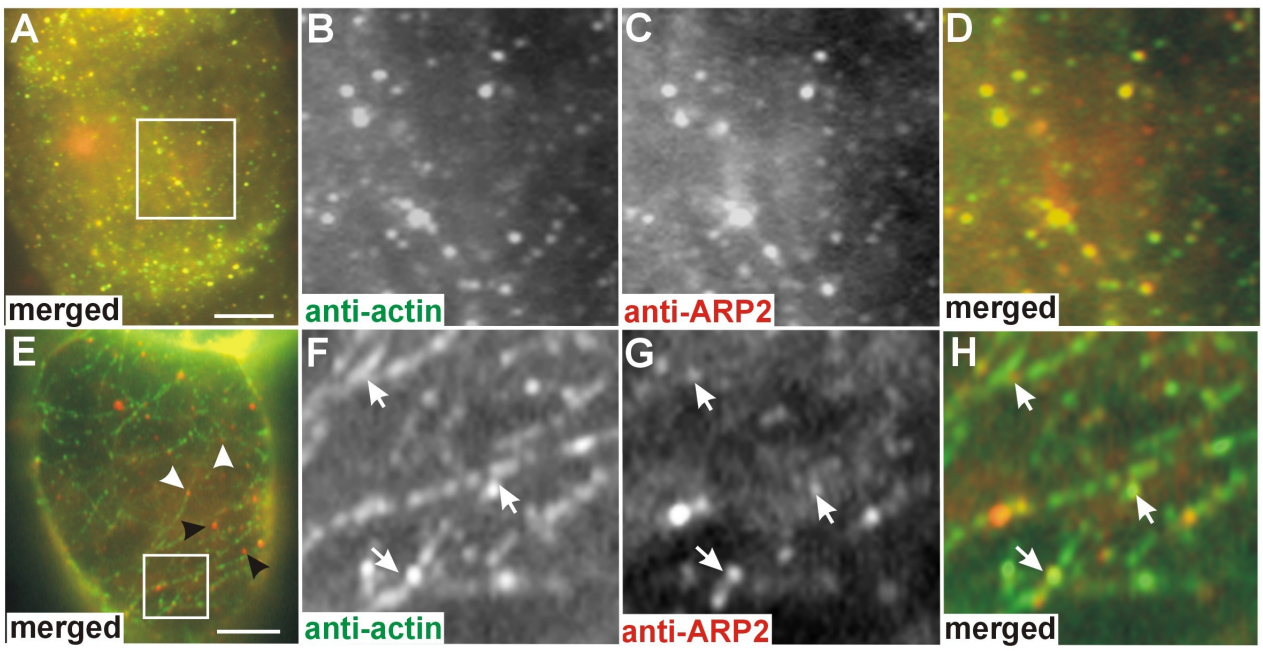

Figure 16. Co-localization of ARP2 with transient actin structures after 12 h at 0 ° C and 5 min at 25 ° C. Fluorescence, microscopy. Immunofluorescence staining with anti-actin (green channel) and anti-SpARP2 (red channel) antibodies. Details boxed in panels A and E are shown in panels B–D and F–H, respectively. **A–D** ARP2 and actin co-localization in dots. **E–H** ARP2 and actin co-localization in branchings (F–H, arrows) and along AFs (E, white arrowheads). Black arrowheads in (E) indicate ARP2 dots that do not co-localize with actin. Bar = 10 μm.

5.2.5. Transient actin structures were not detected in cells recovering from LatB-induced depolymerization of AFs

LatB was used as a tool to induce specific depolymerization of AFs (Fig. 17). First, I investigated the effect of LatB on architecture and viability of BY-2 cells from 3-day-old cultures. Neither of the LatB concentrations tested (100 and 500 nM for 12 hours) affected the viability of cells significantly. The viability ranged from 90 to 95 % in all experiments (details not shown). As usual, control cells formed many radially oriented cytoplasmic strands that connected the cortical and the perinuclear regions (Fig. 17A). When treated with 500 nM LatB, a gradual disruption of cytoplasmic strands occurred, the vacuolar complex fused into one big central vacuole and the nucleus shifted into the layer of a cortical cytoplasm. After 12 hours, none or only one thick cytoplasmic strand connected the nuclear region with the opposite side of the cortical cytoplasm (Fig. 17B).

The concentration of LatB required for complete depolymerization of AFs was tested, and in the subsequent recovery processes, AFs and ARPs were visualized. Treatment with 100 nM for 12 hours did not result in complete depolymerization of AFs (Fig. 17C), and only treatment with 500 nM for 12 hours was sufficient (Fig. 17D). After 12 hours of treatment with 500 nM LatB, the cells were washed to remove LatB and to allow re-assembly of AFs. During the initial 5–15 minutes of recovery, no structures resembling the transient actin structures that formed during recovery from cold, such as actin dots or filaments with a dotted signal, were observed. Instead, re-assembly of AFs in the cortical layer commenced with the formation of short AFs that quickly elongated and sometimes branched (Fig. 17E–G). The re-assembly process continued gradually and, as in the cold experiments, the normal arrangement of AFs was re-established within 1 hour in most cells (Fig. 17H). AFs of cytoplasmic strands began to recover simultaneously with cytoplasmic strands (as observed with Nomarski DIC) within 5–10 minutes after restoration of normal conditions, and were fully developed within 30–60 minutes in most cells.

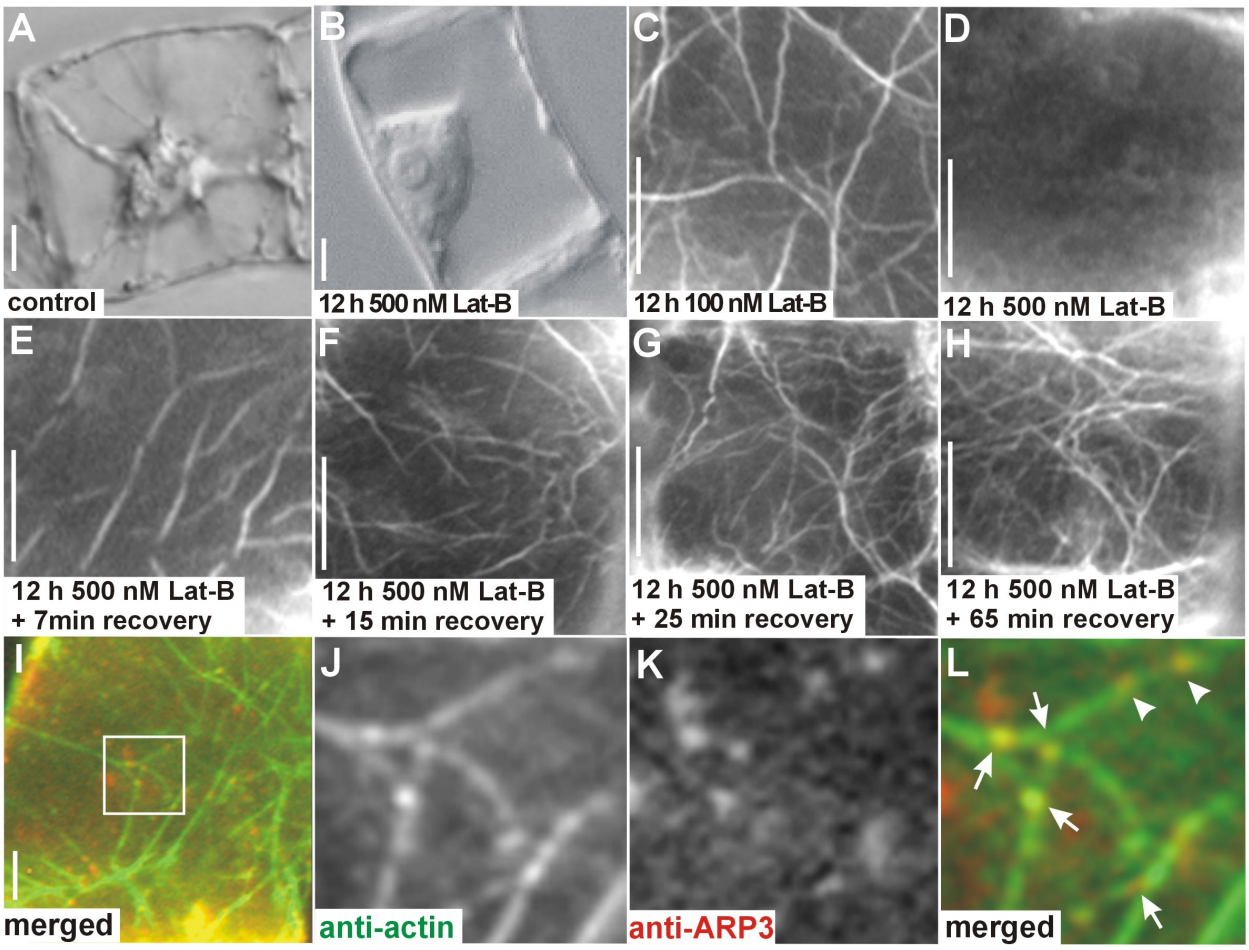

Figure 17. Localization of AFs and ARP3 after LatB treatment and subsequent recovery of AFs in 3-day-old BY-2 cells. Fluorescence microscopy. **A, B** The spatial organization of cytoplasm in control cells that formed many cytoplasmic strands (A) and after 12 h treatment with 500 nm LatB, when degradation of cytoplasmic strands was visible (B), as observed by Nomarski DIC. **C–H** Rhodamine-phalloidin staining. **I–L** Immunofluorescence staining with anti-actin (green channel) and anti-ARP3 (red channel) antibodies. **C** AFs in cells treated with 100 nM LatB for 12 hours. (**D**) AFs in cells treated with 500 nM LatB for 12 hours. (**E–G**) Progressive re-assembly of AFs during recovery from 500 nM LatB treatment. Note the absence of obvious transient actin structures. **H** Normal arrangement of AFs recovered after 60 min in most cells. **I–L** ARP3 (red channel, detected with anti-SpARP3) along AFs (green channel) is indicated by arrowheads and ARP3 co-localization with AFs branching is indicated by arrows. Details boxed in panel I are shown in panels J–L. Bars = 10 μm.

When AFs and ARPs were double-stained in cells recovering from the LatB treatment (Fig. 17I–L), it was found out that ARP2 and ARP3 formed dots along cortical AFs (Fig. 17L, arrowheads) and in junctions of Y-shaped AFs (Fig. 17L, arrows). This distribution is similar to the distribution in control cells as well as the distribution in cells recovering from cold treatment (see Figs. 14B–D and 16F–H).

5.2.6. *In vivo* observations of ARP3::GFP

To observe the localization of the ARP3 *in vivo*, genes encoding for ARP3 and GFP were fused and the fusion gene was stably transformed into tobacco BY-2 cells and transiently transformed into tobacco leave epidermal cells. Similar results were obtained when transformed BY-2 cells or tobacco leaf epidermal cells were observed (Fig. 18 and 19). The signal of GFP was located mainly into cytoplasmic strands (Fig. 18B, 19A; arrows) and cortical layer. In the cortical layer, the diffuse signal was interrupted with circular, non-fluorescent spots of various sizes (Fig. 18C and 19B). In cells transformed with plain *GFP*, the signal was similarly distributed into the cytoplasmic strands, cortical layer, but also to the nucleus (Fig. 18E, F and 19C, D).

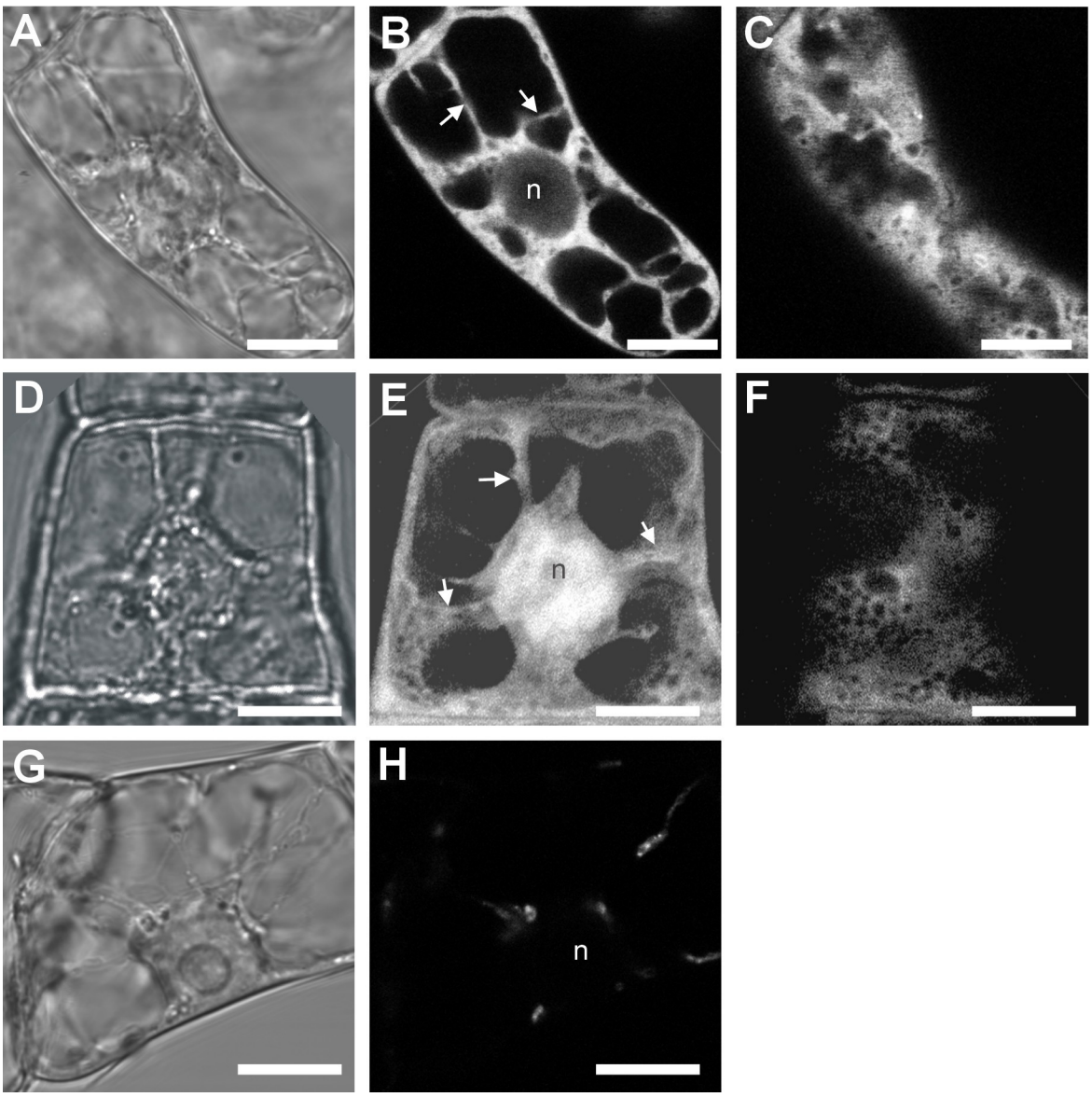

Figure 18. Signal of GFP detected in 3-day-old tobacco BY-2 cells transformed with *ARP3::GFP*. Confocal microscopy. Maximal projections of the two optical sections. **A-C** Cell transformed with *ARP3::GFP*. **D-F** Cell transformed with *GFP*. **G, H** Untransformed cell. (A, D, G) Organization of cytoplasm in median optical sections as shown by Nomarski DIC. (B, E) Signal of GFP in median optical sections localized into cytoplasmic compartments. Arrows point out the signal in cytoplasmic strands. (n) – position of nucleus. (C, F) The diffuse, patterned signal of the GFP in the cortical layer. Bars = 10 μm.

Western blots confirmed the expression of fusion protein, but also revealed the degradation of the fusion protein and the occurrence of plain GFP (Fig. 13). Therefore, *in vivo* observations of Arp3::GFP were prevented by the presence of a pool of the free GFP in the cytoplasm.

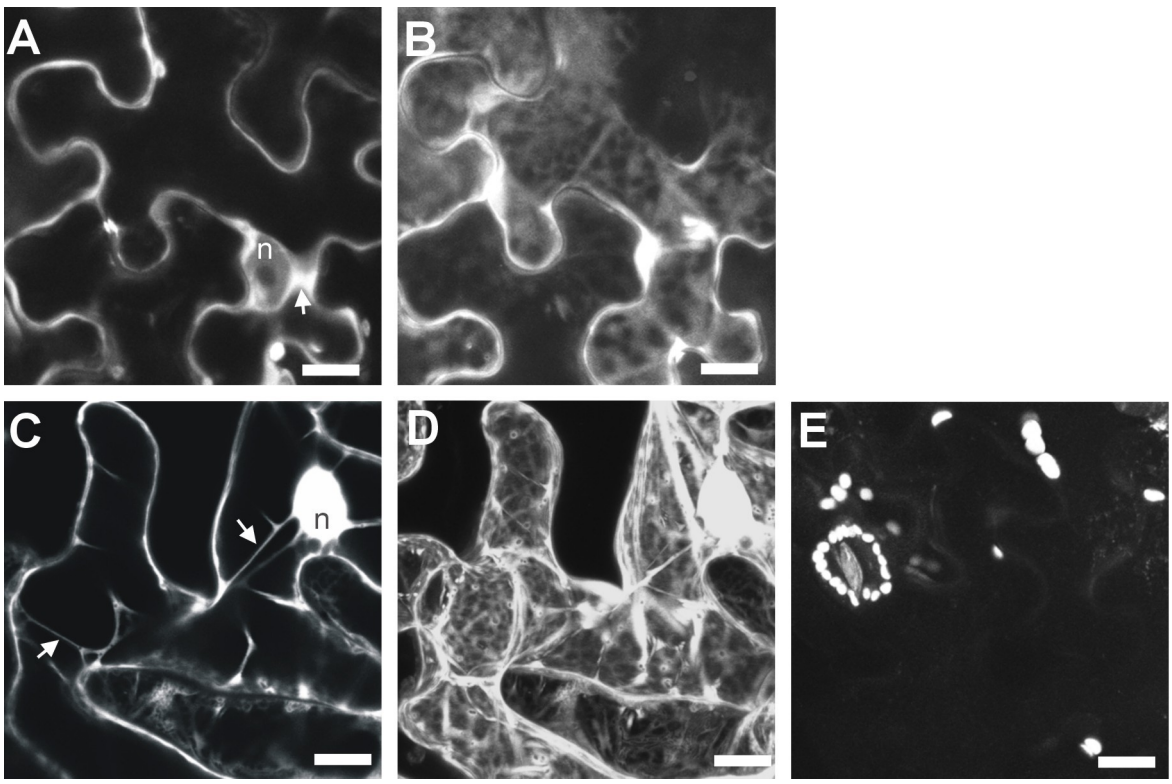

Figure 19. Signal of GFP detected in tobacco leaf epidermal cells transformed with *ARP3::GFP*. Confocal microscopy. Maximal projections of the two optical sections. **A-B** Cell transformed with *ARP3::GFP*. **C-D** Cell transformed with *GFP*. **E** Untransformed cell. (A, C) Signal of GFP in median optical sections localized into cytoplasmic compartments. (B, D) The diffuse signal of GFP in the cortical layer. Arrows in (A) and (C) point out the signal in cytoplasmic strands. (n) – position of nucleus. Bars = 10 μm.

5.3. ARP3 localization during the elongation of tobacco pollen tubes

5.3.1. ARP3 is expressed in pollen tubes

To confirm or disprove the discussed role of the Arp2/3 complex in the tip growth of pollen tubes, total protein extracts from tobacco pollens were blotted and probed with specific antibody against NtARP3 (Fig. 20). Proteins of apparent molecular mass of about 48 kDa and 30 kDa were detected. The band of about 48 kDa corresponds to predicted molecular weight of NtARP3, while the band of about 30 kDa may represent a product of degradation.

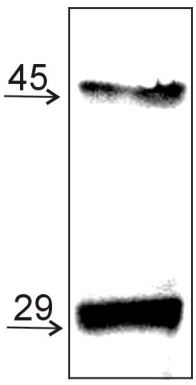

Figure 20. Immunoblot analysis of NtARP3 in total protein extract from tobacco pollen. Blot was probed with mouse anti-NtARP3 antibody. Molecular mass standards are indicated by arrows.

5.3.2. ARP3 localized into the very tip of a pollen tube

Since immunoblot proved the occurrence of the NtARP3 in protein extract from tobacco pollen tubes, the localization of NtARP3 and actin was revealed in following immunostaining experiments using anti-NtARP3 and rhodamine-phalloidin (Fig. 21). In a basal part of a pollen tube, actin filaments formed long cables oriented longitudinally to the growth axis of the tube. In the very tip of the tube, a mesh of randomly oriented fine AFs was detected.

NtARP3 appeared diffusively throughout the cytoplasm, preferentially under the plasma membrane along the whole surface of the tube. In the cortical layer, the diffusive pattern of ARP3 was supplemented by randomly dispersed spots. The most intensive signal was preferentially detected in the very tip of pollen tube, where the network of fine AFs appeared and where the growths of the tube takes place.

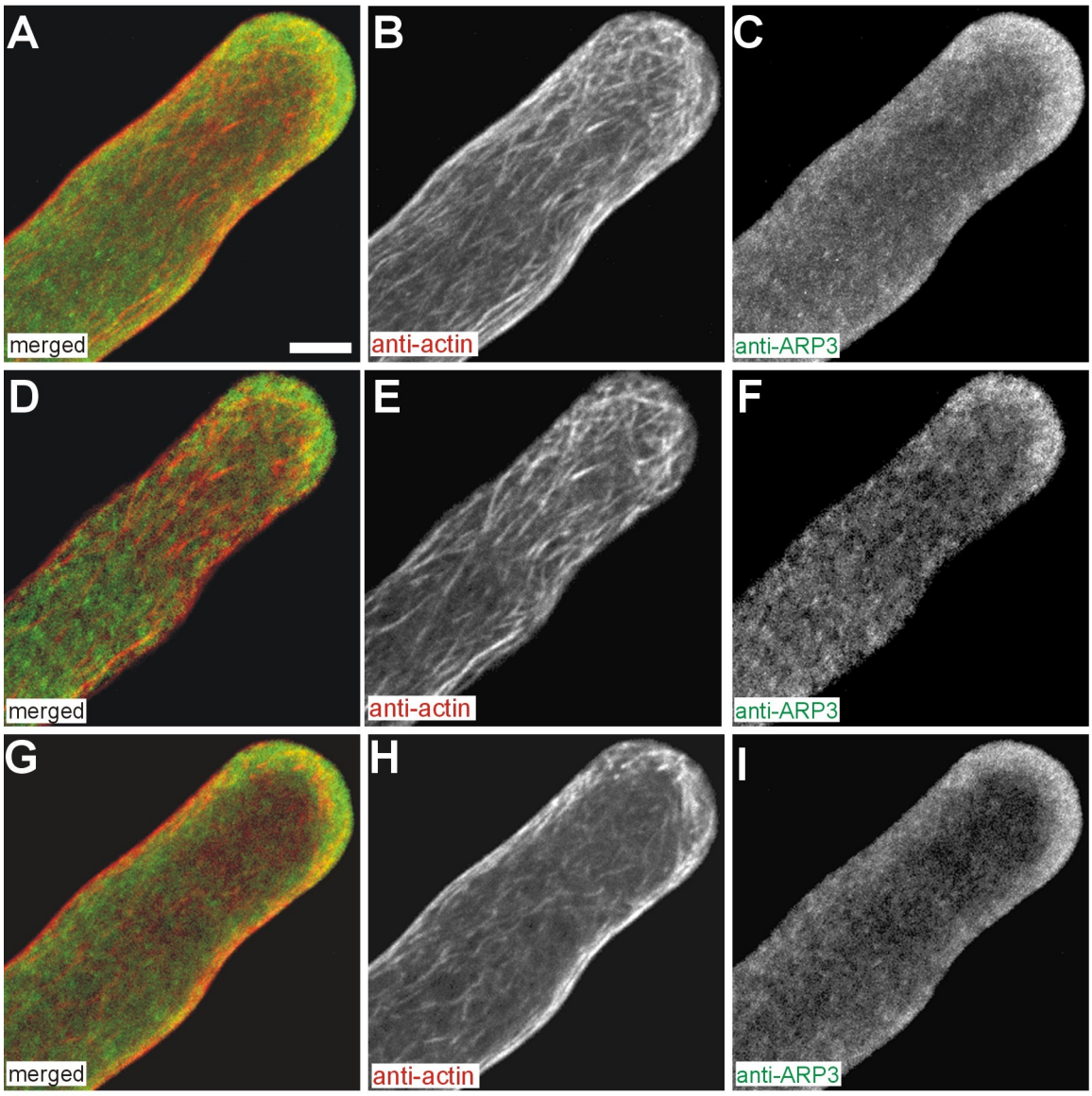

Figure 21. Localization of ARP3 in tobacco pollen tubes. Confocal microscopy. Immunofluorescence staining with anti-NtARP3 (green channel) and rhodamine-phalloidin (red channel). **A-C** Maximal projection of 15 optical sections. In a basal part of a tube, Afs formed a lingitudinal cables. In apical and subapical regions, the network of randomly oriented filaments was detected. **D-F** In the cortical layer, the diffuse pattern of NtARP3 with small spots was localized along the whole surface of the tube, preferentially into the very tip. Maximal projection of two optical sections. **G-I** Diffuse cytoplasmic signal of NtARP3 concentrated at the tip of the pollen tube. Maximal projection of two median optical sections. Bar = 10 μm.

6. DISCUSSION

6.1. AFs organization in control BY-2 cells

To detect changes in AFs organization after treatment with cold or LatB, first, the organization of AFs in untreated cells had to be find out. To visualize AFs in tobacco cell line BY-2, stainings with rhodamine-phaloidin or monoclonal actin antibody were used. My results confirmed the data published by Kakimoto and Shibaoka (1987), who found randomly organized AFs in the cell cortex, and actin cables in cytoplasmic strands and round nucleus in 3-day-old interphase BY-2 cell. Transversely oriented AFs in the cell cortex were predominantly found in elongated cells (Sonobe and Shibaoka 1989). Consistently with this result, I observed that the arrangement of AF network changed during growth cycle (Graph 1) from random orientation predominating in 3-day-old cells (in 79 % of cells) to transversely oriented actin cables in 7-day-old cells (57 % of cells). The elongation processes predominantly occurring in 7-day-old cells may account for the reorientation of AFs from randomly oriented network in intensively dividing 3-day-old cells to transversely oriented network in 7-day-old cells. Since MTs are known to play an important role in deposition of cell wall and both cytoskeletal structures were shown to cooperate (Collings et al. 1998, Blancaflor 2000), longitudinal orientation of AFs may reflect the requirements of the cell for transportation pathways of both AFs and MTs when cellular elongation primarily takes place. However, such a hypothesis has not been tested yet and the reason for the reorientation of AFs remains to be elucidated.

Recently, arrangement of AFs in living BY-2 cells detected using GFP fused to second actin binding domain of fimbrin (Higaki et al. 2006) revealed the high degree of similarity in results obtained with both techniques (fixing and labelling versus *in vivo* detection) which indicates a suitability of the fixation procedure.

For evaluation of quantitative results of AFs arrangement in 3-day-old and 7-day-old cells treated with cold and subsequently recovering, the success of the staining procedure is an important factor. The percentage of successfully stained cells varied not only between 3-day-old and 7-day-old cells, but also between cold treated cells and cells recovering from cold. In 3-day-old controls, the percentage of cells with unsuccessfully stained (damaged cells) AFs was 10-15 % (Graph 1). After 12 hours at 0 ° C, the number unsatisfactorily stained cells increased to approximately 40 % suggesting that the most of these cells may have died during the cold treatment (see Chapter 6.3). On contrary, the number of unsatisfactorily stained 7-day-old cells reached approximately 40 % not only in cold treated cells (Graph 3B), but also in control (Graph 1) and in cells recovering from cold

(Graph 3B). In this case, the number of damaged cells could not relate with the decline in viability. 7-day-old cells posses large vacuoles and much less of cytoplasmic strands than 3-day-old controls. Therefore, they are extremely fragile for staining of cytoskeletal structures. During staining procedure, an insufficient fixing of proteins in the cortical layer of elongated cell is more probable and even degradation of cytoskeletal proteins caused by lytic enzymes released from vacuoles could be expected.

6.2. ARP2 and ARP3 co-localize with AFs in control BY-2 cells

The staining patterns of anti-SpARP2, anti-SpARP3 and anti-NtARP3 antibodies were identical. In control cells, the antibodies recognized protein epitopes in a form of dots closely associated with AFs in the cortical cytoplasm, cytoplasmic strands and around the nucleus. ARP dots were also localized at junctions of branched AFs. Similar distribution of ARPs was observed in cells re-assembling their actin network during recovery after cold and LatB treatments.

In plants, co-localization of ARP3 and AFs was shown by Van Gestel et al. (2003). Using anti-ARP3 against yeast protein, the authors observed punctuate and filamentous signals co-localizing with actin structures. In contrast, I have never observed a filamentous pattern. This difference could be explained by a procedure used in the experiments of Van Gestel et al. (2003) and rather by difference in antibodies used. All antibodies used in my experiments gave identical staining pattern in control BY-2 cells. More than that, immunoblots proved that the anti-ARP3 raised against tobacco protein used in my study specifically recognized tobacco ARP3, suggesting that the staining pattern observed with the use of this antibody reflects the real situation.

In animals, ARPs have been shown to localize to sites with high actin dynamics (Moreau et al. 1996; Welch et al. 1997a; Bretschneider et al. 2004). Thus, the occurrence of ARPs described in my thesis may reflect high AF nucleation activity in the metabolically active, exponentially growing cells. The ARP dots localized along AFs may represent the Arp2/3 complexes with potential branching activity, the rarely observed single ARP dots that did not co-localize with actin possibly represent inactive Arp2/3 complexes.

Alternatively, ARPs composing the isolated dots may participate in other processes. Recently, the role of the Arp2/3 complex in diverse processes occurring within the cell are extensively studied. In yeasts, requirement of the Arp2/3 complex for vacuole fusion (Eitzen et al. 2002) and mitochondrial motility (Boldogh et al. 2001) was demonstrated and particularly, its role was proposed in various endocytic processes such as formation of cortical actin patches (reviewed in

Merriefield 2004, Aycscough 2005), vesicle formation at the trans-Golgi network (Carreno et al. 2004) and regulation of actin dynamics at Golgi-associated trafficking (Luna et al. 2002, Matas et al. 2004). In plants, the importance of AFs in vesicle recycling (Baluška et al. 2002, Baluska et al. 2004), distribution of ER (Boevink et al 1998), Golgi traffic (Nebenfuhr et al. 1999) or vacuolar dynamics (Uemura et al. 2002) was shown previously. Plants, like yeasts, may use the Arp2/3 complex to control the organel movement and various endocytic and exocytic processes via AFs organization. Indeed, decreased motility of Golgi bodies, peroxisomes and mitochondrias and vacuole fragmentation was observed in *A. thaliana* mutants in the Arp2/3 complex subunits (Mathur et al. 2003a, b; Saedler et al. 2004). ARP dots observed in my experiments may participate in some of these processes. Consequently, except for localization of the Arp2/3 complex subunits in the area of leading edge, Welch et al. (1997a) detected also punctuate signal in the cortical region of a fibroblast body (Fig. 4), which was not further functionally addressed. Similarities in the detected pattern of the Arp2/3 complex subunits in cortex fibroblast body and tobacco BY-2 cells tempt to speculate about analogue, non-motile functions of Arp2/3 complex in both of the organisms.

6.3. 3-day-old cells are more sensitive to cold treatment than 7-day-old cells

Tobacco BY-2 cells proved to be a highly sensitive experimental model for detailed investigation of the processes of depolymerization and re-assembly of the actin cytoskeleton in response to cold temperature. Exposing the cells to 0 ^{o} C for only a few minutes affected their cytoplasmic architecture and particularly the organization of the cytoskeleton, while the viability remained almost unaffected.

FDA viability tests are based on a detection of active processes in living cells, namely, enzymatic activities and membrane integrity (Steward et al. 1999). Since cells just released from 0 ° C generally have very low enzymatic activities and cold-damaged membranes (Kacperska 1999), an immediate use of the FDA test would be unsuitable. Therefore, the viability of cells released from the cold treatment was assessed after additional two hours of recovery at 25 ° C.

Using this approach, the viability of 3-day-old cells varied between 50 % and 30 % at the end of 12 hours at 0 ° C in four independent experiments (Graph 2 shows results of one representative experiment). The decline in the viability of 7-day-old cells was not so steep and even after prolonged exposure to cold temperature the viability reached 78 % (Graph 2). This difference may be connected with with the generally decreased metabolic activity of 7-day-old cells. 3-day-old cells constantly repeat the cell cycle, they are highly metabolically active, and therefore extra sensitive to

external stimuli. Non-dividing 7-day-old cells elongate rapidly due to a water absorption, which is passive rather than active process and so their response to stress factors is probably more moderate.

6.4. Cold affects actin network

AFs in transvacuolar cytoplasmic strands disappeared within 5 minutes at 0 ° C, simultaneously with the disintegration of the cytoplasmic strands as seen with the Nomarski DIC. Woods et al. (1984) have observed similar disintegration of cytoplasmic strands in response to cold in various plant species, and suggested that this was the result of disruption of AFs. The scaffolding role of AFs in the formation of transvacuolar strands has been demonstrated in experiments using actin-depolymerizing drugs. A breakdown of cytoplasmic strands was observed after treating tobacco BY-2 cells with latrunculin B for 60 minutes (Van Gestel et al. 2003) or root hairs of *Vicia sativa* with cytochalasin D for 30 minutes (Esseling et al. 2000). Therefore the disruption of the transvacuolar cytoplasmic strands observed in my experiments is likely to be the result of cold-induced depolymerization of the cytoplasmic AFs.

Fine AFs in the cell cortex of 3-day-old cells were apparently less sensitive to cold than cytoplasmic strands. They depolymerized later within 20 minutes of the cold treatment, at about the same time whan the degradation of cortical MTs started (data not shown). Possibly, the destabilization of one resulted in disorganization of the other. The mutual cooperation of AFs and MTs was also shown by Blancaflor (2000) by selective drug-induced stabilization or destabilization of actin and microtubular cytoskeleton.

The most resistant actin structures were the thick actin cables of 7-day-old cells that endured in the cortical cytoplasm even after prolonged cold treatment. After 12 h at 0 ° C, most of the 7-day-old cells (57 %) still contained actin filaments (Graph 3), but in 3-day-old cells, the same treatment did not cause the depolymerization of AFs in only 18 % of cells. Similar observation made Egierszdorff and Kacperska (2001) who demonstrated that thick actin cables in stationary oilseed rape cell suspension were generally more resistant to freezing temperature than the fine filamentous network of younger cells. A possible reason for higher sensitivity of AFs in 3-day-old cells to cold remains unclear. Involvement of different actin isoforms that lower the turnover of AFs, various actin associated proteins stabilizing the AFs array in 7-day-old cells or even other signaling molecules and subcellular structures can participate in different characteristics of AFs network in cells of various age and, therefore, various needs.

Actin was shown to be able to form, at least *in vitro*, a variety of nonfilamentous polymeric or

crystalline supramolecular assemblies (Steinmetz et al. 1997). Actin rods, whose incidence was observed at the end of the cold period mainly in 3-day-old cells (Fig. 9F), may represent a population another polymeric actin form such as tube-like assemblies or actin paracrystals described by Steinmetz et al. (1997). Actin rods occurred preferentially in 3-day-old cells after 12 hour cold period (20 %; compare Graph 3 and Graph 4), which indicates that they originated by *de novo* polymerization at 0 ° C and that their occurrence could relate with the degree of AF network degradation. It is possible that high pool of monomeric actin emerging in response to prolonged exposure of cells to non-physiological temperatures spontaneously polymerized into other polymeric actin forms, however, further investigation will be necessary to support this hypothesis and to elucidate the structure, composition and function of cold-induced actin rods.

The immunoblot analysis did not detect any appreciable changes in the amounts of total, soluble and sedimentable actin after cold treatment in 3-day-old BY-2 cells. (Fig. 11). It is also know that translational activity of BY-2 cells was severely reduced by the cold treatment (Dr. Čapková, unpublished data). Therefore it seems that the pool of actin was stable, neither degraded, nor augmented by newly synthesized proteins. However, stable amounts of actin in soluble and microsomal fractions during prolonged exposure to cold temperature are surprising. AFs completely depolymerized after 12 h at 0°C. Monomeric actin is not expected to interact with membranes any more. The probable explanation is that the high concentration of actin in the cytoplasm made it impossible to study subtle changes in concentration of actin in various protein fractions due to the leaking between them during the extraction procedure. Second possibility is that actin interacts with membrane even in its monomeric form. However, this hypothesis needs further explanation.

6.5. Transient actin structures formed during recovery of cells from cold treatment

Incubation of cells at 0 ° C for 12 hours was apparently sufficient to depolymerize AFs in most 3-day-old cells. After transfer back to 25 ° C, a rapid re-polymerization of actin into small dots, rods connected with actin filaments and dotted filaments became detectable within 30 seconds of recovery in exponential cells (Fig. 10A-E). The formation of the unique "transient actin structures" during the early stages of actin re-polymerization is of particular interest. The incidence of similar actin structures in plant cells has not been described yet neither their composition and function. We hypothesized that actin dots in the cell cortex and around the nucleus correspond to sites of AFs nucleation (SANs). Cold-induced actin rods may also serve as independent nucleation sites during AF recovery.

Later during the recovery period, there appeared thin and branched AFs connecting the dots and rods ("beads-on-string" structures, or bright dots at the junctions of Y-shaped filaments). This may be presumably an outcome of AF assembly from the initiation sites and thus may represent a second step in the recovery of AFs from cold. Some cells formed a dense actin network without dotted signal already 30 seconds after transfer to control temperature. In these cells, maybe, cold treatment did not cause the complete depolymerization of AFs. The cold-stable AFs would offer free B-ends for AFs polymerization. The limiting step of AFs nucleation could be omitted and, therefore, after only 30 seconds of recovery fine actin network detected. In contrast to exponential cells, very low number of 7-day-old cells with transient actin structures were observed (Graph 3B), and transversal actin net re-appeared gradually, usually without previous formation of actin dots. Different modes of actin re-polymerization in exponential and stationary cells may relate to a degree of the preceding cold-induced AFs depolymerization. In exponential cells, where AFs depolymerization was complete, re-assembly of a new actin filament required *de novo* nucleation. In stationary cells and partially also in some exponential cells that retained some remnants of AFs (including cold-induced actin rods), re-assembly could occur by means of addition of new monomers to existing free filament ends. In this case, no transient actin structures would be formed and actin network would reconstitute immediately into filaments. To test this hypothesis, 3-day-old cells were treated by shorter period of 0 ° C so that the actin network was not completely disrupted and cells still contained remnants of AFs (6 hours at 0 ° C; Graph 4). During subsequent recovery, almost no cells with transient actin structures were observed. This may support the hypothesis described above. More detailed evaluation of the data, however, reveals a small discrepancy. The number of 12-hour-cold-treated cells with completely depolymerized AFs (24 %) and the number of subsequently recovering cells with transient actin structures (25 %) correspond to each other, suggesting that complete depolymerization of AFs preceded the formation of transient actin structures. However, the number of 6-hour-cold treated cells with completely depolymerized AFs (13 %) does not correlate with the number of subsequently recovering cells with transient actin structures (0,3 %). This may indicate that the hypothesis of subsequent formation of transient actin structures in cell with previously completely depolymerized AFs network in not valid. However, another explanation exists. For example, in cells with completely depolymerized AFs after 6-hour cold treatment, another cellular structures such as membranes or microtubules, may resist cold damage and serve as supporting structures for quick polymerization of AFs during recovery processes. Therefore, transient actin structures either did not form at all, or their re-organization into actin filaments was too quick to be detectable.

An overview of changes in the organization of AFs detected during the cold treatment and subsequent recovery is shown in a graphical model in Fig. 22, together with a proposed course of re-organization of the actin cytoskeleton.

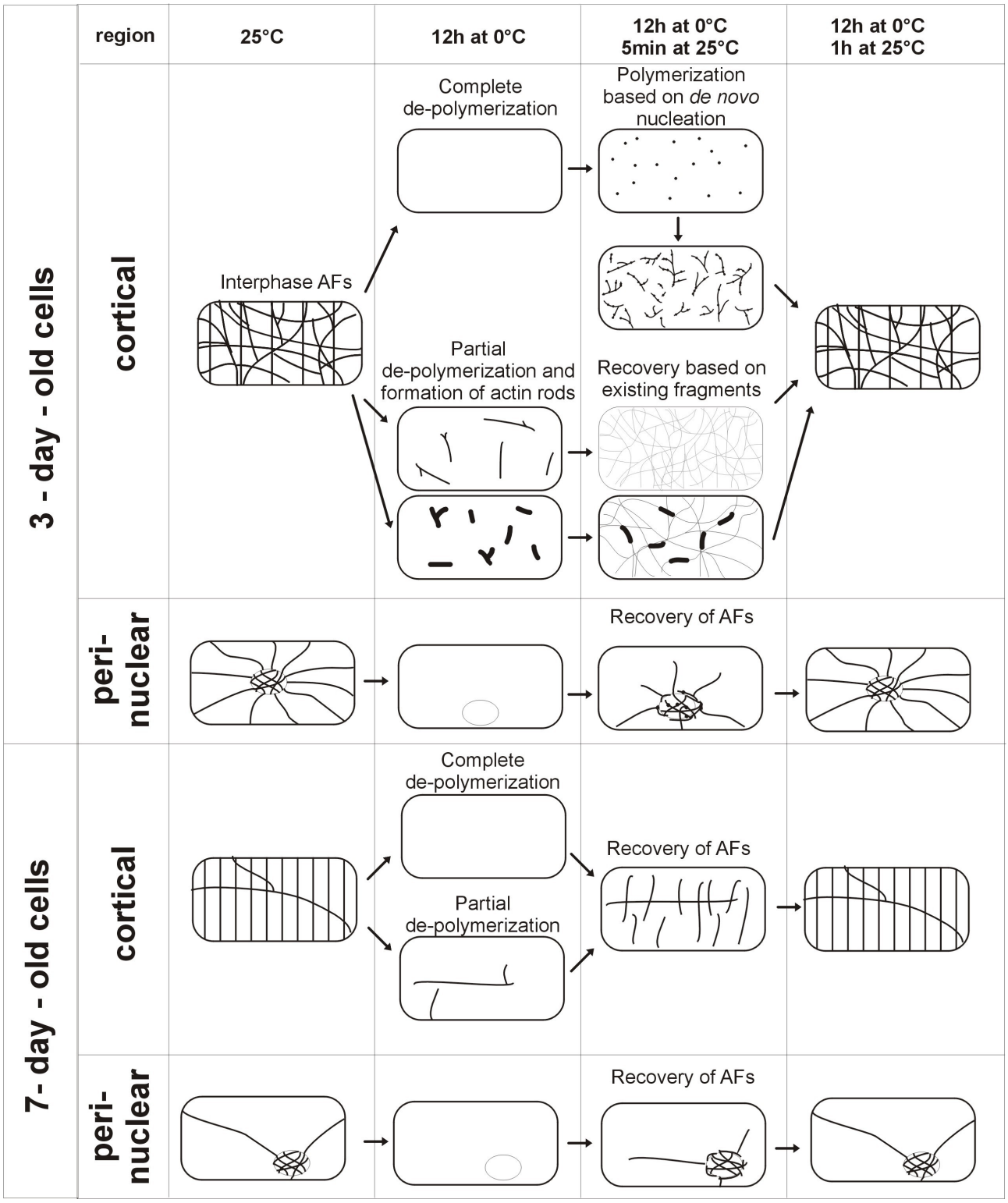

Figure 22. A model summarizing important stages in the re-assembly of AFs during the cold treatment at 0 ° C and subsequent recovery at 25 ° C in interphase BY-2 cells. Arrows indicate proposed course of cytoskeletal organization. In 3-day-old cells, cold treatment resulted in complete depolymerization of AFs in the perinuclear region and in the cytoplasmic strands, and complete or partial depolymerization in the cortical region. Polymerization of actin into dots in the cell cortex and in the perinuclear region during early phases of recovery probably occurred in those cells, in which cold-induced depolymerization was complete. The cells retaining short fragments of actin at the end of the cold treatment were able to polymerize actin into net immediately, without formation of actin dots. In the perinuclear region, actin basket formed around nucleus during early phases of recovery. AFs emerged from it pointing towards the cortical region, thus re-forming the cytoplasmic strands.

In 7-day-old cells, cold treatment caused only partial depolymerzation of AFs in cortical region, and during subsequent recovery, AFs re-polymerized from the ends of existing filaments without forming transient actin structures. In perinuclear region, the degradation and re-forming of actin basket and cytoplasmic strands occurred similarly to 3-day-old cells.

6.6. Sites of AFs nucleation

6.6.1. ARPs co-localize with hypothetical SANs in cells recovering from cold treatment

Besides formins, Arp2/3-driven AFs polymerization was well described to assist in AFs nucleation in animals (for review see Cvrčková et al. 2004). Recently, its function in regulation of AFs organization in plants was suggested (for review see Deeks and Hussey 2005, Mathur 2006), but evidence containing the data on distribution of the Arp2/3 complex subunits, the role of the complex in processes of AFs initiation and the correlation with AFs in plants are missing. Since the putative SANs were detected in BY-2 cells recovering from cold, I focused on the hypothetical role of the Arp2/3 complex subunits during processes of AFs initiation after cold-induced destruction.

Both ARP2 and ARP3, visualized by means of various antibodies, co-localized with transient actin dots (potential SANs, Fig. 16A-D), as well as with branches of newly formed AFs that were observed in cells recovering from cold-induced AF depolymerization (Fig. 16E-H). ARP dots appeared also along AFs and only rarely as single, isolated dots. The occurrence of components of the Arp2/3 complex in potential SANs is of particular interest and, in plants, has not been described before. The co-localization of ARPs with transiently formed actin structures may reflect their function in *de novo* AF nucleation (in animals previously reported in Ma et al. 1998; Mullins and Pollard 1999; Rohatgi et al. 1999) and in AF nucleation on a filament template, resulting in a network of branched AFs (for review see Welch and Mullins 2002). ARPs localized along re-assembling AFs or as isolated dots during recovery after depolymerization may represent the initiation nucleation points, or may participate in actin-mediated endocytic processes or in intracellular movement (see Chapter 6.2). Since the subcellular distribution of ARPs was not affected either by cold or LatB treatment, it seems probable that in cell, SANs occur independently on the degree of the organization of AFs network.

6.6.2. Drug-induced depolymerization of AFs is not sufficient for formation of potential SANs

To observe whether the formation of SANs represents an essential step during processes of AFs re-polymerization, I used LatB to degrade AFs in BY-2 cells and to observe the processes of subsequent re-formation of AFs after washing out the drug (Fig. 17).

Treatment with 500 nM LatB for 12 hours induced complete depolymerization of AFs, as detected by optical microscopy. After the drug had been washed out, AFs started to re-assemble quickly and, within 60 minutes of recovery, a control-like actin network was re-formed. However, transient actin dots – potential SANs – were never observed during any stage of LatB recovery. This

indicates that simple actin depolymerization is not sufficient for the formation of the transient structures during actin recovery.

Low temperature has a great impact on other subcellular structures. It mainly affects membranes (Murata and Los 1997) and the architecture of the vacuome. It has been shown that the Arp2/3 complex plays an important role in vacuolar organization in *A. thaliana* trichomes (Mathur et al. 2003a), localizes to the vacuolar membrane and regulates vacuolar fusion in yeasts (Eitzen et al. 2002). Thus, actin nucleation and polymerization might occur in close cooperation and interaction with cellular membranes such as a tonoplast, plasma membrane or endoplasmic reticulum. AFs physically interact with microtubules and these two cytoskeletons affect each other (Collings et al. 1998). Further, low temperature causes MTs to depolymerize (Kerr and Carter 1990; Bartolo and Carter 1991a, b). Abdrakhamanova and co-workers (2003) have suggested that MTs have a role in a cold acclimation of winter wheat, leading to freezing tolerance. Thus, cold-induced degradation of MTs may represent another factor affecting the dynamics of the actin cytoskeleton.

We suggested that the nucleation of AFs observed in recovering BY-2 cells affected by low temperature is a two-phase process. During the first phase, actin accumulates around potential SANs. A nature of SANs has to be further investigated, nevertheless, I showed that ARPs are components of these structures. During the second phase, polymerization of AF occurs. We proposed that the polymerization process requires an interaction between AFs and other cellular structures, such as membranes and microtubules. During early phases of recovery from the cold treatment, these structures would be unable to serve as the support or "cellular memory" for actin polymerization. A massive accumulation of actin around SANs would then reflect a lag phase between actin nucleation and polymerization, before the support structures recover from cold treatment. During the recovery from LatB treatment, however, no obvious actin accumulation around potential SANs was detected. In these cells, the effect of LatB was restricted to AFs and the system of cellular membranes and particularly the microtubular cytoskeleton remained unaffected. Thus, re-assembly of AFs could occur immediately with the support of other cellular structures. Accumulation of non-polymerized actin around potential SANs was either too quick to be seen or did not occur at all.

6.7. Anti-ARPs do not cross-react with actin

A cross-reactivity test on immunoblots showed that the two anti-ARPs raised against fission yeast ARP2 and ARP3 recognized proteins with different molecular mass to actin (Fig. 12C). A molecular mass of the protein band recognized by anti-SpARP2 in a soluble protein fraction, but not in the membrane fraction (Fig. 12A), corresponded to the putative molecular mass of tobacco ARP2, which is, according to my results, encoded by 389 AA with theoretical molecular mass about 44 kDa (for sequences see Supplements). The putative molecular masses of ARP2 from *A. thaliana* (44 kDa, 389 AA, GenBank accession no. AF507910) correspond to my results. In a membrane protein fraction, but not in the soluble protein fraction, both antibodies against SpARP3 and NtARP3, recognized a protein slightly larger than 45 kDa (Fig. 12A, B), which corresponds to the predicted molecular mass of tobacco ARP3. My data showed that the tobacco ARP3 comprises 428 AA of putative molecular mass about 48 kDa (see Supplements), which is in accordance with predicted molecular masses of *A. thaliana* ARP3 (47,6 kDa, 427 AA, GenBank accession no. AC007357).

To confirm the specificity of antibody against NtARP3, proteins isolated from cells and leaves transformed with *ARP3::GFP* were used for immunoblotting. The expression of fusion protein was parallelly verified by immunodetection with anti-GFP. In transformed tissues, but not in untransformed control, both antibodies (anti-GFP and anti-NtARP3) recognized protein slightly larger than 70 kDa corresponding to putative molecular mass of fusion protein ARP3-GFP (approximately 80 kDa), but also proteins of approximately 48 and 30 kDa, which may reflect the degradation of fusion protein and release of GFP (about 33 kDa) and ARP3 (about 48 kDa). The 30 kDa protein detected with anti-NtARP3 not only in total protein fractions from BY-2 cells and epidermal leaf cells (Fig. 13), but also from proteins isolated from tobacco pollen tubes (Fig. 20), may correspond to degradation product of ARP3 or may reflect an unspecific binding of the antibody. However, the immunostaining pattern of all antibodies used in my experiments was identical, suggesting that also results obtained with tobacco specific anti-ARP3 were reliable.

Both ARP2 and ARP3 are known to exist in the same protein complex but co-sedimented with different protein fractions. Therefore, they may have different roles within this complex. The ARP3 protein co-sedimenting only with the membrane fraction, could mediate interactions of the Arp2/3 complex with membranes. ARP3 detected in association with membranes (Fig. 15) supports this hypothesis. A primarily membrane function of ARP3 in tobacco cells was also suggested by Van Gestel et al. (2003). This hypothesis is consistent with studies of mammalian cells. ARP3 has been shown to bind to Golgi membranes in an ADP-ribosylation factor 1 (ARF1)-dependent manner; Matas et al. 2004), mediating regulation of retrograde (Golgi-to-ER; Luna et al. 2002) and anterograde (ER-to-Golgi) membrane trafficking at the ER/Golgi interface (Fucini et al. 2002).

6.8. Cells expressing ARP3 fused to GFP

To observe the localisation of ARP3 in living cell, the protein was fused to GFP and transformed to BY-2 cells to be stably expressed, and injected into abaxial epidermis of tobacco leafs to be expressed transiently. The immunobloting revealed that in both cases, the fusion protein was expressed, however, it probably underwent partial degradation and the fluorescence of free GFP interfered with fluorescence of GFP linked to ARP3 (Fig. 13). Indeed, the pattern of the plain GFP that was expressed in BY-2 cells as well as in tobacco leafs as a control corresponded to the pattern of fusion protein localization, confirming non-specificity of fluorescence signal detected in transformed cells (Fig. 18 and 19). The only observable difference between the cells expressing ARP3 linked to GFP and plain GFP was the intense nuclear signal in cells expressing plain GFP comparing to cells expressing ARP3::GFP. Plain GFP is known to enter the nucleus spontaneously. It is likely that plain GFP as a product of partial degradation of ARP3::GFP caused the weak fluorescence in nucleus. The cytoplasmic fluorescence of ARP3::GFP could be explained in two ways. GFP linked to ARP3 may collide with the function of the protein. The localization of the functionless ARP3::GFP would correspond with the localization of the free GFP. If GFP tail did not interfere with the normal function of the protein, then the specific fluorescence of the protein may have not been detectable due to the background fluorescence of degraded GFP in cytoplasm.

6.9. The Arp2/3 complex is involved in the expansion of pollen tubes

The role of the Arp2/3 complex in the directional expansion of some plant cell types, such as pollen tubes, has been repeatedly and intensively discussed. The only and the most confusing evidence for the minor role of the Arp2/3 complex involvement in the pollen tip growth came from studies on mutants in genes encoding for the Arp2/3 complex subunits or in some of regulation proteins. These plant mutants, surprisingly, produced normal fertile seeds. This indirect evidence of the uselessness of the Arp2/3-induced AFs polymerization for pollen function has not been disproved yet. My experiments showed that ARP3 was localized to the cortical region and accumulated at the very tip of growing tobacco pollen tube (Fig. 21). Such a localization could be considered, at least partially, as similar to the leading edge of moving fibroblasts. Therefore, the Arp2/3 complex in growing pollen tube may play a role similar to the role in lamellipodia of motile cells in organizing of AFs to drive the tip growth, as suggested by Pollard et al. (2000). Considering the fact that pollen tube growth is apparently not disturbed in mutant plants, we must search for other explanations. Since mutant pollen tubes were not studied in detail, some minor, yet

unobserved, alternations in growing rate, organization of AFs, etc. might occur that do not interfere with pollen tube function. Indeed, minor defects in pollen tube growth were postulated but not described (Li et al. 2003). The other explanation would assume the existence of control mechanism maintaining the functional Arp2/3 complex even when some of its subunits was eliminated. This hypothesis, however, needs evidence. Consequently, the knockdown of ARPC1 subunit of the Arp2/3 complex by RNAi in *P. patens* (Harries et al. 2005) led to various developmental defects including the lack of the tip-growing cells. This suggests that Arp2/3-driven actin polymerization could contribute directly to membrane protrusion in plants as well as in animal lamellipodia.

Although equal internal turgor pressure would predestine the plant cell to gain the more or less oval shape (such as seen in mesophyl cells), the plant body is comprised of wide range of cellular types. The most proclaimed examples are oval mesophyl cells, lobed cells of leaf epidermis, elongated root hairs, pollen tubes, or various forms of xylem elements or trichomes. The emergence of those diverse cell types is probably provided by universal mechanism. The controlled expansion of local protrusions of plant cells encompasses orchestrating of numerous processes on the cell boundary - in the cell wall, plasma membrane and underlying cytoskeletal structures. The need for the dynamic actin cytoskeleton in creating the zonal characteristics of cell that leads to local expansions is extensively discussed (Mathur 2006). The Arp2/3 complex as an efficient modulator of the actin cytoskeleton still deserves attention even though the recent evidence support rather minor role of the complex in plant cell development. Our knowledge of Arp2/3 complex-driven processes in plants is based mainly on mutant analyses. In this regard, the study of Harries et al. (2005) is unique as well as the attempts to directly localize the complex subunits in plant cells. To confirm or disprove the disputed role of the Arp2/3 complex in plant development, the more studies using various approaches have to be applied and critically reviewed.

6.10. Conclusions: Arp2/3 complex in non-motile cells?

Three years ago, the existence of the Arp2/3 complex in plants was still disputable. Wide range of emerging studies brought evidence about the apparent, but probably indispensable role of the complex in plants. Generally, the function of the complex in expansion of some types of plant cells was proven, but the data seem far from being concrete and undebatable. The most attacked question: - What about the role of the protein complex typically participating in motile processes, in generally non-motile cells? - may find a simple answer in accepting intracellular movement and compartment reconstruction as an analogue for the motility of the whole cells. Moreover, even plant alternative to animal leading edges can be found in growing pollen tubes or root hairs, however, the role of the Arp2/3 complex was not detailed even in intracellular processes, and so discussion about

uncertain role of the Arp2/3 complex in plant leading edges became more or less dormant.

In my work, I took advantage of combining molecular-biological, biochemical and cytological approaches to slightly uncover the function of the Arp2/3 complex in BY-2 cells and in growing pollen tubes. My data brought evidence, that the Arp2/3 complex co-localizes with AFs in unaffected BY-2 cells, and participates in processes of AFs nucleation and polymerization in cells recovering from cold-induced AFs degradation. The hypothesized function of the complex in endocytic processes, organel movement, etc. has been suggested but needs further evidence. On the other hand, it was shown several times that expression levels of gene transcripts for complex subunits are ubiquitously low and, interestingly, most genes encoding for the Arp2/3 signalling pathway including the complex subunits are single-copied. This may indicate that the complex participates only in a few concrete and defined processes Or else, the importance of the complex may be manifested by the existence of mechanisms assuring the functionality of the complex. Which of hypothesis proposed takes place in plants remains an interesting question to be elucidated. The detection of one protein of the Arp2/3 complex exclusively in the very tip of growing pollen tube re-opens the discussion about the possible role of the Arp2/3 complex in plant cell morphogenesis throughout the generation and growth of plant-specific leading edges.

7. CONCLUSIONS

This doctoral thesis aimed to elucidate the processes of AFs initiation and polymerization in tobacco BY-2 cells and to investigate potential involvement of the Arp2/3 complex in processes of the early stages of AFs recovery after cold-induced degradation.

Main results of my thesis could be summarized into following statements:

- Cold treatment followed by recovery conditions (12 hours 0 ° C + 5-60 minutes 25 ° C) proved to be an appropriate tool to investigate mechanisms of actin nucleation and polymerization.
- Cells in exponential phase of growth (3-day-old) were more sensitive to low temperature (0 ° C), which caused gradual depolymerization of AFs in both 3-day-old and 7-day-old tobacco BY-2 cells. Unlike 7-day-old cells, total degradation of AFs occurred in most 3-day-old cells.
- Recovery conditions induced re-establishment of AFs array in 3-day-old and 7-day-old tobacco BY-2 cell. AFs re-polymerized rapidly in the cortical region, and on the nuclear envelope. Complete reconstitution of AFs was preceded by the formation of transient actin structures (dots, dotted filaments) in 3-day-old cells, but not in 7-day-old cells, as a possible consequence of the degree of previous AFs degradation. Degradation of AFs caused by LatB was not sufficient to induce the formation of transient actin structures.
- Proteins of the Arp2/3 complex appearing as dots after immunostaining co-localized with AFs in tobacco BY-2 cells. ARPs also co-localized with transient actin dots during recovery of AFs in cold-treated 3-day-old cells.
- **We hypothesized** that **transient actin dots represent sites of AFs nucleation** and that **the Arp2/3 complex plays a role in processes of AFs nucleation and organization** in BY-2 cells.
- In tobacco pollen tubes, ARP3 protein was detected preferentially in the growing apex using specific antibody against tobacco ARP3. **We propose** that **the Arp2/3 complex is involved in processes of local expansion of pollen tubes** similarly to its function during formation and progression of leading edge in animal cells.

As a part of this Ph.D. thesis

- methods for immunostaining of AFs in tobacco BY-2 cells and tobacco pollen tubes were optimized, as well as the production and immunostaining of "membrane ghosts" from tobacco BY-2 cells
- polyclonal antibody against tobacco ARP3 was produced
- tobacco ARP3 was fused to GFP and cloned into binary vector allowing stable or transient transformation of plant cells
- tobacco cell line stably expressing tobacco ARP3 fused to GFP was obtained

8. PUBLICATIONS

Data proclaimed in this Ph.D. thesis were published in following original publications:

Pokorna J, Schwarzerova K., Zelenkova S., Petrasek J., Janotova I, Capkova V and Opatrny Z. Sites of actin reorganisation in cold-treated tobacco cells. *Plant Cell Environ* (2004) 27, 641-653. Times Cited: 3.

Fiserova J., Schwarzerova K., Petrasek J. and Opatrny Z., Proteins of Arp2/3 complex are localised to sites of actin filament nucleation in tobacco BY-2 cells. *Protoplasma* (2006) 227: 119-128. Times Cited: 0.

Schwarzerova K., **Pokorna** J., Petrasek, J., Zelenkova S., Capkova V., Janotova I. And Opatrny Z.: The structure and function of cortical cytoplasm in cold-treated tobacco cells: The role of the cytoskeleton and the endomembrane system. *Cell Biology Internal* 27 (2003) 263-265. Times Cited: 1.

Other original publication:

Borikova, P., **Pokorna**, J., Opatrny Z.: Is the lethal and malforming effect of the potential antigiberelline retardant ANC on the tobacco BY-2 cell line mediated by the cytoskeleton? *Cell Biology Internal* 27 (2003) 175-176. Times Cited: 0.

9. REFERENCES

Abdrakhamanova A, Wang QY, Khokhlova L, Nick P (2003) Is microtubule disassembly a trigger for cold acclimation? Plant Cell Physiol 44: 676-686

Akashi T, Kawasaki S, Shibaoka H (1990) Stabilization of cortical microtubules by the cell wall in cultured tobacco cells. Planta 182: 363-369

An GH (1985) High-efficiency transformation of cultured tobacco cells. Plant Physiol 79: 568-570

Ayscough KR (2005) Coupling actin dynamics to the endocytic process in *Saccharomyces cerevisiae*. Protoplasma 226: 81-88

Baluska F, Hlavacka A, Samaj J, Palme K, Robinson DG, Matoh T, McCurdy DW, Menzel D, Volkmann D (2002) F-actin-dependent endocytosis of cell wall pectins in meristematic root cells. Insights from brefeldin A-induced compartments. Plant Physiol 130: 422-431

Baluska F, Samaj J, Hlavacka A, Kendrick-Jones J, Volkmann D (2004) Actin-dependent fluid-phase endocytosis in inner cortex cells of maize root apices. J Exp Bot 55: 463-473

Bartolo ME, Carter JV (1991a) Effects of microtubule stabilization on the freezing tolerance of mesophyll cells of spinach. Plant Physiol 97: 182-187

Bartolo ME, Carter JV (1991b) Microtubules in mesophyll cells of nonaclimated and cold-aclimated spinach. Plant Physiol 97: 175-181

Basu D, El Assal SED, Le J, Mallery EL, Szymanski DB (2004) Interchangeable functions of *Arabidopsis* PIROGI and the human WAVE complex subunit SRA1 during leaf epidermal development. Dev 131: 4345-4355

Basu D, Le J, El Essal SED, Huang S, Zhang CH, Mallery EL, Koliantz G, Staiger CJ, Szymanski DB (2005) DISTORTED3/SCAR2 is a putative *Arabidopsis* WAVE complex subunit that activates the Arp2/3 complex and is required for epidermal morphogenesis. Plant Cell 17: 502-524

Biyasheva A, Svitkina T, Kunda P, Baum B, Borisy G (2004) Cascade pathway of filopodia formation downstream of SCAR. J Cell Sci 117: 837-848

Blagg SL, Stewart M, Sambles C, Insall RH (2003) PIR121 regulates pseudopod dynamics and SCAR activity in *Dictyostelium*. Curr Biol 13: 1480-1487

Blancaflor EB (2000) Cortical actin filaments potentially interact with cortical microtubules in regulating polarity of cell expansion in primary roots of maize (*Zea mays* L.). J Plant Growth Regul 19: 406-414

Boevink P, Oparka K, Cruz SS, Martin RB, Betteridge A, Hawes C (1998) Stacks on tracks: the plant Golgi apparatus traffics on an actin/ER network. Plant J 15: 441-447

Bogdan S, Klambt C (2003) Kette regulates actin dynamics by inhibiting WAVE and activating WASP activity. Eur J Cell Biol 82: 63-63

Boldogh IR, Yang HC, Nowakowski WD, Karmon SL, Hays LG, Yates JR, Pon LA (2001) Arp2/3 complex and actin dynamics are required for actin-based mitochondrial motility in yeast. P Natl Acad Sci USA 98: 3162-3167

Borths EL, Welch MD (2002) Turning on the Arp2/3 complex at atomic resolution. Structure 10: 131-135

Brembu T, Winge P, Seem M, Bones AM (2004) NAPP and PIRP encode subunits of a

putative wave regulatory protein complex involved in plant cell morphogenesis. Plant Cell 16: 3168-3168

Bretschneider T, Diez S, Anderson K, Heuser J, Clarke M, Muller-Taubenberger A, Kohler J, Gerisch G (2004) Dynamic actin patterns and Arp2/3 assembly at the substrate-attached surface of motile cells. Curr Biol 14: 1-10

Carreno S, Engqvist-Goldstein AE, Zhang CX, McDonald KL, Drubin DG (2004) Actin dynamics coupled to clathrin-coated vesicle formation at the trans-Golgi network. J Cell Biol 165: 781-788

Collings DA, Asada T, Allen NS, Shibaoka H (1998) Plasma membrane-associated actin in bright yellow 2 tobacco cells - Evidence for interaction with microtubules. Plant Physiol 118: 917-928

Cvrckova F, Rivero F, Bavlnka B (2004) Evolutionarily conserved modules in actin nucleation: lessons from *Dictyostelium discoideum* and plants. Protoplasma 224: 15-31

Davis SJ, Vierstra RD (1998) Soluble, highly fluorescent variants of green fluorescent protein (GFP) for use in higher plants. Plant Mol Biol36: 521-528

Deblaere R, Bytebier B, Degerve H, Deboeck F, Schell P, VanMontagu M, Leemans J (1985) Efficient octopine Ti-plasmid-derived vectors for *Agrobacterium*-mediated gene-transfer to plants. Nucleic Acids Res 13: 4777-4788

Deeks MJ, Hussey PJ (2005) Arp2/3 and scar: Plants move to the fore. Nat Rev Mol Cell Biol 6: 954-964

Deeks MJ, Hussey PJ, Davies B (2002) Formins: intermediates in signal-transduction cascades that affect cytoskeletal reorganization. Trends Plant Sci 7: 492-498

Deeks MJ, Kaloriti D, Davies B, Malho R, Hussey PJ (2004) *Arabidopsis* NAP1 is essential for Arp2/3-dependent trichome morphogenesis. Curr Biol 14: 1410-1414

Devreotes PN, Zigmond SH (1988) Chemotaxis in eukaryotic cell - a focus on leukocytes and *Dictyostelium*. Annu Rev Cell Biol 4: 649-686

Djakovic S, Dyachok J, Burke M, Frank MJ, Smith LG (2006) BRICK1/HSPC300 functions with SCAR and the ARP2/3 complex to regulate epidermal cell shape in *Arabidopsis*. Dev 133: 1091-1100

Dower WJ, Miller JF, Ragsdale CW (1988) High-efficientcy transformation of *Escherichia* coli by high voltage electroporation. Nucleic Acids Res 16: 6127-6145

Duncan MC, Cope MJTV, Goode BL, Wendland B, Drubin DG (2001) Yeast Eps15-like endocytic protein, Pan1p, activates the Arp2/3 complex. Nat Cell Biol 3: 687-690

Eden S, Rohatgi R, Podtelejnikov AV, Mann M, Kirschner MW (2002) Mechanism of regulation of WAVE1-induced actin nucleation by Rac1 and Nck. Nature 418: 790-793

Egierszdorff S, Kacperska A (2001) Low temperature effects on growth and actin cytoskeleton organisation in suspension cells of winter oilseed rape. Plant Cell Tiss Org 65: 149-158

Eitzen G, Wang L, Thorngren N, Wickner W (2002) Remodeling of organelle-bound actin is required for yeast vacuole fusion. J Cell Biol 158: 669-679

El Assal SED, Le J, Basu D, Mallery EL, Szymanski DB (2004) *Arabidopsis* GNARLED encodes a NAP125 homolog that positively regulates ARP2/3. Curr Biol 14: 1405-1409

El Assall SE, Le J, Basu D, Mallery EL, Szymanski DB (2004) DISTORTED2 encodes an ARPC2 subunit of the putative *Arabidopsis* ARP2/3 complex. Plant J 38: 526-538

Esseling J, de Ruijter N, Emons AMC (2000) The root hair actin cytoskeleton as backbone,

highway, morphogenetic instrument and target for signalling. In: Ridge RW, Emons AMC (ed) Root Hairs. Cell and Molecular Biology. Springer-Verlag, Tokyo, pp 29-52

Evangelista M, Klebl BM, Tong AHY, Webb BA, Leeuw T, Leberer E, Whiteway M, Thomas DY, Boone C (2000) A role for myosin-I in actin assembly through interactions with Vrp1p, Bee1p, and the Arp2/3 complex. J Cell Biol 148: 353-362

Frank M, Egile C, Dyachok J, Djakovic S, Nolasco M, Li R, Smith LG (2004) Activation of Arp2/3 complex-dependent actin polymerization by plant proteins distantly related to Scar/WAVE. P Natl Acad Sci USA 101: 16379-16384

Frank MJ, Cartwright HN, Smith LG (2003) Three Brick genes have distinct functions in a common pathway promoting polarized cell division and cell morphogenesis in the maize leaf epidermis. Dev 130: 753-762

Frank MJ, Smith LG (2002) A small, novel protein highly conserved in plants and animals promotes the polarized growth and division of maize leaf epidermal cells. Curr Biol 12: 849-853

Fu Y, Wu G, Yang ZB (2001) Rop GTPase-dependent dynamics of tip-localized F-actin controls tip growth in pollen tubes. J Cell Biol 152: 1019-1032

Fucini RV, Chen JL, Sharma C, Kessels MM, Stamnes M (2002) Golgi vesicle proteins are linked to the assembly of an actin complex defined by mAbp1. Mol Biol Cell 13: 621-631

Gautreau A, Ho HYH, Li JX, Steen H, Gygi SP, Kirschner MW (2004) Purification and architecture of the ubiquitous Wave complex. P Natl Acad Sci USA 101: 4379-4383

Geitmann A, Emons AMC (2000) The cytoskeleton in plant and fungal cell tip growth. J Microsc-Oxford 198: 218-245

Goode BL, Wong JJ, Butty AC, Peter M, McCormack AL, Yates JR, Drubin DG, Barnes G (1999) Coronin promotes the rapid assembly and cross-linking of actin filaments and may link the actin and microtubule cytoskeletons in yeast. J Cell Biol 144: 83-98

Harries PA, Pan AH, Quatrano RS (2005) Actin-related protein2/3 complex component ARPC1 is required for proper cell morphogenesis and polarized cell growth in *Physcomitrella* patens. Plant Cell 17: 2327-2339

Hasezawa S, Kumagai F, Nagata T (1997) Sites of microtubule reorganization in tobacco BY-2 cells during cell-cycle progression. Protoplasma 198: 202-209

Hepler PK, Vidali L, Cheung AY (2001) Polarized cell growth in higher plants. Annu Rev Cell Dev Biol 17: 159-187

Higaki T, Kutsuna N, Okubo E, Sano T, Hasezawa S (2006) Actin microfilaments regulate vacuolar structures and dynamics: Dual observation of actin microfilaments and vacuolar membrane in living tobacco BY-2 cells. Plant Cell Physiol 47: 839-852

Hogetsu T (1986) Re-formation of microtubules in *Closterium ehrenbergii* Meneghini after cold induced depolymerization. Planta 167: 437-443. In: Hasezawa S, Kumagai F, Nagata T (1997) Sites of microtubule reorganization in tobacco BY-2 cells during cell-cycle progression. Protoplasma 198: 202-209

Hudson AM, Cooley L (2002) Understanding the function of actin-binding proteins through genetic analysis of *Drosophila* oogenesis. Annu Rev Gen 36: 455-488

Ibarra N, Pollitt A, Insall RH (2005) Regulation of actin assembly by SCAR/WAVE proteins. Biochemical Society Transactions 33: 1243-1246

Innocenti M, Zucconi A, Disanza A, Frittoli E, Areces LB, Steffen A, Stradal TEB, Di Fiore PP, Carlier MF, Scita G (2004) Abi1 is essential for the formation and activation of a WAVE2 signalling complex. Nat Cell Biol 6: 319-327

Kacperska A (1999) Plant responses to low temperature: signalling pathways involved in plant acclimation. In: Margesin R, Schinner F (ed) Cold-adapted organisms. Springer-Verlag Berlin Heidelberg, Berlin, pp 79-104

Kakimoto T, Shibaoka H (1987) Actin filaments and microtubules in the preprophase band and phragmoplast of tobacco cells. Protoplasma 140: 181-186

Kaksonen M, Sun Y, Drubin DG (2003) A pathway for association of receptors, adaptors, and actin during endocytic internalization. Cell 115: 475-487

Kelleher JF, Atkinson SJ, Pollard TD (1995) Sequences, structural models, and cellular localization of actin related proteins ARP2 and ARP3 from *Acanthamoeba*. J Cell Biol 131: 385-397

Kerr GP, Carter JV (1990) Tubulin isotypes in rye roots are altered during cold acclimation. Plant Physiol 93: 83-88

Klahre U, Chua NH (1999) The *Arabidopsis* ACTIN-RELATED PROTEIN 2 (AtARP2) promoter directs expression in xylem precursor cells and pollen. Plant Mol Biol 41: 65-73

Koncz C, Schell J (1986) The promoter of Tl DNA gene 5 controls the tissue-specific expression of the chimeric genes carried by a novel type of *Agrobacterium* binary vector. Mol Gener Gen 204: 383-396

Kost B, Spielhofer P, Chua NH (1998) A GFP-mouse talin fusion protein labels plant actin filaments in vivo and visualizes the actin cytoskeleton in growing pollen tubes. Plan J 16: 393-401

Kuhn JR, Pollard TD (2005) Real-time measurements of actin filament polymerization by total internal reflection fluorescence microscopy. Biophysical J 88: 1387-1402

Le J, El Assal SED, Basu D, Saad ME, Szymanski DB (2003) Requirements for *Arabidopsis* ATARP2 and ATARP3 during epidermal development. Curr Biol 13: 1341-1347

Le J, Mallery EL, Zhang CH, Brankle S, Szymanski DB (2006) *Arabidopsis* BRICK1/HSPC300 is an essential WAVE-complex subunit that selectively stabilizes the Arp2/3 activator SCAR2. Curr Biol 16: 895-901

Li SD, Blanchoin L, Yang ZB, Lord EM (2003) The putative *Arabidopsis* Arp2/3 complex controls leaf cell morphogenesis. Plant Physiol 132: 2034-2044

Lovy-Wheeler A, Wilsen KL, Baskin TI, Hepler PK (2005) Enhanced fixation reveals the apical cortical fringe of actin filaments as a consistent feature of the pollen tube. Planta 221: 95-104

Luna A, Matas OB, Martinez-Menarguez JA, Mato E, Duran JM, Ballesta J, Way M, Egea G (2002) Regulation of protein transport from the golgi complex to the endoplasmic reticulum by CDC42 and N-WASP. Mol Biol Cell 13: 866-879

Ma L, Rohatgi R, Kirschner MW (1998) The Arp2/3 complex mediates actin polymerization induced by the small GTP-binding protein Cdc42. P Natl Acad Sci USA 95: 15362-15367

Machesky LM, Atkinson SJ, Ampe C, Vandekerckhove J, Pollard TD (1994) Purification of a cortical complex containing 2 unconventional actins from *Acanthamoeba* by affinity achromatography on profilin agarose. J Cell Biol 127: 107-115

Machesky LM, Gould KL (1999) The Arp2/3 complex: a multifunctional actin organizer. Curr Opin Cell Biol 11: 117-121

Marchand JB, Kaiser DA, Pollard TD, Higgs HN (2001) Interaction of WASP/Scar proteins with actin and vertebrate Arp2/3 complex. Nat Cell Biol 3: 76-82

Matas OB, Martinez-Menarguez J, Egea G (2004) Association of Cdc42/N-WASP/Arp2/3 signaling pathway with golgi membranes. Traffic 5: 838-846

Mathur J (2005) The ARP2/3 complex: giving plant cells a leading edge. Bioessays 27: 377-

Mathur J (2006) Local interactions shape plant cells. Curr Opin Cell Biol 18: 40-46

Mathur J, Chua NH (2000) Microtubule stabilization leads to growth reorientation in *Arabidopsis* trichomes. Plant Cell 12: 465-477

Mathur J, Mathur N, Kernebeck B, Hulskamp M (2003a) Mutations in actin-related proteins 2 and 3 affect cell shape development in *Arabidopsis*. Plant Cell 15: 1632-1645

Mathur J, Mathur N, Kirik V, Kernebeck B, Srinivas BP, Hulskamp M (2003b) *Arabidopsis* CROOKED encodes for the smallest subunit of the ARP2/3 complex and controls cell shape by region specific fine F-actin formation. Dev 130: 3137-3146

Mathur J, Spielhofer P, Kost B, Chua NH (1999) The actin cytoskeleton is required to elaborate and maintain spatial patterning during trichome cell morphogenesis in *Arabidopsis* thaliana. Dev 126: 5559-5568

McCollum D, Feoktistova A, Morphew M, Balasubramanian M, Gould KL (1996) The Schizosaccharomyces pombe actin-related protein, Arp3, is a component of the cortical actin cytoskeleton and interacts with profilin. EMBO J 15: 6438-6446

McCormac AC, Elliott MC, Chen DF (1998) A simple method for the production of highly competent cells of *Agrobacterium* for transformation via electroporation. Mol Biotech 9: 155-159

McKinney EC, Kandasamy MK, Meagher RB (2002) *Arabidopsis* contains ancient classes of differentially expressed actin-related protein genes. Plant Physiol 128: 997-1007

Merrifield CJ (2004) Seeing is believing: imaging actin dynamics at single sites of endocytosis. Trends Cell Biol 14: 352-358

Miller KG (2002) Extending the Arp2/3 complex and its regulation beyond the leading edge. J Cell Biol 156: 591-593

Mizuno K (1992) Induction of cold stability of microtubules in cultured tobacco cells. Plant Physiol 100: 740-748

Moreau V, Madania A, Martin RP, Winsor B (1996) The *Saccharomyces cerevisiae* actin-related protein arp2 is involved in the actin cytoskeleton. J Cell Biol 134: 117-132

Morrell JL, Morphew M, Gould KL (1999) A mutant of Arp2p causes partial disassembly of the Arp2/3 complex and loss of cortical actin function in fission yeast. Mol Biol Cell 10: 4201-4215

Mullins RD, Heuser JA, Pollard TD (1998) The interaction of Arp2/3 complex with actin: Nucleation, high affinity pointed end capping, and formation of branching networks of filaments. P Natl Acad Sci USA 95: 6181-6186

Mullins RD, Pollard TD (1999) Rho-family GTPases require the Arp2/3 complex to stimulate actin polymerization in *Acanthamoeba* extracts. Curr Biol 9: 405-415

Murata N, Los DA (1997) Membrane fluidity and temperature perception. Plant Physiol 115: 875-879

Murgia I, Maciver SK, Morandini P (1995) An actin related protein from *Dictyostelium* discoideum is develpmentaly regulated and associated with mitochondria. Febs Lett 360: 235-241

Nagata T, Nemoto Y, Hasezawa S (1992) Tobacco BY-2 cell line as the "HeLa" cell in the cell biology of higher plants. Int Rev Cytol 132: 1-30

Nebenfuhr A, Gallagher LA, Dunahay TG, Frohlick JA, Mazurkiewicz AM, Meehl JB, Staehelin LA (1999) Stop-and-go movements of plant Golgi stacks are mediated by the acto-myosin system. Plant Physiol 121: 1127-1141

Nick P (2000) Control of the response to low temperatures. In: Nick P (ed) Plant

Microtubules Potential for Biotechnology. Springer-Verlag Berlin Heidelberg 2000, Berlin, pp 121-135

Olyslaegers G, Verbelen JP (1998) Improved staining of F-actin and co-localization of mitochondria in plant cells. J Microsc-Oxford 192: 73-77

Örvar BL, Sangwan V, Omann F, Dhindsa RS (2000) Early steps in cold sensing by plant cells: the role of actin cytoskeleton and membrane fluidity. Plant J 23: 785-794

Picton JM, Steer MW (1982) A model for the mechanism of tip extension in pollen tubes. J Theor Biol 98: 15-20

Pilát Z (2005) Identifikace proteinového komplexu Arp2/3 v rostlinných buňkách. Diploma Thesis. Charles University in Prague. Czech Republic.

Pollard TD (1986) Rate constants for the reactions of ATP-actin and ADP-actin with the ends of actin filaments. J Cell Biol 103: 2747-2754

Pollard TD, Blanchoin L, Mullins RD (2000) Molecular mechanisms controlling actin filament dynamics in nonmuscle cells. Ann Rev Biophys Biomol Struct 29: 545-576

Popov N, Schmitt S, Mathies H (1975) Eine störungsfreie Mikromethode zur Bestimmung des Proteingehaltes in Gewebshomogenaten. Acta Biol Germ 34: 144-146

Quader H, Hofmann A, Schnepf E (1989) Reorganization of the endoplasmic reticulum in epidermal cells of onion bulb scales after cold stress: Involvement of cytoskeletal elements. Planta 177: 273-280

Robinson RC, Turbedsky K, Kaiser DA, Marchand JB, Higgs HN, Choe S, Pollard TD (2001) Crystal structure of Arp2/3 complex. Science 294: 1679-1684

Rohatgi R, Ma L, Miki H, Lopez M, Kirchhausen T, Takenawa T, Kirschner MW (1999) The interaction between N-WASP and the Arp2/3 complex links Cdc42-dependent signals to actin assembly. Cell 97: 221-231

Romeis T, Ludwig AA, Martin R, Jones JDG (2001) Calcium-dependent protein kinases play an essential role in a plant defence response. EMBO J 20: 5556-5567

Saedler R, Mathur N, Srinivas BP, Kernebeck B, Hulskamp M, Mathur J (2004) Actin control over microtubules suggested by DISTORTED2 encoding the *Arabidopsis* ARPC2 subunit homolog. Plant Cell Physiol 45: 813-822

Sambrook J, Russell DW (2001) Molecular cloning: A laboratory manual. III./A3.9: Cold Spring Harbor, NY: Cold Spring Harbor Laboratory Press

Sawa M, Suetsugu S, Sugimoto A, Miki H, Yamamoto M, Takenawa T (2003) Essential role of the *C.elegans* Arp2/3 complex in cell migration during ventral enclosure. J Cell Sci 116: 1505-1518

Seastone DJ, Harris E, Temesvari LA, Bear JE, Saxe CL, Cardelli J (2001) The WASp-like protein Scar regulates macropinocytosis, phagocytosis and endosomal membrane flow in *Dictyostelium*. J Cell Sci 114: 2673-2683

Sheahan M, Steiger CJ, Rose RJ, McCurdy DW (2004) A green fluorescent protein fusion to actin-binding domain 2 of *Arabidopsis* fimbrin highlights new features of a dynamic actin cytoskeleton in live plant cells. Plant Physiol 136: 3968-3978

Sonobe S, Shibaoka H (1989) Cortical fine actin filaments in higher plant cells visualized by rhodamin-phalloidin after pretreatment with *m*-maleimidobenzoyl *N*-hydrxysuccinimide ester. Protoplasma 35: 451-460. In: Collings DA, Asada T, Allen NS, Shibaoka H (1998) Plasma membrane-associated actin in bright yellow 2 tobacco cells - Evidence for interaction with microtubules. Plant Physiol 118: 917-928

Steinmetz MO, Stoffler D, Hoenger A, Bremer A, Aebi U (1997) Actin: From cell biology to atomic detail. J Struct Biol 119: 295-320

Steffen A, Rottner K, Ehinger J, Innocenti M, Scita G, Wehland A, Stradal TEB (2004) Sra-1 and Nap1 link Rac to actin assembly driving lamellipodia formation. EMBO J 23: 749-759

Steward N, Martin R, Engasser JM, Goergen JL (1999) A new methodology for plant cell viability assessment using intracellular esterase activity. Plant Cell Rep 19: 171-176

Stradal TEB, Rottner K, Disanza A, Confalonieri S, Innocenti M, Scita G (2004) Regulation of actin dynamics by WASP and WAVE family proteins. Trends Cell Biol 14: 303-311

Stradal TEB, Scita G (2006) Protein complexes regulating Arp2/3-mediated actin assembly. Curr Opin Cell Biol 18: 4-10

Svitkina TM, Borisy GG (1999) Arp2/3 complex and actin depolymerizing factor cofilin in dendritic organization and treadmilling of actin filament array in lamellipodia. J Cell Biol 145: 1009-1026

Svitkina TM, Bulanova EA, Chaga OY, Vignjevic DM, Kojima S, Vasiliev JM, Borisy GG (2003) Mechanism of filopodia initiation by reorganization of a dendritic network. J Cell Biol 160: 409-421

Szymanski DB (2005) Breaking the WAVE complex: the point of *Arabidopsis* trichomes. Curr Opin Plant Biol 8: 103-112

Szymanski DB, Marks MD, Wick SM (1999) Organized F-actin is essential for normal trichome morphogenesis in *Arabidopsis*. Plant Cell 11: 2331-2347

Uemura T, Yoshimura SH, Takeyasu K, Sato MH (2002) Vacuolar membrane dynamics revealed by GFP-AtVam3 fusion protein. Genes to Cells 7: 743-753

Uruno T, Liu JL, Zhang PJ, Fan YX, Egile C, Li P, Mueller SC, Zhan X (2001) Activation of Arp2/3 complex-mediated actin polymerization by cortactin. Nat Cell Biol 3: 259-266

Van Gestel K, Slegers H, von Witsch M, Samaj J, Baluska F, Verbelen JP (2003) Immunological evidence for the presence of plant homologues of the actin-related protein Arp3 in tobacco and maize: subcellular localization to actin-enriched pit fields and emerging root hairs. Protoplasma 222: 45-52

Vantard M, Blanchoin L (2002) Actin polymerization processes in plant cells. Curr Opin Plant Biol 5: 502-506

Vidali L, Hepler PK (2001) Actin and pollen tube growth. Protoplasma 215: 64-76

Vidali L, McKenna ST, Hepler PK (2001) Actin polymerization is essential for pollen tube growth. Mol Biol Cell 12: 2534-2545

Voinnet O, Rivas S, Mestre P, Baulcombe D (2003) An enhanced transient expression system in plants based on suppression of gene silencing by the p19 protein of tomato bushy stunt virus. Plant J 33: 949-956

Vuillard L, Braunbreton C, Rabilloud T (1995) Non-Detergent Sulfobetaines - A New Class of Mild Solubilization Agents for Protein-Purification. Biochem J 305: 337-343

Wasteneys GO, and Williamson RE (1989) Reassembly of microtubules in *Nitella tasmanica*: assembly of cortical microtubules in branching clusters and its relevance to steady-ctate microtubule assambly. J Cell Sci 93: 705-714. In: Hasezawa S, Kumagai F, Nagata T (1997) Sites of microtubule reorganization in tobacco BY-2 cells during cell-cycle progression. Protoplasma 198: 202-209

Weaver AM, Karginov AV, Kinley AW, Weed SA, Li Y, Parsons JT, Cooper JA (2001) Cortactin promotes and stabilizes Arp2/3-induced actin filament network formation. Curr Biol 11:

370-374

Welch MD, DePace AH, Verma S, Iwamatsu A, Mitchison TJ (1997a) The human Arp2/3 complex is composed of evolutionarily conserved subunits and is localized to cellular regions of dynamic actin filament assembly. J Cell Biol 138: 375-384

Welch MD, Iwamatsu A, Mitchison TJ (1997b) Actin polymerization is induced by Arp2/3 protein complex at the surface of *Listeria monocytogenes*. Nature 385: 265-269

Welch MD, Mullins RD (2002) Cellular control of actin nucleation. Annu Rev Cell Dev Biol 18: 247-288

Widholm JM (1972) The use of fluorescein diacetate and phenosafranine for determining viability of cultured plant cells. Stain Tech 47: 189-194

Wilsen KL, Lovy-Wheeler A, Voigt B, Menzel D, Kunkel JG, Hepler PK (2006) Imaging the actin cytoskeleton in growing pollen tubes. Sex Plant Rep 19: 51-62

Winter D, Podtelejnikov AV, Mann M, Li R (1997) The complex containing actin-related proteins Arp2 and Arp3 is required for the motility and integrity of yeast actin patches. Curr Biol 7: 519-529

Woods CM, Reid MS, Patterson BD (1984) Response to chilling stress in plant cells. 1. Changes in cyclosis and cytoplasmic structure. Protoplasma 121: 8-16

Yarar D, To W, Abo A, Welch MD (1999) The Wiskott-Aldrich syndrome protein directs actin-based motility by stimulating actin nucleation with the Arp2/3 complex. Curr Biol 9: 555-558

Zallen JA, Cohen Y, Hudson AM, Cooley L, Wieschaus E, Schejter ED (2002) SCAR is a primary regulator of Arp2/3-dependent morphological events in *Drosophila*. J Cell Biol 156: 689-701

Zhang XG, Dyachok J, Krishnakumar S, Smith LG, Oppenheimer DG (2005) IRREGULAR TRICHOME BRANCH1 in *Arabidopsis* encodes a plant homolog of the actin-related protein2/3 complex activator Scar/WAVE that regulates actin and microtubule organization. Plant Cell 17: 2314-2326

SUPPLEMENTS

Sequences used to design primers

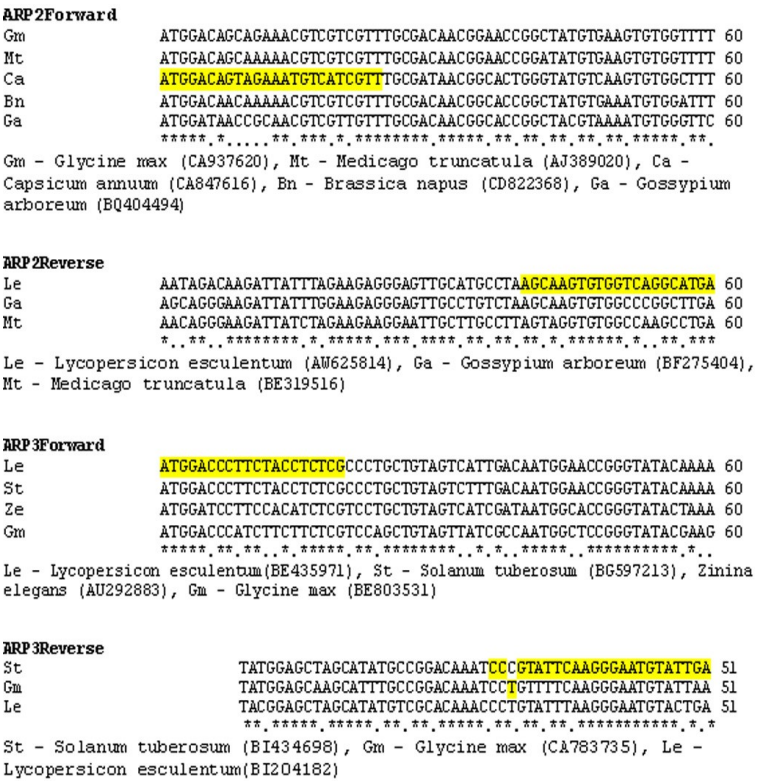

Figure 23. Sequences used to design primers for amplification of *NtARP2* and *NtARP3* genes. Final primer sequences are highlighted in yellow.

Sequence of NtARP2

>NtARP2

```
atggacagtagaaatgtcatcgtttgcnacaacggcaccgggtatgtcaagtgtggcttt
 M  D  S  R  N  V  I  V  C  X  N  G  T  G  Y  V  K  C  G  F
gcgggtgagaattttcccacatctgtattcccttgtgttgtggggaggccaacgctaaga
 A  G  E  N  F  P  T  S  V  F  P  C  V  V  G  R  P  T  L  R
tatgaagaatctcttatggaacaagacttgaaggatactattgtgggagatgattgcttg
 Y  E  E  S  L  M  E  Q  D  L  K  D  T  I  V  G  D  D  C  L
aagttgcggcatcagttggatatatcatatcctgtcaacaatggaattgtgcaaaactgg
 K  L  R  H  Q  L  D  I  S  Y  P  V  N  N  G  I  V  Q  N  W
gatgatatggggcatgtgtgggatcatgcatttttcaacgaactgaaggtagatccgacc
 D  D  M  G  H  V  W  D  H  A  F  F  N  E  L  K  V  D  P  T
gaatgcaaaattctgctgacagatccacctctcaatccatcgaaaaatcgtgaaaagatg
 E  C  K  I  L  L  T  D  P  P  L  N  P  S  K  N  R  E  K  M
gtagaaactatgtttgagaagtacaactttgctggggtcttcatccaaattcaagctgtt
 V  E  T  M  F  E  K  Y  N  F  A  G  V  F  I  Q  I  Q  A  V
ctaacactgtatgctcaaggtttgttgactgggctagtcatagactctggtgatggagtt
 L  T  L  Y  A  Q  G  L  L  T  G  L  V  I  D  S  G  D  G  V
```

```
acgcatgttgttcctgttgttgatggatactcattccctcacctcacaaaaagaatgaat
 T  H  V  V  P  V  V  D  G  Y  S  F  P  H  L  T  K  R  M  N
gttgcagggcgccatataacatcttatctggttgatctgctacttcgaagagggtatgca
 V  A  G  R  H  I  T  S  Y  L  V  D  L  L  L  R  R  G  Y  A
atgaataagagtgctgattttgagaccgtcagggatattaaagaaaagctgtgctacatt
 M  N  K  S  A  D  F  E  T  V  R  D  I  K  E  K  L  C  Y  I
agttatgattacaagagagaatatcagttagggcttgagactactattcttgttaagaat
 S  Y  D  Y  K  R  E  Y  Q  L  G  L  E  T  T  I  L  V  K  N
tatactcttccagatgggagggtacttaaagttggcacagagaggttccaggcacctgag
 Y  T  L  P  D  G  R  V  L  K  V  G  T  E  R  F  Q  A  P  E
gctctttttactccagatcttattgatgttgaaggtgatggcatggcagacatggtattt
 A  L  F  T  P  D  L  I  D  V  E  G  D  G  M  A  D  M  V  F
cgttgcatccaggagatggatattgataacaggatgatgctctaccaacatattgttttg
 R  C  I  Q  E  M  D  I  D  N  R  M  M  L  Y  Q  H  I  V  L
agtggcggaagtactatgtatcctggcttacctagtcgccttgagaaagaaattttggac
 S  G  G  S  T  M  Y  P  G  L  P  S  R  L  E  K  E  I  L  D
cgctatcttgatgttgttttgaaggggaacaaagatggtttgaagaaattgcgcttacga
 R  Y  L  D  V  V  L  K  G  N  K  D  G  L  K  K  L  R  L  R
atagaagatccaccaagaagaaagcatatggtgtaccttggaggtgcggttctggcagga
 I  E  D  P  P  R  R  K  H  M  V  Y  L  G  G  A  V  L  A  G
attatgaaggatgcccctgagttttggatcaatagacaagattatttagaagagggagtt
 I  M  K  D  A  P  E  F  W  I  N  R  Q  D  Y  L  E  E  G  V
gcttgcttaagcaagtgtggtcaggcatga
 A  C  L  S  K  C  G  Q  A  -
```

Sequence of NtARP3

>NtARP3

```
atggacccttctacctctcgcccagctgtagtcattgacaatggaaccgggtatacaaaa
 M  D  P  S  T  S  R  P  A  V  V  I  D  N  G  T  G  Y  T  K
atgggttttgctggaaatgttgaaccatctttcatactgcctacagttgtcgctgttaac
 M  G  F  A  G  N  V  E  P  S  F  I  L  P  T  V  V  A  V  N
gaatcatttatcaatcagcctcgagctttgactaagagcagcaacttagctcagtacagt
 E  S  F  I  N  Q  P  R  A  L  T  K  S  S  N  L  A  Q  Y  S
gcaggagttatggctgatcttgatttctttattggggaagaggcattgagtagatctaaa
 A  G  V  M  A  D  L  D  F  F  I  G  E  E  A  L  S  R  S  K
tctagtagcacttacaatcttagctatcctattaaacatggacaggttgataactgggat
 S  S  S  T  Y  N  L  S  Y  P  I  K  H  G  Q  V  D  N  W  D
gcaatggagcggttctggcagcagtgtgtattcaattatctgcgctgtgaccctgaggat
 A  M  E  R  F  W  Q  Q  C  V  F  N  Y  L  R  C  D  P  E  D
cactattttctgttgactgaaagccctatgactgcaccagagaaccgagaatatactggt
 H  Y  F  L  L  T  E  S  P  M  T  A  P  E  N  R  E  Y  T  G
gaaattatgtttgagactttcaatgttccgggactttatatagctgtgcagccggttctt
 E  I  M  F  E  T  F  N  V  P  G  L  Y  I  A  V  Q  P  V  L
gctctggcagctgggtacacagcatctaagtgtgagatgactggagtcgtagtggatgtt
 A  L  A  A  G  Y  T  A  S  K  C  E  M  T  G  V  V  V  D  V
ggagatggtgctacccatgttgtacctgttgctgaaggttatgttattgggagtagcatt
 G  D  G  A  T  H  V  V  P  V  A  E  G  Y  V  I  G  S  S  I
aagtcaatccctgttgctgggaaagatgttactcttttcattcaacagctcatgaaggaa
 K  S  I  P  V  A  G  K  D  V  T  L  F  I  Q  Q  L  M  K  E
aggggagagcatgttccagcagaggattccttagaagtagcacgaaaagtgaaggaaatg
 R  G  E  H  V  P  A  E  D  S  L  E  V  A  R  K  V  K  E  M
tattgctatacttgttctgacattgtgaaggagtctaataagcatgataaagagccaggg
 Y  C  Y  T  C  S  D  I  V  K  E  S  N  K  H  D  K  E  P  G
aagtacatcaagcaatggagaggtacaaaaccaaagacaggagcaccatattcatgtgat
 K  Y  I  K  Q  W  R  G  T  K  P  K  T  G  A  P  Y  S  C  D
gttggctatgagcgatttcttggtcctgaggttttcttcaatcctgagatctataatagt
 V  G  Y  E  R  F  L  G  P  E  V  F  F  N  P  E  I  Y  N  S
gattttacgacccctttacctgatgtgattgacaaatgtatccagtctgcaccaattgac
 D  F  T  T  P  L  P  D  V  I  D  K  C  I  Q  S  A  P  I  D
acaagaagagctttatataagaatattgttctatccggaggatcaaccatgttcaaagac
 T  R  R  A  L  Y  K  N  I  V  L  S  G  G  S  T  M  F  K  D
```

```
ttccatagaagattgcagcgagatctcaagaagattgtggatgaccgtgttcctgcatca
 F  H  R  R  L  Q  R  D  L  K  K  I  V  D  D  R  V  P  A  S
gatgctcggttaggtggaaatgtcaaagcacaaccagttgaagtgaatgttgtcagcaat
 D  A  R  L  G  G  N  V  K  A  Q  P  V  E  V  N  V  V  S  N
cctatccagagatatgcagtttggtttggaggttctgtactagcttcaactccggaattt
 P  I  Q  R  Y  A  V  W  F  G  G  S  V  L  A  S  T  P  E  F
tttgcggcttgccatacaaagacagaatacgaggaatatggagctagcatatgccgcaca
 F  A  A  C  H  T  K  T  E  Y  E  E  Y  G  A  S  I  C  R  T
aaccctgtattcaagggaatgtattga
 N  P  V  F  K  G  M  Y  -
```